2013-09-13

Vibro-Acoustic Monitoring of Pipeline Leakage and Corrosion

Sharma, Vishash

UNIVERSITY OF CALGARY

Vibro-Acoustic Monitoring of Pipeline Leakage and Corrosion

by

Vishash Sharma

A THESIS

SUBMITTED TO THE FACULTY OF GRADUATE STUDIES

IN PARTIAL FULFILMENT OF THE REQUIREMENTS FOR THE

DEGREE OF MASTER OF SCIENCE

DEPARTMENT OF MECHANICAL AND MANUFACTURING ENGINEERING

CALGARY, ALBERTA

SEPTEMBER, 2013

ABSTRACT

Pipeline networks are economical means of transporting oil and gas. Most pipelines have been designed with a typical life span of 25 to 30 years. Existing pipelines are aging and quite susceptible to failure, due to poor construction of joints, corrosion, fatigue and material cracks. Accidents, terrorist activities, sabotage or theft can also cause leak disasters. Prevention of catastrophic failures of pipelines is critical for public safety and the environment. In order to maintain the healthy state of pipelines, continuous and accurate monitoring of pipelines is crucial, especially for corrosion and leakage. In order to reduce the impact of petroleum product spills, quick and effective leakage detection is needed to mitigate the problem.

The focus of this study is the development of a novel pipeline monitoring scheme to detect faults such as corrosion and leakage. Dynamic properties, such as frequency response functions (FRFs) and transient responses, of the pipeline system can change when faults occur. In the case of a corroded pipeline or leaky pipeline system, the mass and stiffness of the pipeline changes, thereby changing the FRFs of the pipeline system. The variation in the dynamic parameters is used to predict the presence of the corrosion or leakage in the pipeline system.

Experimental modal analysis was performed using a small-scale pipeline setup in various operating and physical conditions. In parallel, finite element analysis was undertaken for the same physical and operating conditions of the pipeline. A novel adaptive neuro fuzzy inference system (ANFIS) based scheme was developed for pipeline monitoring using fuzzy rules and neural networks. The trained ANFIS architecture was tested with a number of sets of dynamic parameters that were obtained by simulating leakage and corrosion in the pipeline and by varying the pressure and flow rate.

The results show that the ANFIS-based pipeline monitoring system can accurately predict the corrosion or leakage in the pipeline with an acceptable band of errors. The predicted results validates that the ANFIS-based pipeline monitoring system is less time-consuming and more flexible through the use of fuzzy rules incorporated with real-world systems.

Acknowledgements

I am heartily thankful to my supervisor, Dr. Simon Park, for his patience in seeing this project through and in having the confidence that I would succeed in tackling the many problems encountered along the way. Words fail me for the expression of my appreciation to my wife, Seema, and my daughter, Yashasvi, for their loving support. I wish to express my warm and sincere thanks to my colleagues, Majid Mehrpouya and Matthew Kindree, in the Micro Engineering Dynamics Automation Laboratory (MEDAL) at the University of Calgary: they have supported me in many respects during the project. I am also very grateful to Cathie Heys for her support during my writing of the thesis, making it more grammatically sound.

Vishash Sharma

TABLE OF CONTENTS

LIST OF TABLES

LIST OF FIGURES

LIST OF SYMBOLS, ABBREVIATIONS AND NOMENCLATURE

Symbols	Definition
ANFIS	Adaptive Neuro Fuzzy Inference System
MEDAL	Micro Engineering Dynamics Automation Laboratory
AE	Acoustic Emission
FE	Finite Element
NDT	Non Destructive Testing
FRF	Frequency Response Function
MFL	Magnetic Flux Leakage
EMAT	Electromagnetic-Acoustic Transducers
EIS	Electrochemical Impedance System
CFD	Computational Fluid Dynamics
RTTM	Real-Time Transient Modelling
EMA	Experimental Modal Analysis
DAC	Data Acquisition System
FAM	Fuzzy Associative Memories
LSE	Least Square Estimation
IMP	Integrity Management Plan
SCC	Stress Corrosion Cracking
GPR	Ground Penetration Radar
API	American Petroleum Institute
FFT	Fast Fourier Transform
DOF	Degree of Freedom
NPS	Nominal Pipe Size
[M]	Mass Matrix
[C]	Damping Coefficient Matrix
[K]	Stiffness Matrix
[X(s)]	Displacement matrix
[H(s)]	Transfer Function
ω	Excitation Frequency
ζ	Modal Damping Ratio
ϕ	Modal Transfer Function
$\{P\}$	Eigenvector Matrix
i, j, k	Matrix Indices
m	Modal Mass
{u}	Normalised Mass Matrix
ω_n	Natural Frequency

ANN	Artificial Neural Network
RMS	Root Mean Square
MF	Membership Function
RMSE	Root Mean Squared Error
L/min	Litres per Minute
kPa	Kilo -Pascal
N	Number of samples
F	Periodic Force
ADC	Analogue to Digital Converter
S	Auto Spectrum
ODS	Operating Deflected Shapes
ρ	Mass density
p	pressure
u	Displacement vector
f^B	Body force vector
v	Velocity vector
n	Neumann boundary condition
α	Penulty factor
β	Bulk Modulus
δ	Differential operator
V_f	Fluid Boundary
S_f	Neumann Boundary
S_u	Dirichlet Boundary

CHAPTER 1: INTRODUCTION

A pipeline is a conduit made from pipes connected end-to-end for long distances and is used to transport oil, gas or other fluid. Pipeline networks are the most economical and safest means for the transport of oil and gas. The distribution of oil or gas in pipelines must occur under safe and reliable conditions; however, the pipeline may be damaged by environmental and weather conditions, as well as aging or pressure changes [Barradas et al., 2009]. Pipelines are designed to support impacts or internal overpressure, but occasionally pressure surges may lead to line breaks and leaks. In some cases, pipelines are underground or under the sea. To further complicate the scenario, the fluid or gas in transport does not operate under steady-state conditions, making it even more difficult to perform a fault inspection. Additionally, small leaks are harder to detect, because they are a consequence of corrosion and aging in the pipeline.

1.1 Motivation

Pipelines are among the major factors affecting the economies of each and every nation. Canada has been endowed with an abundance of hydrocarbon natural resources, which started the development of the Canadian pipeline system nearly 60 years ago. Today, that system comprises about 585,000 kilometres of pipelines within Canada [Murray et al., 2011].

There have been some major incidents of pipeline failure in the recent past, such as BP pipeline failure and Enbridge pipeline incidences. The pipeline industry relies on non-destructive testing (NDT) methods, such as penetrant, ultrasonic and electromagnetic testing, to detect and characterise the degradation and damage. Thousands of kilometres of pipelines are examined using electromagnetic and ultrasonic methods. The developers of NDT methods are challenged

by the pipeline environment when implementing the most effective measurement technology to monitor the pipeline health. Inspection tools must meet measurement specifications for long distances and negotiation of tight bends.

In-line inspection equipment is commonly used to examine a large portion of long distance transmission pipeline systems that transport energy products from well gathering points to local distribution companies. A piece of equipment that is inserted into a pipeline and driven by product flow is called a pig (pipeline inspection gauge). Pigs that are equipped with sensors and data recording devises are called intelligent pigs.

Some pipelines have excessive physical or operational barriers that prevent the use of available pigs, and such pipelines are termed as unpiggable. Pipelines can contain dirt, debris and deposited solids such as salts. Solid deposits can form an adherent solid barrier that affects pig (pipeline inspection gauge) passage, adversely impacts the accuracy of measurement and can be very difficult to remove. Crawler technologies are being implemented that overcome these barriers, sometimes with alternative inspection methods [Barradas et al., 2009]. After internal inspection, the details of the anomalies are commonly quantified after excavation using more conventional NDT methods.

Magnetic flux leakage can be implemented to overcome such physical barriers while adequately detecting the corrosion in the pipeline. However, there is a limitation to the magnetic flux leakage method when used for seamless pipelines. For example, pipelines constructed of seamless pipe can present unique log interpretation problems, especially for magnetic flux leakage tools [Battelle et al., 2006]. For ultrasonic inspection tools, the inclusion content is an important factor and can vary significantly from joint to joint, with one joint permitting a high quality inspection and the next being not inspectable [Battelle et al., 2006].

In terms of implementing an integrity management plan (IMP), the first step is the evaluation of potential threats that exist in the pipeline or segment being considered. Once credible threats are established, appropriate integrity assessment methods are then selected. Where instrumented non-destructive tools are appropriate, several preliminary aspects must then be considered; otherwise, alternative integrity assessment methods that may include pressure testing and direct assessment are required.

Apart from regulatory monitoring and requirements by local legislation in relation to pipeline systems, it is also necessary to develop an intelligent system to monitor damage to pipeline systems from leakage or failures, considering the all possible causes of pipeline failure and pipeline environment conditions, so that measurements are accurate and predictions are reliable. In fact, it is the responsibility of competent professionals all around the world to put effort into devising an intelligent monitoring system that cannot only counter the unfortunate events of failure, but can also predict the health of pipeline, so that preventive maintenance can be carried out in a timely fashion.

1.2 Objectives

It is difficult to use conventional NDT methods to detect damage, such as the loosening of bolted connections, in a complex network of pipes, since there is no obvious material loss associated with the damage, and the material of the pipeline is naturally discontinuous at its joint boundaries. The vibration-based damage detection methods that are used, utilize the change in the vibration characteristics of a pipeline, such as natural frequencies, mode shapes and frequency response functions (FRFs), to detect the locations and extent of damage in the pipeline structure, overcoming the disadvantages of conventional NDT methods.

Once a database on the variation of dynamic parameters is available for known cases of pipeline failures, a novel architecture based on an artificial intelligent methodology can then be developed by training the system (tuning the prediction parameters for the health monitoring of the pipeline) to acquire the artificial intelligence to predict the condition of the pipeline, when it is put under test against the dynamic variable database generated by the fusion of the vibro-acoustic signals obtained from acoustic sensors and accelerometers installed on an operational pipeline.

The focus of this research is the development of a pipeline monitoring scheme to predict damage to pipelines, due to corrosion and leakage by utilising a three-step process:

i. Investigation of Pipeline Conditions through Changes in Dynamic Properties based on Experimental Modal Analysis

To investigate the changes in dynamic properties due to changes in pipeline conditions, an experimental modal analysis (EMA) was performed in the laboratory using a small-scale experimental setup for an empty pipeline, a pipeline with water flow, a pipeline with corrosion with water flow, and a leaky pipeline. Accelerometers and acoustic emission sensors were employed to obtain dynamic parameters such as FRFs, natural frequencies and time-domain signals.

Most pipeline damage, such as cracks, fatigue and corrosion, is manifested as a reduction in stiffness. As a function of structural stiffness and mass, the linear vibration characteristics of a structure, including the natural frequencies and mode shapes, change due to the structural stiffness reduction. Damage at different locations to different degrees can lead to different patterns in the changes of the natural frequencies and mode shapes.

Hence, one can use the changes in dynamics to detect the extent of damage by solving an inverse problem.

ii. Investigation of Pipeline Conditions through Changes in Dynamic Properties based on Finite Element Analysis

A finite element (FE) analysis was done for the pipeline for the operating conditions that were used during the EMA in the laboratory, in order to estimate the variation in the dynamic characteristics of the pipeline in various operating conditions of the pipeline.

iii. Development of Pipeline Monitoring Scheme by Implementing an Adaptive Neuro Fuzzy Inference System

An adaptive neuro fuzzy inference system (ANFIS) has the characteristics that allow us to solve problems by providing learning ability, parallel operation, structural knowledge representation and better integration with other design control methods.

The ANFIS-based pipeline monitoring scheme was trained to tune the decision parameters to predict an event of leakage or corrosion. The dynamic parameters, such as variation in FRFs, natural frequencies and time-domain signals from acoustic emission sensors were used as input variables to train the ANFIS-based pipeline monitoring scheme. The decision parameters or consequent parameters of the ANFIS-based pipeline monitoring are basically the resultant output of the scheme to predict the health of the pipeline. The trained pipeline monitoring scheme is capable of predicting the condition of

a pipeline based on the unknown dynamic response obtained through the fusion of acoustic emission and accelerometer sensors.

The datasets for the variations in dynamic parameters from the EMA and FE analysis for the same operating conditions of the pipeline ensures the reliability of datasets, which were then used to develop the ANFIS-based pipeline monitoring scheme.

The design and development of the pipeline health monitoring scheme was based on actual data obtained from EMA and FE analysis for the dynamic parameters of the pipeline for the same operating conditions of the pipeline. The ANFIS-based pipeline monitoring scheme then evolve using the estimated variations in dynamic parameters and fusion of time-domain signals from acoustic emission sensors, ensuring the robustness of the ANFIS-based system for monitoring pipeline health.

1.3 Organisation of Thesis

The organisation of the thesis is described in the following paragraphs.

Chapter 2 presents various methods implemented for pipeline monitoring, from those used by the Roman Empire and even earlier to those that currently used in the world of pipeline networks. The main features, including the limitations, are discussed for each monitoring system.

Chapter 3 gives the details on the EMA and FE analysis of a pipeline. The experimental setup for the EMA to obtain the responses of a pipeline in the frequency and time domains is described. The methodology for and results from the FE analysis are then presented. The comparison of the results is given for both the cases i.e. responses from EMA and FE analysis for the same set of operating conditions of the pipeline.

Chapter 4 depicts the training and testing of the ANFIS-based pipeline monitoring scheme. Results and discussions are presented in two parts and are followed by a summary of the results. First, the training of the ANFIS-based scheme is described; and, the results of the predictions made after testing the ANFIS architecture are given. This is followed by detailed discussions on the predictions made by the ANFIS system.

Chapter 5 provides conclusions, describing the uniqueness of the proposed methodology and the assumptions and limitations. The last part of this chapter gives the details on proposed future work related to pipeline monitoring.

CHAPTER 2: LITERTURE SURVEY

Thousands of years ago – long before the Romans – the Chinese were making use of timber to construct primitive interlinked conduits/pipelines for the transportation of irrigation water [Ryder et al., 2008]. Throughout history, pipelines have consistently been the most efficient mass transportation method for liquids and gas. However, it is only in the last century that the pipeline design, construction and operation have affected the evolution of the pipeline into a safe and reliable method of transporting vast quantities of hydrocarbons over long distances.

With increasing public awareness and concern for the environment, recent pipeline leak incidents have shown that the cost to a company can be far more than downtime and cleanup expenses [Ryder et al., 2008]. As more stringent statutory regulations are introduced in developed countries, cost-effective and reliable leak detection systems are in demand.

This chapter describes the causes of failures in pipelines and reviews various methods of pipeline monitoring. The flaws in a pipeline can be divided broadly in two categories: technological and manufacturing flaws, and operational flaws. The following manufacturing flaws are hazardous for further operations of a pipeline [Shcherbinin et al., 2011]:

- Areas of high concentrations of non-metallic inclusions, different types of voids, rolling tears, laps, blisters and cracks, leading to the nucleation and development of deep corrosion pits and blowholes;
- The cracking of a pipe wall in the areas of exposed segregation and delamination zones of the metal of a pipe;

- The nucleation of various cracks in the zones of the thermal influence of weld joints and the after bending of sheet edges;
- Poor quality steel, leading to the sharp thinning of the wall in the lower part of a pipe under the action of an aggressive medium (the rates of uniform overall corrosion and pit development vary from 0.15 to 1.5 mm/yr.); and,
- High internal stresses, especially in zones of high tensile stresses.

The main causes of the appearance of such flaws are non-optimal and non-uniform chemical compositions of pipe steels, poor quality rolling, non-optimal and outdated manufacturing technology for pipes, the scatter of process parameters, the violation of technical discipline, and the absence of control of the results of intermediate technological operations.

Technological and manufacturing flaws are subsequently manifested to a degree during the operation of pipelines. During the construction and operation of pipelines, flaws of the following types appear in pipes [Shcherbinin et al., 2011]:

- Uniform (overall) corrosion, leading to a change in the thickness of a pipe wall or the dimensions of a pipe.
- Pitting, i.e. deep point corrosion damage flaws that lead to the appearance of blowholes in a pipe wall. If corrosion damage covers a large area, this corrosion process is called pit damage.
- Cracking of pipe steels under the action of tensile stresses in a corrosive medium (stress corrosion cracking, SCC). In the case of damage by SCC, the propagation of cracks in the metal proceeds under the simultaneous action of mechanical tensile

stress and corrosion. Cracks propagate perpendicularly to the direction of tensile stress under small external strains of the metal.

- Flaws associated with the construction of pipelines, namely damage of insulating protective coatings, strain of pipe walls (warpage, indentations, corrugations and other distortions in the shape of a pipe), and incomplete fusions in weld seams (pores, shells, slag inclusions, cracks).
- Operational flaws that occur due to variable mechanical loads (cyclic and vibrational), leading to the cracking of the metal of a pipe wall in the zone of a joint with shutoff valves and pipeline tees and also in a zone with abnormal seams.
- Flaws that occur due to seasonal movements of soils, namely the appearance of stressed areas in the zone of the buckling of a pipe with the subsequent cracking in the zone of field (annular) weld seams.

SCC is a special hazard and creates the complications during detection with NDT methods. In the metal of a pipe damaged by the SCC mechanism, most of the corrosion cracks at the centre of damage are at the development stage, and only approximately 30% of them are stabilised. However, many stabilised corrosion cracks still remain as hazardous flaws; and the damage, which may be initiated again and pass into the category of crack development during the tests of a gas pipeline or other accompanying activities, is concentrated at the crack tips.

The retesting of pipelines (i.e. the creation of an internal pipeline pressure exceeding its operational value) is sometimes inefficient, as small product leaks can remain undetected in the case of the underground location of a pipeline. Moreover, retesting is undesirable, as it may lead to the coalescence of developing cracks with the formation of a through flaw in a pipe or to the

activation of cracks that are stable under operational pressures. Among the factors that promote the destruction of the steel pipes that are under operation are as follows [Shcherbinin et al., 2011]:

- Increased temperature of a pipeline,
- Presence of insulation flaws,
- Manufacture of pipes from a steel hardened by controlled rolling,
- Presence of non-metallic inclusions in steel,
- Presence of internal residual stresses in pipes and the application of external tensile stresses,
- Action of cyclic and seasonal temperature and strain loads, and
- Retesting of pipelines.

2.1 Causes of Pipeline Failures

2.1.1 External Corrosion

The outside surface of a carbon steel pipeline buried in a soil or water environment will corrode. Usually, there is no corrosion allowance for increasing the thickness of a pipeline to specifically account for the external corrosion of pipelines. Hence, the outside surface of the pipeline may see excessive corrosion, unless it is protected with a coating (e.g. coal tar).

2.1.2 Internal Corrosion and Erosion

Petroleum pipelines carrying oil, gas or petroleum products are not immune to corrosion and erosion, although the hydrocarbon fluids themselves are not corrosive. However, the presence of corrosive constituents, such as water, salts, carbon dioxide (CO_2) and hydrogen

sulphide (H_2S) or even abrasive material, such as sand, contribute largely to internal corrosion and erosion [Shawki et al., 2002]. Failures due to internal corrosion and erosion have been noticed in petroleum production and transportation pipelines. The failure cases have been very diverse in nature, due to a great number of reasons that can result from the design stage, including material selection, to the basic requirements of operation, testing and maintenance.

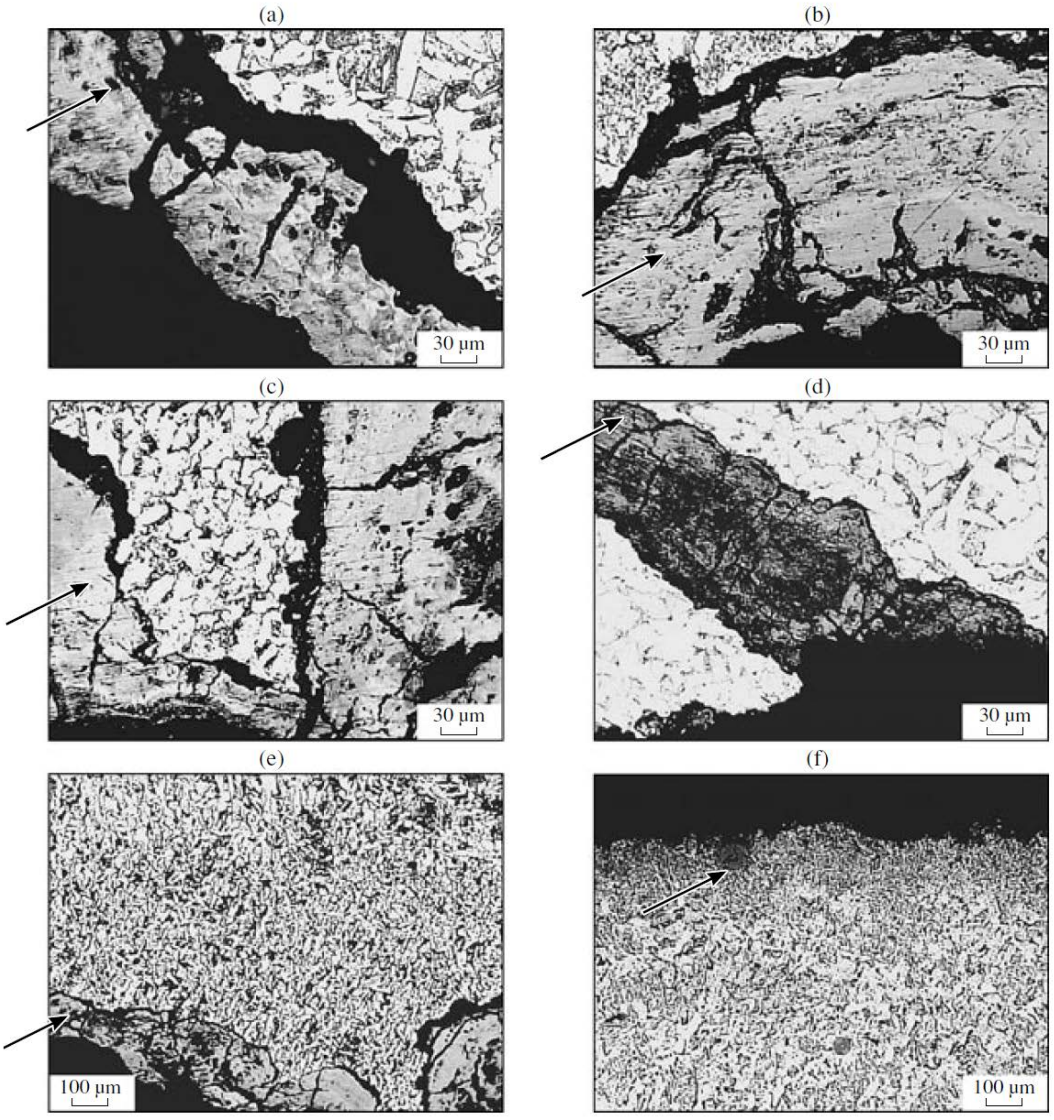

Figure 2.1: Micro sections of corroded areas at the inner: a, b, c, d - welded joint; e - base metal; f - outer faces of the pipe wall. Arrows indicate oxides. [Andriashin et al., 2006]

2.1.3 External Damages

External damage in the form of dents and gouges, which are deformations in the wall of a pipe, serve as crack initiation sites. Dents typically result from a purely radial deformation, whereas a gouge has a component of deformation along the surface of the pipe. For example, a pipe impinging on a rock results in a dent. If the pipeline also slides on the rock, a dent with a gouge is created. Third-party external damage, usually caused during construction and excavation, is a common cause of gouges. A gouge normally results in a highly deformed, work hardened surface layer and may involve metal removal [Diaz et al., 2001]. Mechanical damage can result in the immediate failure of the pipe, delayed failure or no failure over the designed life of the pipeline.

2.2 Review of Pipeline Monitoring Methods

Structural and functional monitoring can significantly improve pipeline management and safety. Regular monitoring with parameters featuring the structural and functional conditions of the flow line can help prevent failure, detect a problem and its position and undertake maintenance and repair activities in time [Inaudi et al., 2013]. Thus, safety is increased, maintenance cost optimised and economic losses decreased. Typical structural parameters to be monitored are strain and curvature, while the most interesting functional parameters are temperature distribution, leakage and third-party intrusion. Since flow lines are usually tubular structures with kilometric lengths, structural monitoring of their full extent is an issue in itself.

2.2.1 Manual Detection

Pipeline regulations and codes require operators to maintain and inspect their pipelines to appropriate standards. Maintenance of a pipeline is an essential part of maintaining the overall integrity of the entire pipeline system. Therefore, pipelines are routinely inspected and monitored. A traditional leak detection method is the use of experienced personnel who walk along a pipeline, looking for unusual patterns near the pipeline, smelling substances that can be released from the pipeline and listening to noises generated by product escaping from a pipeline hole. The results of such a leak detection method depend on the individuals' experience and whether a leak develops before or after inspection. Another leak detection method is the use of trained dogs that are sensitive to the smell of substances released from a leak.

Patrolling by aircraft and road and by walking along pipeline routes can check for unwanted or unplanned excavations around the pipeline and encroachment of population/buildings. Sub-sea pipelines are regularly surveyed using a survey boat and associated equipment to check the pipeline route [Hopkins et al., 2002].

Manual inspection methods are mainly limited by accessibility to the operating pipeline; however, most of the parts of a pipeline are usually buried. The use of an airplane or a helicopter is a very expensive proposition for an aboveground pipeline.

2.2.2 Hardware-Based Detection

Pipeline management presents challenges that are quite unique. Their long length, high value, high risk and often difficult access conditions require continuous monitoring as well as optimization of maintenance intervention. The main concern for pipeline owners comes from

possible leakages that can have a severe impact on the environment and put the pipeline out of service for repair.

There is a limited arsenal of tools available for pipe detection; and, each technique has advantages and shortcomings. The selection of a hardware system should be optimized to accurately detect and locate leaks during steady-state, shut-in and transients operations for onshore and offshore pipelines of all sizes. The different methods can be deployed in parallel in order to ensure the highest possible reliability.

2.2.2.1 Portable Devices

Local methods of inspection with NDT instruments (ultrasonic, eddy current and magnetic) include strain gauging and acoustic systems for the detection of leaks and geodetic measurements. These monitoring methods are performed with systems of contact transducers that are connected to a supervisory control centre by different telecommunication channels, including satellites. Transducers for temperatures, corrosion, stress levels, strains, leaks and detection of sagging of underwater passages may be used. Some of the portable devices are described in the following paragraphs.

Infrared Thermography

Some leaks can be detected through the identification of temperature changes in the immediate surroundings. Infrared thermography is used to detect hot water leaks. This method's equipment can be used from moving vehicles, aircraft or as a portable system in ground cover. Several miles or hundreds of miles of pipeline per day can be inspected [Weil et al., 1993] using the infrared thermography technique.

The detection and analysis process involves the use of the infrared thermography radiometric imager to measure, display and store a temperature image or map. One of the perceived limitations of infrared thermography is that it is too cold to use this technique in temperate climates, since there is rarely the extreme solar exposure that enables successful use of thermographs to detect pipeline faults.

Ground Penetrator Radar

Ground penetrator radar (GPR) has a long and sometimes checkered history in pipeline monitoring [Cist et al., 2001]. Although it is perhaps the best general pipe locator available, it is often mistakenly assumed to be a silver bullet. GPR uses a radar transmitter and receiver to accurately pinpoint buried pipeline leaks without digging. The leaking substances can be 'seen' at the source by the radar via the changes in the surrounding soil's electrical parameters. A colour graphic data format then displays the leak [Graf et al., 1990; Hennigar et al., 1993].

GPR is not, however, able to detect pipeline faults in highly conductive clay and silty soils. Sometimes clutter from other objects can obscure pipes. Most commonly, subtleties in processing and interpretation mean that less skilled surveyors may fail to detect pipes that would otherwise be clearly resolved. This means that GPR can never be 100% successful at locating pipes. However, the expansion of the GPR's capabilities into fully three-dimensional images has made detection much more robust, and interpretation much simpler. This means that GPR is really now entering into a new phase of capability, making it far more versatile than ever before.

Gas Sampling

If the product inside a pipeline is highly volatile, a vapour monitoring system can be used to detect the level of hydrocarbon vapour in the pipeline surroundings. This is usually done

through gas sampling; the methods of which typically use a flame ionisation detector housed in a handheld or vehicle-mounted probe to detect methane or ethane. The primary advantage of gas sampling methods is their sensitivity to very small concentrations of gases, allowing for the detection of even very tiny leaks [Sivathanu et al., 2001]. The technique is also immune to false alarms. The disadvantages of the technology are that detection is very slow and limited to the local area from which the gas is drawn into the probe for analysis. Therefore, the cost of monitoring long pipelines using gas sampling methods is very high.

Soil Monitoring

In soil monitoring methods, the pipeline is first injected with a small amount of a tracer chemical, which seeps out of the pipe in the event of a leak. This is detected by dragging an instrument along the surface above the pipeline. The advantages of this type of method include very low false alarms and high sensitivity. However, these techniques are very expensive for use in monitoring, since trace chemicals have to be continuously added to the natural gas. In addition, it cannot be used for detecting leaks from pipelines that are exposed.

Fibre-Optic Sensor

The ability to measure temperatures and strains at thousands of points along a single fibre is particularly relevant for the monitoring of elongated structures, such as pipelines. Sensing systems based on Brillouin and Raman scattering are used to detect pipeline leakages, verify pipeline operational parameters, and prevent failure of pipelines installed in landslide areas [Inaudi et al., 2007].

Recent developments in distributed fibre sensing technology allow the monitoring of 60 km of pipeline from a single instrument and of up to 300 km with the use of optical amplifiers. New application opportunities have demonstrated that the design and production of sensing cables is a critical element for the success of any distributed sensing instrumentation project.

Although some telecommunication cables can be effectively used for sensing ordinary temperatures, the monitoring of high and low temperatures or distributed strains presents unique challenges that require specific cable designs. This contribution presents advances in long-range distributed sensing and novel sensing cable designs for distributed temperature and strain sensing. Fibre-optic systems have the disadvantage of being difficult to retrofit to an existing line. In addition, damage to the sensing cables can render a system non-functional [DNV et al., 2006].

Pressure Wave Detectors

Another important aspect of oil transportation is the interface piping systems for transmission to and from ships. Research has been conducted on effective methodology for safe monitoring of ships' piping systems. Detection of ship pipeline leakage is one of the most important techniques to be developed, as it can help to prevent damage to the ship, which would prevent it from safe operation [Peng et al., 2010; Xie et al., 2010].

The negative pressure wave technique is an effective method for fluid leakage detection and location. However, it is difficult to distinguish the source that has led to the fluid pressure drop. In order to solve the problem, the wavelet transform algorithm has been adopted to define inflexion of the negative pressure wave when it propagates along the pipe. The wavelet threshold noise technique has been used to separate the characteristic inflexion of a negative pressure wave when calculating the leaking position.

Pure frequency domain analysis is a newly developed and proposed method for leak detection in pipelines [Guo et al., 2008; Yang et al., 2008]. In the research studies, transient signals were generated by the sharp closure of a valve from the small constant opening. The genetic algorithm was integrated into the method to calibrate the location and quantity of leakage. There are two main distinctions with this method: the boundary conditions are not constrained, and the leak detection is analysed in the entire frequency domain without calculation of the inverse Fourier transformation of any point. The proposed leak detection method shows potential for being applied to the pipeline system with a single leak.

Magnetic Method

The integrity of pipelines is monitored using intelligent inspection tools (i.e. intelligent pigs). The material state of a pipeline is assessed by determining localized magnetic flux leakage (MFL). The MFL technique is performed by magnetizing the steel pipe near the saturation flux density and then detecting a local flux leakage caused by surface anomalies.

The effect of a magnetic field on the hydrogen absorption and corrosion behaviors of API X80, X70, and X52 line pipe steel grades were analyzed [Roubidoux et al., 2011]. The purpose of this work was the determination of the fundamental mechanisms by which a magnetic field alters the corrosion and hydrogen absorption behaviors of these steels. The conditions that a pipeline experiences in the field were simulated in a laboratory setting using permanent magnets and cathodic potentials. Two permanent magnets of one tesla each were used to simulate the remnant magnetic field present in a pipeline in order to alter a pigging operation. The cathodic protection return currents were simulated by polarizing the working electrode (steel sample) to cathodic potentials. Using experimental electrochemical methods and theoretical modeling, it

was found that a magnetic field changes the passivation behavior, shifts the corrosion potential to more anodic potentials and increases the total absorbed hydrogen content.

This approach provides an accurate measurement of wall thickness only at the point of physical contact and not along the circumference of the pipe. In principle, this technique could be adapted for non-contact measurements using electromagnetic-acoustic transducers (EMATs). However, the accuracy of the measurement degrades with thicker objects, due to the particular transducer design: it was specifically designed for thinner materials. With a properly designed transducer, the accuracy of the thickness measurement can be better than 1%. This kind of accuracy is simply not possible using the existing devices on the market, because they require prior knowledge of the material, which is not available for a natural gas pipeline that is degraded from use over a period of time.

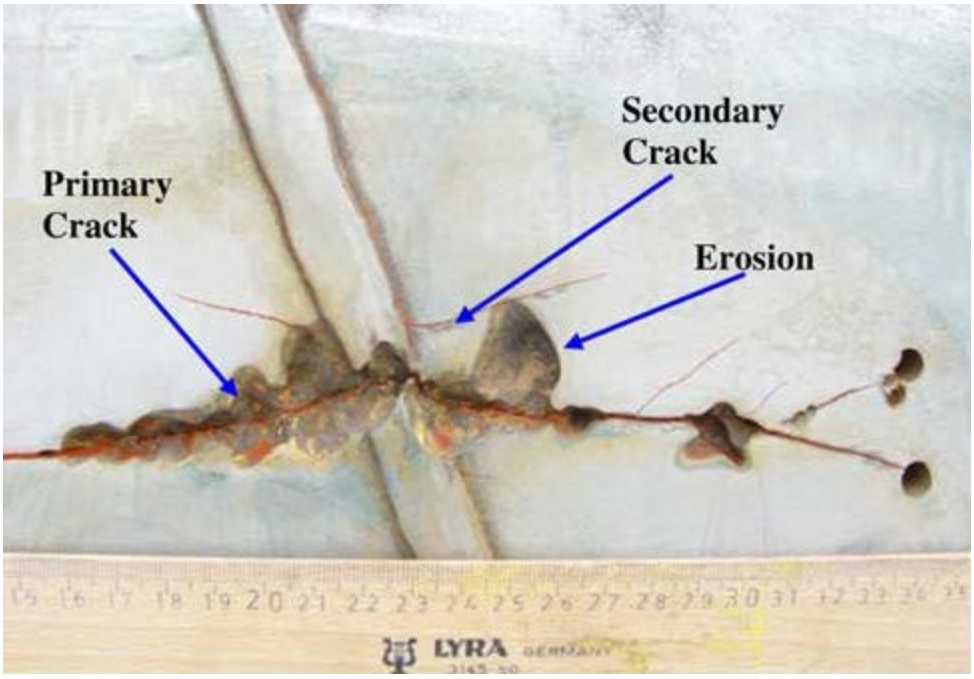

Figure 2.2: Longitudinal primary and secondary cracks on the outside surface as revealed by magnetic particle testing [Lobley et al., 2009]

Eddy Current Method

The eddy current inspection technique is based on the principle of electromagnetism. When an alternating current is applied to the conductor, a magnetic field develops in and around the conductor. If another electrical conductor is brought into close proximity to this changing magnetic field, the eddy current is induced in this second conductor. Eddy currents are induced electrical currents that flow in a circular path.

The major limitation of the eddy current inspection method is that only conductive materials can be inspected. Moreover, the surface must be accessible to the probe; and, surface finish and roughness may interfere. Reference standards are needed for the setup, and the depth of penetration is limited.

Electrochemical Impedance Spectroscopy

External corrosion of the pipeline surface occurs via a chemical attack from surrounding media. Electrons held by the metal are transferred to electrolyte species during electrochemical oxidation-reduction half-cell reactions. Metal dissolution is the anodic reaction; and, iron, which is the major component in pipeline metal alloys, is oxidised to ferrous ions.

In situ analysis of an electrochemical system is often performed using electrical methods, since the electrical response can be attributed to the kinetics of the surface reactions. Electrochemical impedance spectroscopy (EIS) is a frequency response technique where a sinusoidal potential is applied to an electrochemical system, and the responding sinusoidal current signal is measured [Jeffers et al., 1999]. Typically, a spectrum is generated by sweeping a range of frequencies and measuring the impedance at each point. EIS has been shown to be a sensitive technique for monitoring non-stationary behaviour and has been proven to be ideal for

exploring corrosion systems where film formation contributes to reaction kinetics and transport properties over time.

The major disadvantage of EIS is that it requires specialist knowledge for application in the field and that the obtained data requires a detailed analysis for the determination of the rate of corrosion. Moreover, the cost of the data acquisition equipment is high.

2.2.3 Software-Based Monitoring Schemes

Unlike hardware methods, software leak detection methods use instrumentation to measure different internal parameters of a pipeline. The more parameters that are used for a particular software method, the more accurate are the results. The most common forms of software leak detection include balancing systems, pressure analysis and the real-time transient method [Odusina et al., 2008].

Based on a flow model using the computational fluid dynamics (CFD) technique, it is possible to predict the flow behaviour and measure flow rates in case of leakage in a pipeline. This method can give the location of the leak by analysing any deviations from the baseline. However, the gradient intersection is dependent on instrument sensitivity to accurately report leaks and locations. Smaller leaks tend to be ignored if they do not show a significant deviation from the set baseline, and this is unacceptable in the industry. This method is not able to provide an estimate of the leak magnitude.

The most sensitive and accurate software leak detection method is real-time transient modelling (RTTM), which involves the simulation of a pipeline's internal conditions by using advanced fluid mechanics and hydraulic modelling [Odusina et al., 2008]. It combines the conservation of momentum calculations, conservation of energy calculations, a continuity

equation and numerous flow equations. The RTTM approach is able to predict the size and location of leaks by comparing the measured data for a segment of pipeline with the predicted modelled conditions. The pressure-flow profile of the pipeline is calculated based on the measurements of the pipeline's inlet and outlet. The two profiles are later overlapped, and the location of the leak can be identified as the point of intersections.

2.2.4 Vibration-Based Pipeline Monitoring

EMA (experimental modal analysis) has grown in popularity since the advent of the digital Fast Fourier transform (FFT) spectrum analyser in the early 1970s. Today, impact (or bump) testing has become widespread as a fast and economical means of finding the modes of vibration of a machine or structure [Schwarz et al., 1999]. The overall structural response is, in fact, the summation of resonance curves. In other words, the overall response of a structure at any frequency is a summation of responses due to each of its modes. It is also evident that close to the frequency of one of the resonance peaks, the response of one mode dominates the frequency response.

If EMA is performed on a pipeline for different operating conditions, such as corrosion and leaks, the overall dynamic response of the pipeline changes. The frequency response functions (FRFs) and time-domain signals are recorded for analysis, in order to arrive at the resulting predictions of the pipeline. Accelerometers and acoustic emission sensors are utilised to gather the data for the FRFs and time-domain signals emanating from the pipeline

Vibro-Acoustic Sensors

Due to the advent of new technology with the development of acoustic sensors, much work has been done on the monitoring of pipeline health using acoustics waves [Sinha et al., 2005]. This technique can be used to measure pipeline walls, detect gas contamination, measure flow, and detect gas leaks and structural defects in the pipe.

Acoustic wave sensors are so named because they utilise a mechanical (or acoustic) wave as the sensing mechanism. As the acoustic wave propagates through or on the surface of a material, any changes to the characteristics of the propagation path affect the velocity and/or amplitude of the wave. Changes in velocity can be monitored by measuring the frequency or phase characteristics of the sensor and can then be correlated to the corresponding physical quantity that is being measured [Bill et al., 2001].

Due to the limitation of the detection range, it is usually necessary to install many sensors along a pipeline. These sensors detect acoustic signals in the pipeline and discriminate leak sounds from other sounds generated by normal operational changes. When a leak occurs, noise is generated as the fluid escapes from the pipeline. The wave of the noise propagates with a speed determined by the physical properties of the fluid in the pipeline. Acoustic detectors detect these waves and, consequently, the leaks.

Acoustic Emission Techniques

Among the methods of operational monitoring and technical testing, the acoustic emission technique has recently attracted a great deal of attention. One of the advantages of acoustic emissions is their relatively long range. A technique has been suggested for calculating parameters of acoustic emissions pulses propagating in a main pipeline as a function of

parameters of developing cracks, pumped products, pipeline dimensions and distances to detector positions [Budenkov et al., 1999].

One of the important tasks when utilising this technique is the calculation of the limiting distance for the detection of acoustic emission pulses and nominal dimensions of the detected cracks. These calculations are based on the impedance properties of the pipeline material and the product in the pipeline. The limiting distance at which an acoustic emission signal can be detected is a function of a growing crack, with due account taken of the properties of the pumped products, the ambient conditions, the dimensions of the pipeline and estimates of the minimal dimensions of cracks detectable in the acoustic emission testing of accident-prone sections of pipelines [Budenkov et al., 1999].

2.3 Limitation of Existing Pipeline Monitoring Methods

The limitations with the existing methods can be summarised as follows:

- Manual pipeline monitoring methods are limited by a lack of accessibility, due to the fact that most portions of a pipeline are buried and that the use of aircraft is very expensive.
- The accuracy of MFL decreases for thicker materials; and, as with the eddy current method, MFL is limited to only magnetic materials.
- Acoustic sensors suffer from a limited detection range.
- Fibre-optic systems have the disadvantage of being difficult to retrofit to an existing line. In addition, damage to the sensing cables can render a system non-functional.

- EIS is a very sensitive method with respect to data analysis, and it needs to be handled by very highly skilled personnel, which is a cost factor to be considered while utilising this method.
- Software-based methods are unable to predict small leaks.

In view of the above limitations, it is quite evident that tremendous efforts are needed for the development of an intelligent methodology that cannot only detect the fault, but also locate it accurately. This paper is an effort to present an inherently intelligent methodology in this direction.

As a first step to get the dynamic response of the pipeline, a finite element (FE) analysis approach was developed for solving time-dependent fluid/structure interaction problems. Using FE analysis, a useful database is provided by estimating the dynamic parameters in each case of failure. The variation in values of the parameters, such as FRFs and mode shape displacements, in each case are fed to an adaptive neuro fuzzy inference system (ANFIS) architecture with known failures, and the adaptive parameters are optimised. This is called the training phase of the ANFIS. After the training of the monitoring scheme, the ANFIS-based architecture is ready to analyse the response from the signals obtained from acoustic sensors and accelerometers.

CHAPTER 3: EXPERIMENTAL MODAL AND FINITE ELEMENT ANALYSES OF PIPELINE

The first step in developing the pipeline health monitoring scheme based on vibro-acoustic data from the pipeline of interest was the generating datasets for training and verification the adaptive neuro fuzzy inference system (ANFIS) based pipeline monitoring scheme. The training datasets were generated by finite element (FE) analysis, and the testing datasets were generated by performing experimental modal analysis (EMA) on a pipeline assembly in the laboratory to collect the datasets for dynamic properties of the pipeline.

The objective was the capture of dynamic parameters for the pipeline, like frequency response functions (FRFs), natural frequencies and time-domain response signals for different operating conditions (i.e. empty pipeline, pipeline with fluid flow, corroded pipeline with and without fluid flow, and leaky pipeline with and without fluid flow). Frequency-domain response signals were obtained mathematically from time-domain response signals.

EMA is a systematic method for the identification of the modal parameters of a structure, which generally include natural frequencies, modal damping and mode shapes. In experimental modal testing, the structure is excited with a measured force at one or more points, and the response is determined at these points. Using these sets of data, the modal parameters are determined, often by the use of multidimensional curve-fitting routines on a digital computer.

Basically modes (or resonances) are inherent properties of a structure. Resonances are determined by the material properties (mass, stiffness, and damping properties) and boundary conditions of the structure. Each mode is defined by a natural (modal or resonant) frequency, modal damping and a mode shape. If either the material properties or the boundary conditions of

a structure change, its modes change. For instance, if mass is added to a vertical pump, it vibrates differently because its modes have changed.

At or near the natural frequency of a mode, the overall vibration shape (operating deflection shape) of a machine or structure tends to be dominated by the mode shape of the resonance. An operating deflection shape is defined as any forced motion of two or more points on a structure [Schwarz et al. 1999]. Specifying the motion of two or more points defines a shape. Stated differently, a shape is the motion of one point relative to all others. Motion is a vector quantity, which means that it has both a location and a direction associated with it. Motion at a point in a direction is also called a degree of freedom (DOF).

An experiment was performed to mimic the various operating conditions of a pipeline by constructing a small-scale water pipeline was constructed. Accelerometer and acoustic sensors were installed on nominal pipe size 25.4 mm (1”). EMA was performed for various pipeline operating conditions e.g. empty pipe, normal pipe with water flow, corroded pipe, corroded pipe with water flow, leaking pipe.

The experimental tests were performed in both the time and frequency domains. In the frequency-domain tests, the goal was detection of changes in the modal parameters, i.e. corrosion and leakage. The time-domain signals were captured for a long period for detection of corrosion and leakage along the pipe through the changes in the acoustic emission (AE) signals and accelerometer sensor signals.

3.1 Experimental Setup

The pipe used in the experiments was 25.4 mm (1”) with outer diameter of 33.0 mm (1.33”), schedule 40 carbon steel pipes. The experimental setup was constructed using 3 spools

of pipes. Each spool of pipe was 457 mm (18") in length. All the three spools were joined by threaded fittings, i.e. couplings, elbows and tees. The overall length of the pipe assembly was approximately 1500 mm. One end of the pipe was fixed using a clamp, and the other end was simply supported in the vertical direction. The experiment was performed in a laboratory at ambient temperature. The material properties of the carbon steel pipe are listed in Table 3.1:

Table 3.1: Material properties of carbon steel pipe

Young's modulus	20.35×10^{10} N/m$^{2.}$
Poison ratio	0.3
Thermal coefficient	11.06×10^{-6} /°C

The general setup is as depicted in Figure 3.1.

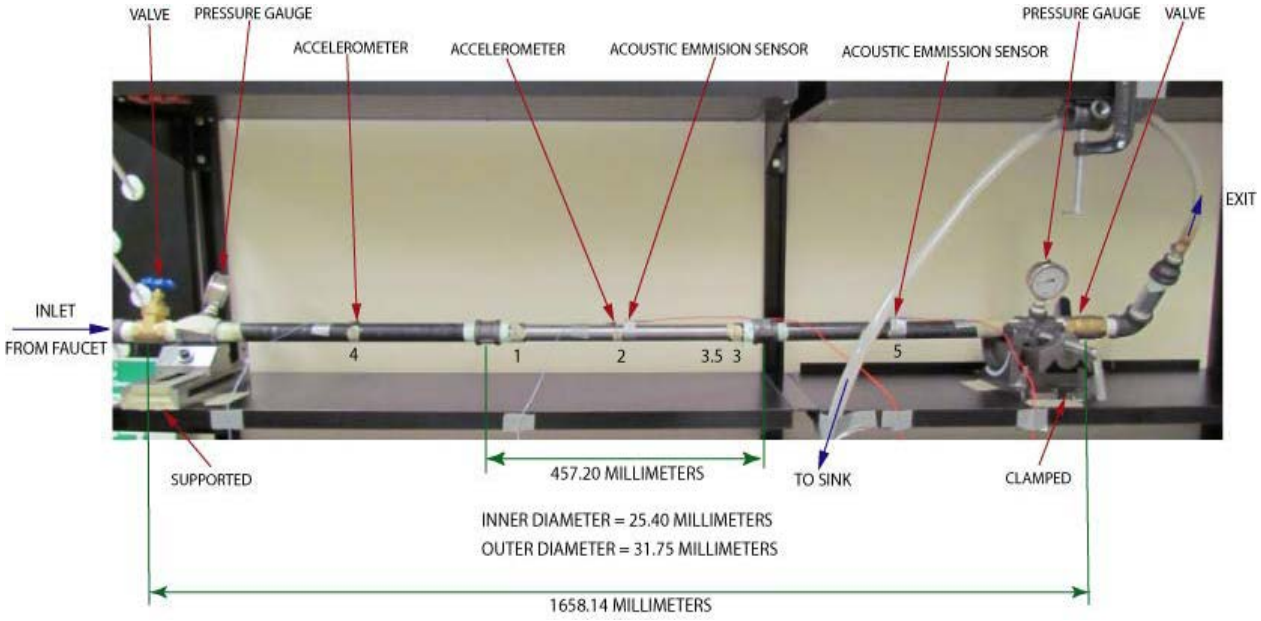

Figure 3.1: Experimental setup for EMA for a pipeline

Water from the faucets in the lab was used as the flowing medium in the pipe assembly. The isolation valves were installed at upstream and downstream of the water flow to control the flow and pressure parameters. Pressure indicators were installed upstream and downstream on the pipe to record the pressure of flow for various operating conditions of pipeline during the experiment. Measuring jars were used to record the flow rate and leakage rate.

3.1.1 Operating Conditions

3.1.1.1 Normal Pipe With and Without Flow

The pipeline assembly was made by connecting three pipe spools of 25.4 mm (1”) using threaded full coupling to ANSI B 16.11 with female threaded ends. The details of the full assembly are listed in Tables 3.2 and 3.3.

Table 3.2: Details of pipeline assembly

Total quantity of pipe spools	3
Connection types for the spools	Threaded couplings
Outer diameter of each pipe spool	33.0 mm
Inner diameter of each pipe spool	26.7 mm
Length of each pipe spool	457.0 mm

Table 3.3: Locations for accelerometers and excitation by the impact hammer

Accelerometer location	Excitation location	Distance from the simple support end (mm)
1	1	485
1	2	680
1	3	915
1	4	230
1	5	1140

The pressure gauges were mounted on the upstream and downstream of the pipeline assembly to record the pressure of flow. In some cases, the pressure gauge showed the recording as zero, which in fact indicates the free flow of water from laboratory faucets through the pipeline assembly without any obstruction to the sink. The pressure of the pipeline is controlled by adjusting the valves to maintain the desired pressure. The operating conditions for normal pipeline assembly are listed in Table 3.4.

Table 3.4: Operating conditions for normal pipe

Normal pipe with or without flow	
Pressure (kPa)	Flow rate (L/min)
0	0 (Empty)
0	10.21
207	7.38

3.1.1.2 Corroded Pipe With and Without Flow

To simulate corrosion in a pipeline, the middle spool of the pipe assembly was used as a test spool to mimic corrosion in a pipeline through the thinning of the pipe wall thickness by 1.6 mm by machining down the spool to the dimensions listed in Table 3.5.

Table 3.5: Details of pipeline assembly to simulate corrosion in a pipeline

Total quantity of pipe spools	3
Connection types for the spools	Threaded couplings
Outer diameter of each pipe spool except the middle pipe spool	33.0 mm
Inner diameter of each pipe spool except the middle pipe spool	26.7 mm
Thinned length of the middle spool to mimic corrosion	355.6 mm
Outer diameter of the thinned portion of the middle spool	29.8 mm
Length of each spool	457.0 mm

Table 3.6: Locations for accelerometer sensors and excitation by hammer in case of corrosion

Accelerometer location	Excitation location	Distance from the simple support end (mm)
1	1	485
1	2	680
1	3	915
1	3.5	910
1	4	230
1	5	1140

Table 3.7: Operating conditions for corroded pipeline assembly

Corroded pipe with or without flow	
Pressure (kPa)	Flow rate (L/min)
0	0
0	8.89
207	5.22

3.1.1.3 Pipe with Opening for Leakage with and without Flow

To mimic leakage in the pipeline assembly, the middle pipe spool was selected. A hole of 5.15 mm was drilled in the middle spool and then this hole was tapped to 6.35 mm with 20NC threads. A set screw was used to control the rate of leakage through the hole while performing

EMA. The details of the pipeline assembly for leakage condition in the pipeline are listed in Tables 3.8 to 3.10.

Table 3.8: The details of the pipeline assembly in case of leakage in the pipeline

Total quantity of pipe spools	3
Connection types for the spools	Threaded coupling
Outer diameter of each pipe spool	33.0 mm
Inner diameter of each pipe spool	26.7 mm
Length of each spool	457.0 mm
Size of the drilled hole	5.15 mm
Threading details of the hole	6.35 mm 20 NC
Location of the hole	In the middle of the middle spool

Table 3.9: Locations for accelerometer sensors and excitation by hammer

Accelerometer location	Excitation location	Distance from the simple support end (mm)
1	1	485
1	2	680
1	3	915
1	4	230
1	5	1140

Table 3.10: Operating conditions for the pipeline assembly with leakage

The pipe with leakage opening with flow or without flow		
Pressure (kPa)	Flow rate (L/min)	Leak rate (L/min)
0	0	Empty
0	7.27	High Leakage
0	8.89	Low Leakage
207	5.45	High Leakage

The FRFs and time-domain signals were recorded using a data acquisition system (DAC) for each of the operating conditions of the pipeline assembly. To capture time-domain signal, two accelerometers and two AE sensors were placed on the top of the pipeline, as shown in Figure 3.1. The flow rates were calculated with a stopwatch and bucket, and the leakage rates were also measured in a similar manner. A licensed version of CutPro-Modal^{TM} was used to store and analyse the time-domain signal and FRF data.

3.2 EMA Methodology

EMAs needed to be carried out to acquire structure dynamics i.e. FRFs, which implicitly contain the system characteristics by means of modal parameters, such as natural frequencies, stiffness and damping coefficients. The impact modal test was performed by exciting the structure by an impulse of an instrumented force hammer with a wide frequency bandwidth and measuring vibrations through accelerometers or AE sensors. The basic concept of FRFs can be understood using the equation of motion for multiple degrees of freedom [Altintas et al. 2006]:

$$\left([M]s^2+[C]s+[K]\right)\{X(s)\}=\{F(s)\} \tag{3.1}$$

Or $[B(s)]\{X(s)\}=\{F(s)\}$ and the transfer function $[H(s)]$ is given by

$$[H(s)]=\frac{\{X(s)\}}{\{F(s)\}}=\frac{adj[B(s)]}{|[B(s)]|} \tag{3.2}$$

The transfer function matrix $[H(s)]$ has $[n\times n]$ dimensions for $n-DOF$ system, and all its elements have a common denominator of $[B(s)]$. The numbers of rows are equal to numbers of coordinate points or measurements, and each column represents a mode. In general, the modal matrix does not have to be square. [*M*], [*C*] and [*K*] are mass, damping and stiffness matrices. Units for damping are N/m-s^{-1}.

The frequency response of the structure can be obtained by replacing $s=j\omega$, where the excitation frequency ω can be scanned in a range covering all natural frequencies. The complete transfer function can be represented as:

$$[H(s)]=\sum_{k=1}^{n}\frac{\{P\}_k\{P\}_k^T}{m_{q,k}}=\sum_{k=1}^{n}\frac{[R]_k}{s^2+2\zeta_k\omega_{n,k}s+\omega_{n,k}^2} \tag{3.3}$$

where $\omega_{n,k}$ and ζ_k are the undamped natural frequency and the modal damping ratio, respectively, for mode k of the system, where each element in the $[n\times n]$ dimensional matrix $[R]_k=\alpha_{il,k}+\beta_{il,k}$ reflects the residues of mode k at row i and column l.

The mode shapes of the system are found from the estimated residues. Alternatively, the displacement vector can be expressed by it mode shapes and modal transfer function.

$$[x]=\left(\sum_{k=1}^{n}\{P\}_k\{P\}_k^T\phi_{q,k}\right)\{F\} \tag{3.4}$$

Where $\{P\}_k$ are the eigenvectors or mode shapes associated with mode k, and $\phi_{q,k}$ is the diagonal modal transfer function matrix.

The modal mass for the mode k using the unscaled modal matrix $[M_x]$ is :

$$m_{q,k} = \{P\}_k^T [M_x] \{P\}_k \tag{3.5}$$

Thus $\frac{\{P\}_k \{P\}_k^T}{m_{q,k}}$ represents the normalisation of each eigenvector with the square root of the modal mass as $\{u\}_k = \{P\}_k / \sqrt{m_{q,k}}$ *and* $\{u\}_k^T = \{P\}_k^T / \sqrt{m_{q,k}}$ .The identified residues, therefore, have the following relationship with the mode shapes:

$$\left(\{P\}_k \{P\}_k^T\right) m_{q,k} = \{u\}_k \{u\}_k^T = \{R\}_k \tag{3.6}$$

where $\{u\}_k$ corresponds to the normalised mode shape giving a unity modal mass. In other words, the mass is unity when the following transformation is used:

$$\{u\}_k^T [M_x] \{u\}_k = 1 \tag{3.7}$$

This is a mathematically convenient way to simplify the identification of mode shapes, modal stiffness and modal damping constants of the structure. In a mathematical modal analysis, one attempts to uncouple the structural equation of motion by means of some suitable transformation, so that the uncoupled equations can be solved. The frequency response of the pipeline can then be found by summing the respective modal responses in accordance with their degree of participation in the pipeline motion. Once the measurements are simultaneously obtained, the time-domain signals are transformed to the frequency domain through discrete fast Fourier transformation [Park et al., 2009]:

$$F(j\omega) = \frac{1}{N} \sum_{n=0}^{N-1} f(nT) \left[\cos \frac{2k\pi}{N} n - j \sin \frac{2k\pi}{N} n \right], \quad k = 0,1,...,\frac{N}{2} \tag{3.8}$$

$$X(j\omega) = \frac{1}{N}\sum_{n=0}^{N-1} x(nT)\left[\cos\frac{2k\pi}{N}n - j\sin\frac{2k\pi}{N}n\right], \quad k = 0,1,...,\frac{N}{2} \tag{3.9}$$

Where F is the force applied at a location on the pipeline setup. X is the displacement measured from the vibration sensor, ω is the frequency in rad/sec, N is the number of samples, and T is the sampling time. In order to minimise noise, the power spectrum is evaluated by multiplying conjugates of the frequency-domain signals, and the spectrum signals are then divided to acquire the transfer function (H) [Park et al., 2009]:

$$H(j\omega) = \frac{X(j\omega)}{F(j\omega)} = \frac{S_{XF}(j\omega)}{S_{FF}(j\omega)} = \frac{X(j\omega)F^*(j\omega)}{F(j\omega)F^*(j\omega)} \tag{3.10}$$

where $*$ is the complex conjugate.

The FRFs can be obtained based on the signal processing procedures, as shown in Figure 3.2.

Similarly, EMA using the impact hammer is performed to acquire the transfer function ($\Phi(s)$). The important things to focus on for during EMA are (1) the impact hammer hits with (or the impact has) sufficient energy contents at the desired frequency range and (2) the coherence of the measurements should be close to one, which indicates the cleanliness of the output signal due to the input signal. Modal parameters such as natural frequencies, stiffness and damping ratios can be identified using the least square method or the nonlinear iteration method. The FRF signal processing block diagram can be described as given in Figure 3.2. The main components of FRF system are the anti-aliasing filter, analogue to digital converter (ADC) and the digital filter.

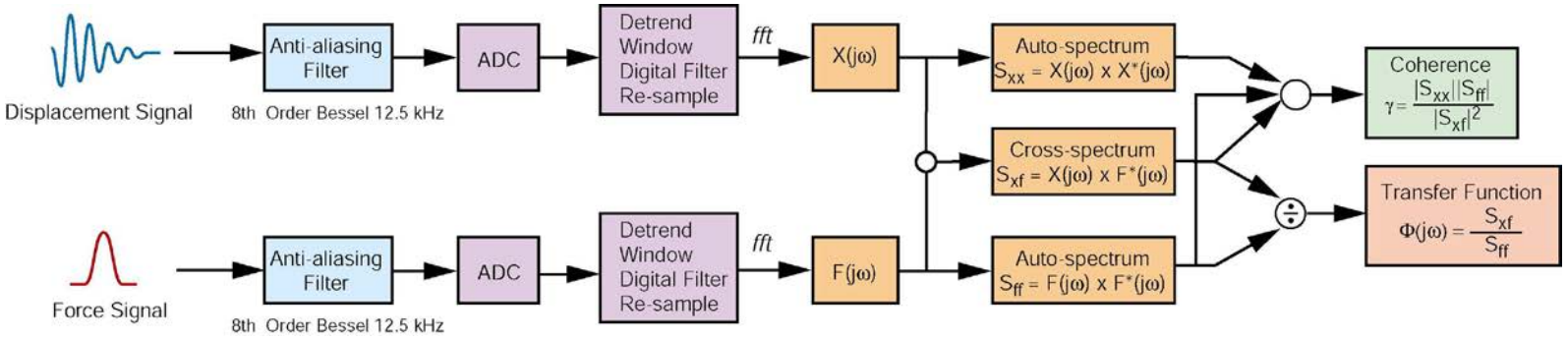

Figure 3.2: Frequency response function signal processing block diagram [Park et al., 2009]

Change of Stiffness *K*

A change in stiffness affects both the resonant frequency as well as the system characteristic at low frequency. This dominance of stiffness at low frequency is the reason that this region of the frequency response function is known as the stiffness region or compliance line.. The variations in magnitude of FRFs and phase angle due to increase in stiffness are shown in Figure 3.3(a) and Figure 3.3(b).

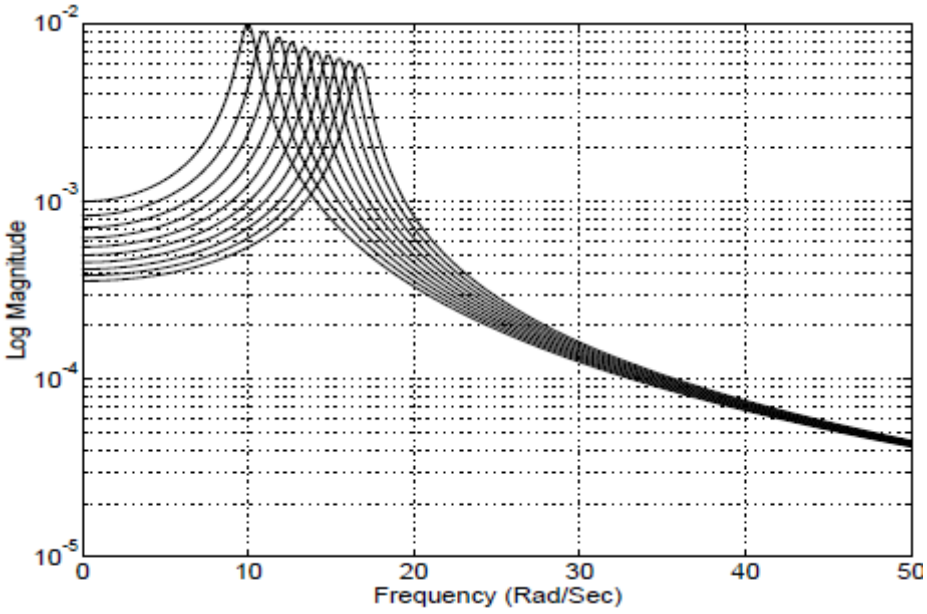

Figure 3.3(a): Variation of FRF due to increase in stiffness [Randall et al., 1998]

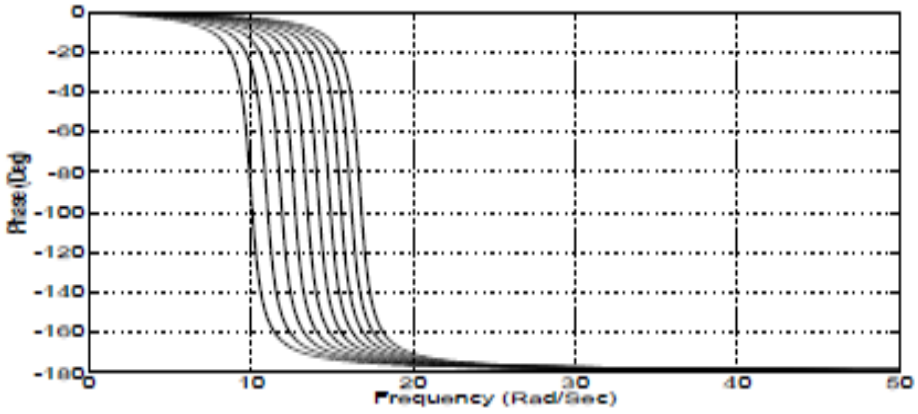

Figure 3.3(b): Variation of phase angle due to increase in stiffness [Randall et al., 1998]

Change of Damping *C*

A change in damping has no apparent effect on the resonant frequency. The only noticeable change involves a change in frequency response function in the region of the resonant frequency. Figure 3.4(a) and Figure 3.4(b) show the variation of magnitudes of FRF and phase angle due to increase in damping ratio ζ. For smaller pipeline sizes, the damping ratio varies from 1% to 3% [Stevenson et.al. 1980]. In this study 2% damping ratio has been used in FE analysis.

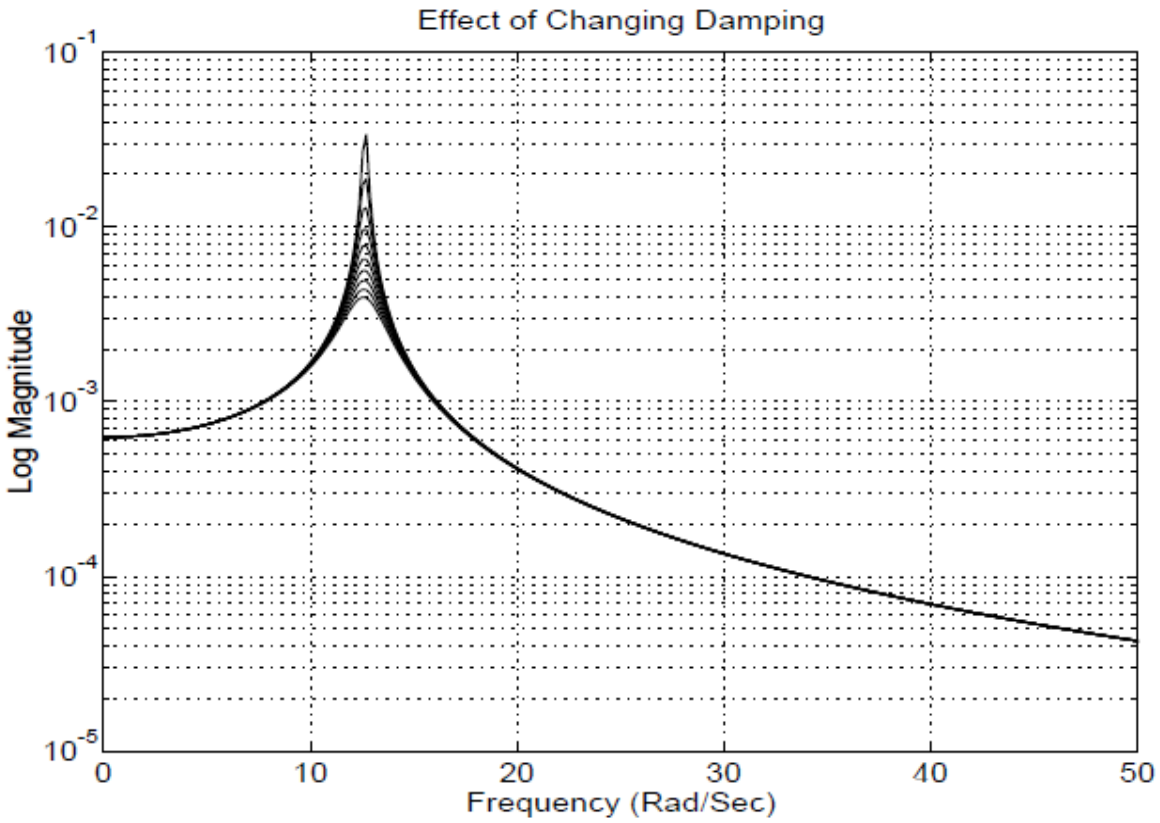

Figure 3.4(a): Variation of FRF due to increase in damping ratio [Randall et al., 1998]

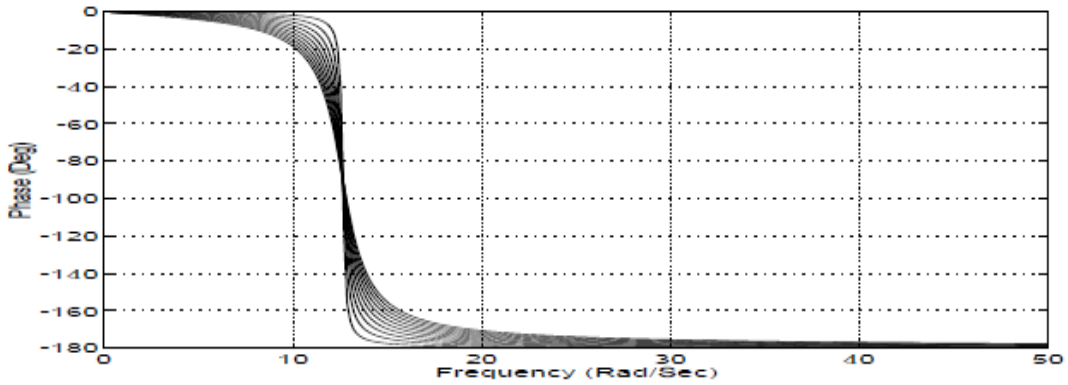

Figure 3.4(b): Variation of phase angle due to increase in damping ratio [Randall et al., 1998]

Change of mass *M*

A change in mass affects both the resonant frequency as well as the system characteristic at high frequency. This dominance of mass at high frequency is the reason that this region of the frequency response function is known as the mass line. Also note that as the mass changes, the apparent damping (sharpness of the resonant frequency) changes accordingly. A change in mass affects both the resonant frequency, the system characteristic at high frequency as well as the fraction of critical damping. Figure 3.5(a) and Figure 3.5(b) show the variation of magnitude of FRF and phase angle respectively, due to increase in mass.

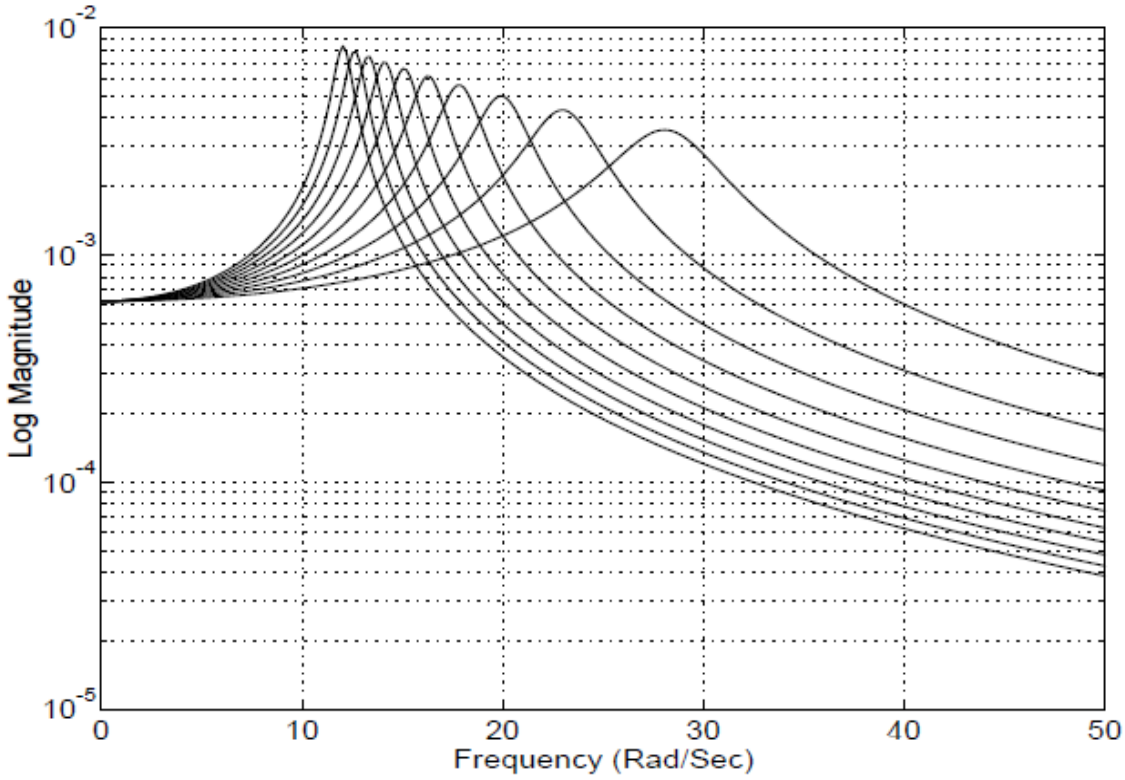

Figure 3.5(a): Variation of FRF due to increase in mass [Randall et al., 1998]

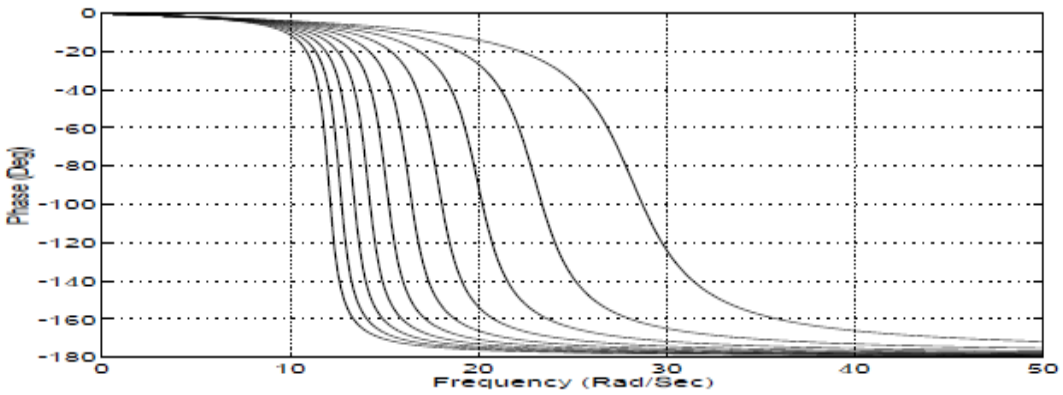

Figure 3.5(b): Variation of phase angle due to increase in mass [Randall et al., 1998]

3.3 EMA Results

All experimental modal parameters are obtained from measured operating deflection shapes (ODSs), i.e. the experimental modal parameters are obtained by artificially exciting a

machine or structure, measuring its ODSs (motion at two or more DOFs) and post-processing the vibration data.

The FRF is a fundamental measurement that isolates the inherent dynamic properties of a mechanical structure. Experimental modal parameters (frequency, damping, and mode shape) are obtained from a set of FRF measurements. The FRF describes the input-output relationship between two points on a structure as a function of frequency [Schwarz et al., 1999]. Since both force and motion are vector quantities, they have directions associated with them. Therefore, an FRF is actually defined between a single input DOF (point and direction) and a single output DOF. A FRF is a measure of the displacement, velocity or acceleration response of a structure at an output DOF per unit of excitation force.

The recorded data for FRFs and time-domain signals were organised to develop combined plots to enable the comparison of evaluated dynamic parameters in each of the pipeline operating conditions. Frequency and time were plotted on the x-axis for FRF and time-domain signals, and displacement and acceleration were plotted on semi-log scale on the y-axis for FRF and time-domain signals. The frequency range was up to 3000 Hz.

At location 1, it is evident that the FRFs for corroded pipe were higher than those of the normal and leaky pipes, due to the thinner wall thickness of the carbon steel pipe. The variation in displacement values was 10 to 15%. A clear shift was observed in the FRF plots for empty and corroded pipes towards right, at approximately 2% to 3% as shown in Figure 3.6.The FRF for the normal and leaky pipes almost matched for a large range of frequencies, but the FRFs showed some shift towards the higher range of frequencies.

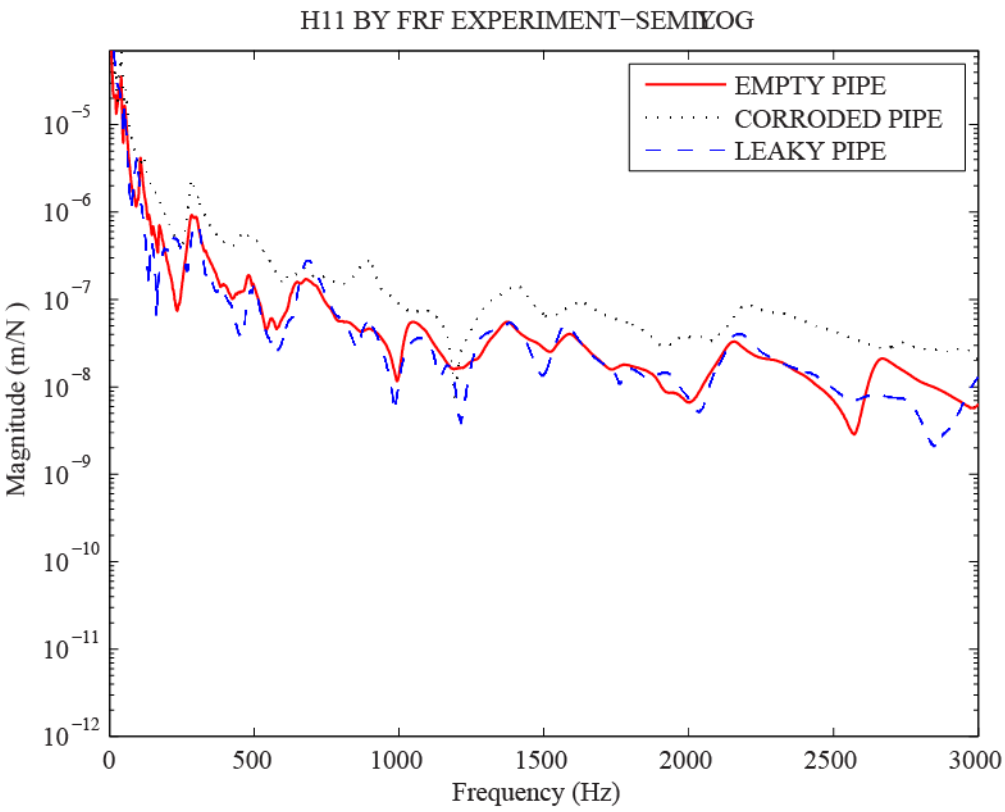

Figure 3.6: Experimental H11 FRF plots for empty pipe

The FRF plot of the pipeline with flow also indicates the values for corroded pipe were higher than the normal and leaky pipes, due to the thinner wall thickness of the carbon steel pipe as shown as in Figure 3.7. The FRF plot for corroded pipeline shows a clear left shift of approximately 10% to 15% along the frequency axis. The variation in magnitude along displacement axis was approximately 10 to 17%. The FRFs for the normal and leaky pipes almost matched, because there was hardly any difference in mass distribution between the normal and leaky pipes. There was a marked difference between the FRF plots for the empty pipeline and the pipeline with flow. The displacement values were lower for the pipeline with flow, which seems to be a prominent effect of water flowing in the pipeline.

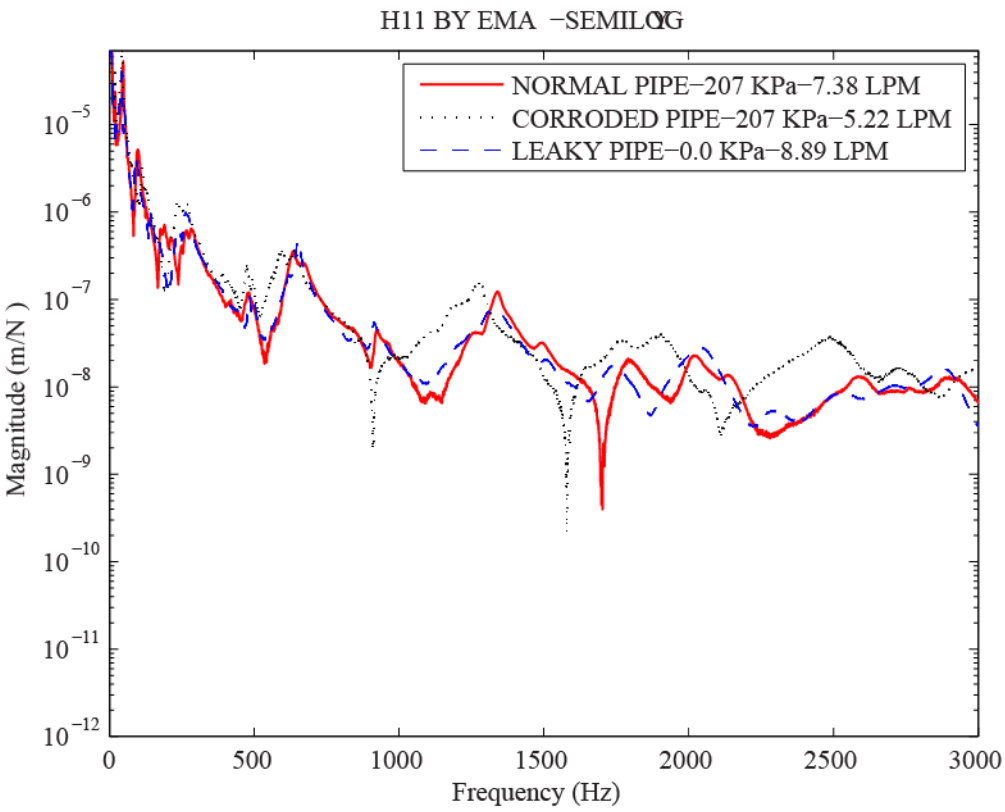

Figure 3.7: FRF plots for pipeline assembly with water flow at location 1

3.4. Finite Element Analysis

The second step in developing the pipeline health monitoring scheme was an FE analysis of the pipeline for the various operating conditions. FE analysis was used to study the dynamic characteristics of the pipeline system for the same set of conditions that were used in the EMA.

The pipeline system was simulated as an analytical model using a FE technique, which was based on the fact that an approximate solution to any complex engineering problem can be reached by subdividing the pipeline into the smaller, more manageable (finite) elements. The FE analysis is a numerical method for solving problems of engineering and mathematical physics. The FE method is quite useful for problems with complicated geometries, loadings, and material

properties where analytical solutions cannot be obtained. The FE method or analysis is a computational technique used to obtain approximate solutions of boundary value problems in engineering by using the discretization of the objects in to small elements and defining the boundary conditions, such as fixed end and simple supported.

Using FEs, the solution of the complex equation that describes the behaviour of the pipeline can often be reduced to a set of linear equations, which can be solved using the standard techniques of matrix algebra. The setup and methodology for FE analysis is described in the following subsections.

3.4.1 FE Methodology

The dynamic behaviour of fluid-filled pipe systems is quite complicated, because it is governed by several coupled waves in the structure and the fluid. Moreover, the layout of individual pipe systems may differ considerably. A pipe system may consist of any combination of typical components, such as straight pipe sections, elbows, pumps, valves, bellows, accumulators and supports.

In linear analysis, for the isentropic and in-viscid fluid models, the momentum and constitutive equations are [Bathe et al., 1997]:

$$\rho ii + \nabla p - f^B = 0 \text{ And } \quad \nabla . u + \frac{p}{\beta} = 0 \tag{3.11}$$

where $u, p, f^B and\ \beta$ are the displacement vector, pressure, body force vector and fluid bulk modulus, respectively. If $f^B = 0$, then in terms of the displacement only [Bathe et al., 1997].

$$\beta \nabla (\nabla . u) - \rho ii = 0 \tag{3.12}$$

Since $\nabla \times \nabla \phi = 0$ for any smooth scalar-valued function, ϕ, then [Bathe et al., 1997]:

$$\frac{\partial}{\partial t}(\nabla \times \upsilon) = 0 \tag{3.13}$$

where υ is the velocity vector.

The motion is, therefore, always circulation preserving, i.e. the vorticity does not change with time. If the fluid starts from rest, there is the irrotationality constraint [Bathe et al., 1997]:

$$\nabla \times u = 0 \tag{3.14}$$

The variational form can be written as [Bathe et al., 1997]:

$$\int_{v_f} \{\beta(\nabla.u)(\nabla.\delta u) + \rho \ddot{u}.\delta u\} dV + \int_{s_f} \overline{p}\,\delta u_n^s dS = 0 \tag{3.15}$$

where u_n^s is the displacement normal to S_f; and, V_f, S and S_f stand for the fluid domain, fluid boundary, Neumann n boundary and Dirichlet boundary condition, respectively. Also $S_u \cup S_f = S$ and $S_u \cap S_f = \phi$.

The above variation form is often used in pure displacement-based formulation. This formulation produces spurious non-zero frequency modes. From the rigid cavity test problem, it was concluded that the observed spurious non-zero frequency modes are rotational modes, because the irrotationality constraints are 'lost' in the FE formulation. The following penalty formulation was, therefore, proposed [Bathe et al., 1997]:

$$\int_{v_f} \{\beta(\nabla.u)(\nabla.\delta u) + \alpha(\nabla \times u)(\nabla \times \delta u) + \rho \ddot{u}.\delta u\} + \int_{s_f} \overline{p}\,\delta u_n^s\, dS = 0 \tag{3.16}$$

where α is a large penalty parameter. However considering the fact that the penalty formulation is too 'stiff', the reduced integration method is normally used for the terms [Bathe et al., 1997]:

$$\int_{v_f} \{\beta(\nabla.u)(\nabla.\delta u) + \alpha(\nabla \times u)(\nabla \times \delta u)\} dV \tag{3.17}$$

With the use of reduced integration, the spurious non-zero frequency modes can be eliminated.

3.4.2. FE Analysis Setup

The pipeline with fluid, coupled with acoustic loads, has been analysed using the multi physics environment of ANSYS Workbench 14.0 software. The details of the modelling are described in the following paragraphs and figures (Figure 3.8 and 3.9).

The presence of the fluid can significantly change the vibration characteristics of the containing pipeline. To determine the extent of this effect, the ANSYS FLUID30 element was used to account for the factors, such as mass, stiffness and damping, that the fluid adds to the overall system. The acoustic properties are added to the element by defining the sound velocity of the fluid medium.

ANSYS acoustic element FLUID30 accomplishes the fluid structure coupling, because there are four degrees of freedom: one for sound pressure and three for optional displacements. Thus, a consistent matrix coupling was set up between the pipeline and fluid elements. The pipe metal interface was modelled using SHELL63. The boundary conditions were simulated by making one end of the pipeline fixed and another end as simply supported.

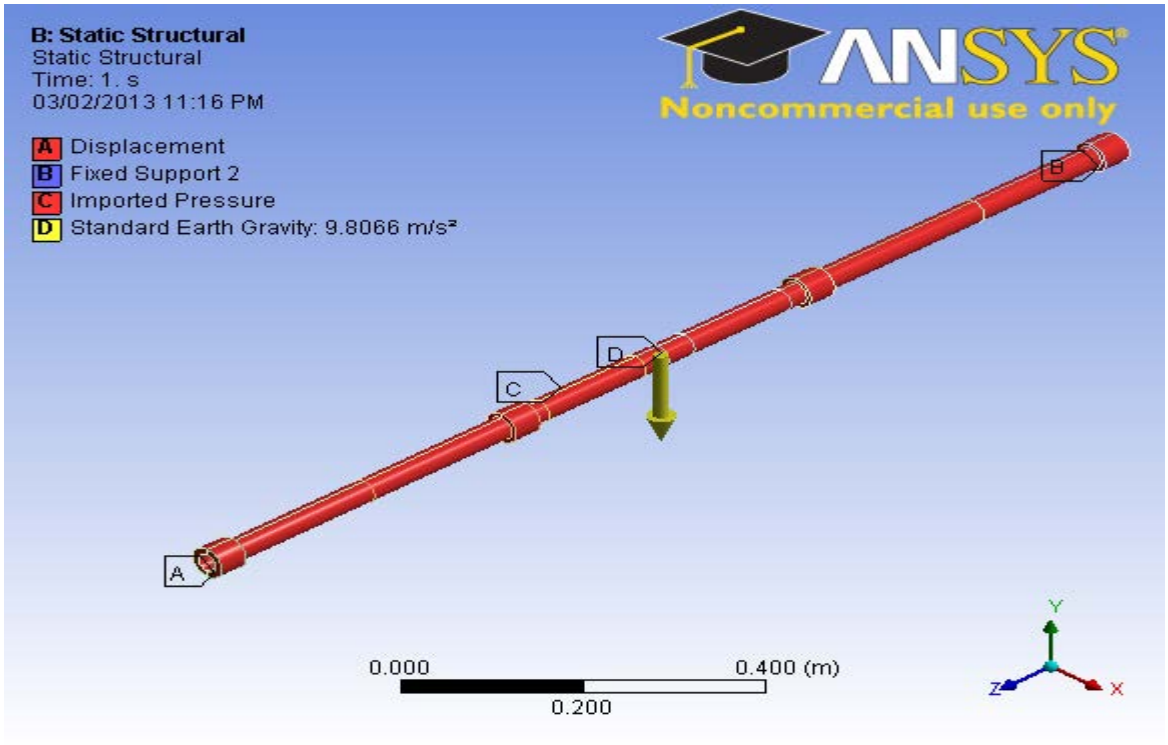

Figure 3.8: Pipeline model in FE analysis

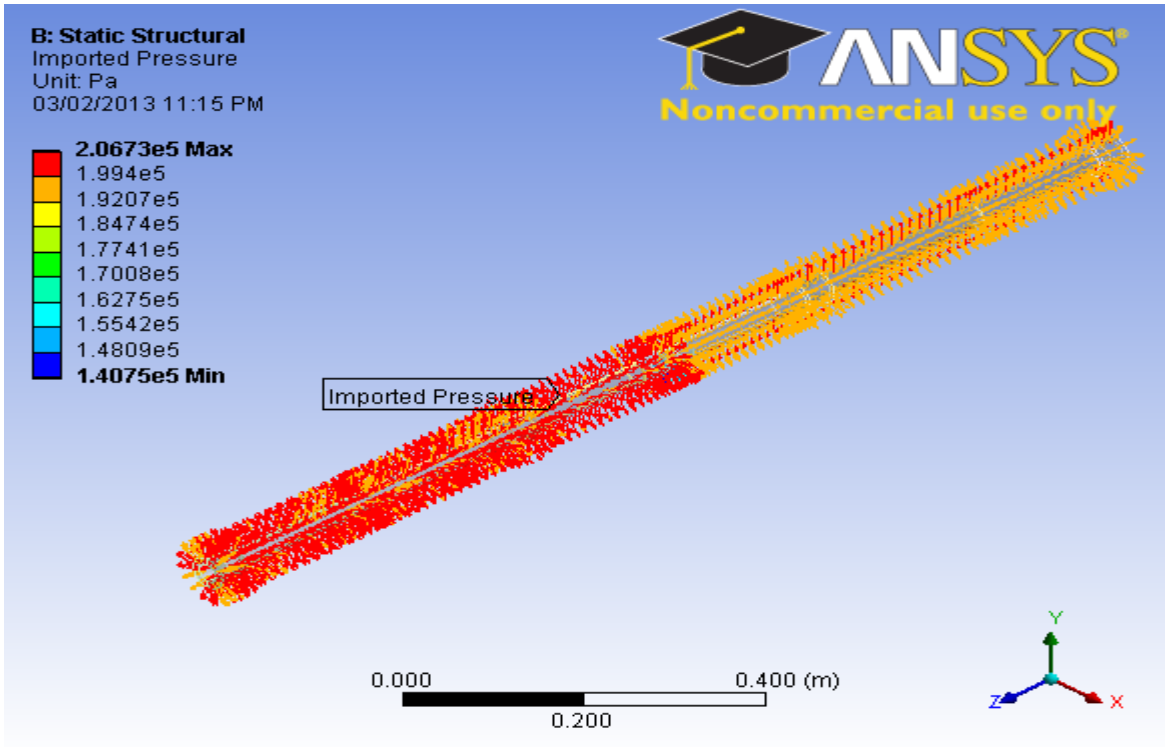

Figure 3.9: Imported pressure in the pipeline

3.4.3 FE Results

FE analysis was carried out for the same set of the operating condition as in EMA, so that comparisons could be done between the results from FE analysis and those of EMA. MATLAB software was utilized to develop the plots, similar to those of EMA. The FRFs were plotted at all the locations, i.e. 1, 2, 3, 4 and 5.

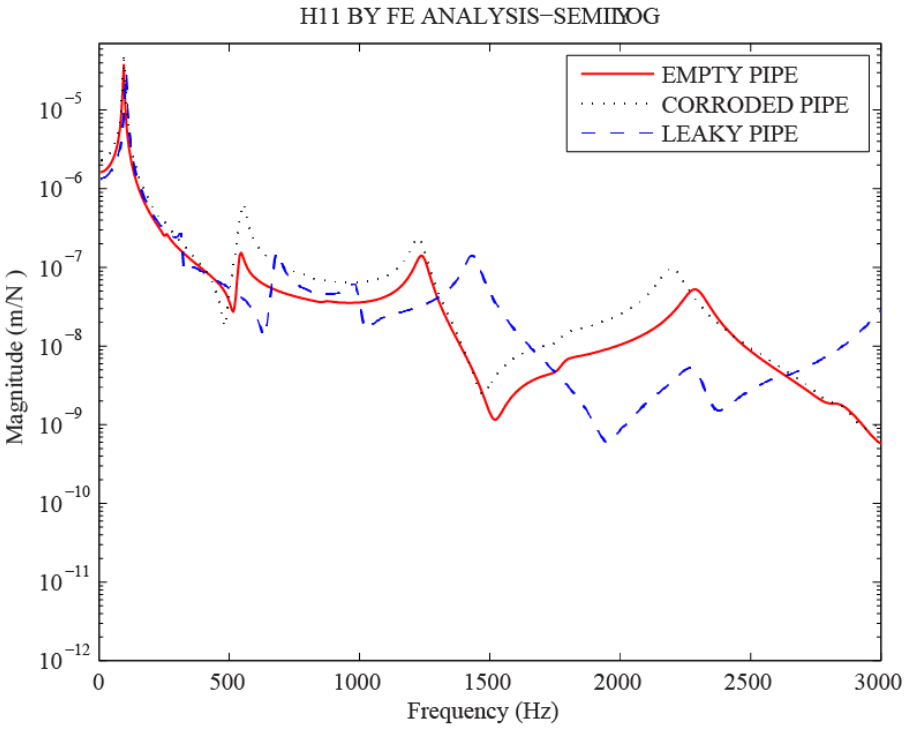

Figure 3.10: FRF plots for the empty pipeline at the location 1 using FE analysis

In the FE analysis for the empty pipeline conditions, the FRFs for the corroded pipe were also higher than those of the normal and leaky pipes, due to the thinner wall thickness of the carbon steel pipe as shown in Figure 3.10. The FRFs for the normal and leaky pipes matched for lower frequencies; however, a shift was observed for the higher frequencies. The change in the

amplitude of the FRF can be attributed to the change in the stiffness of the pipe due to corrosion. As corrosion happens and changes the stiffness properties of the entire system, the setup undergoes more displacement compared to a normal pipe to the same applied force. This change in the FRF magnitude can be monitored continuously to detect any variation in the setup stiffness properties.

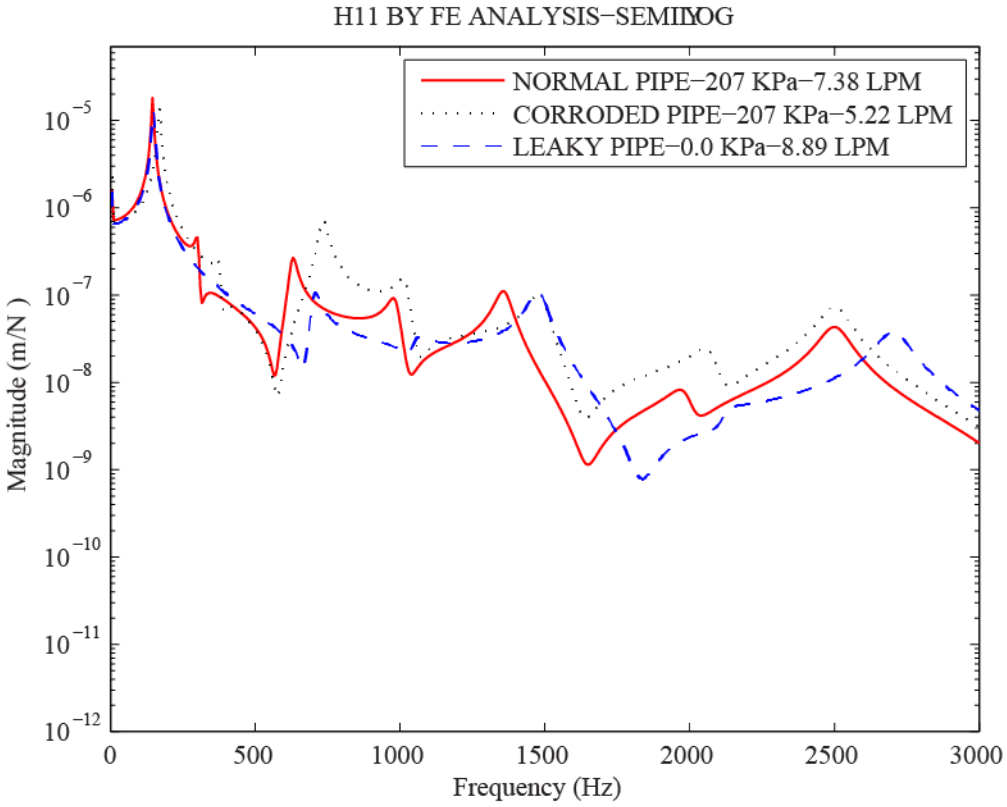

Figure 3.11: FRF plots for pipeline assembly with water flow at location 1 using FE analysis

Similar to the EMA FRF results, the FRF plots of the FE analysis for the pipeline with flow also indicated the higher values for corroded pipe than those of the normal and leaky pipes, due to the thinner wall thickness of the carbon steel pipe as shown in Figure 3.11. The FRFs for the normal and leaky pipes almost matched, because there was hardly any difference in the mass

distribution between the normal and leaky pipes at lower frequencies; and, the FRFs showed a definite shift along the frequency axis for higher frequencies. However the differences between the FRFs have decreased, which is due to water flow in the pipeline.

3.4.4 Natural Frequency Plots using FE Analysis

The natural frequencies were calculated using FE analysis for all the operating conditions of the pipeline. For comparison purposes the natural frequencies were plotted together for the normal, corroded and leaky pipelines without and with water flow. The combined plots are shown in Figures 3.12 and 3.13

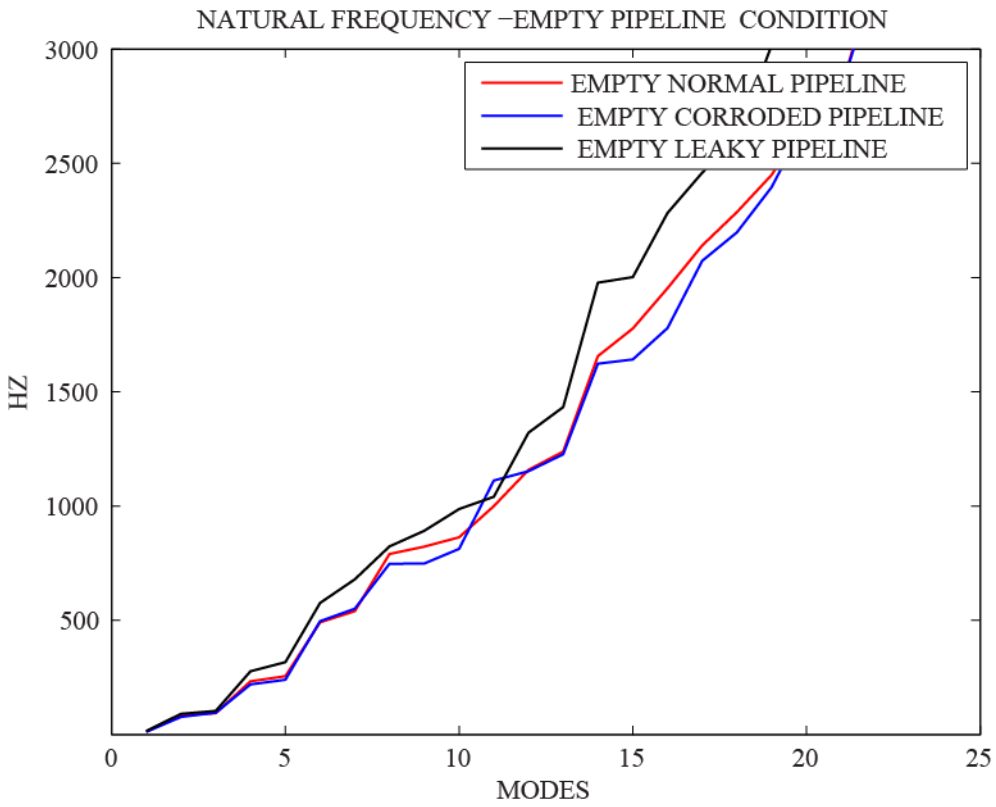

Figure 3.12: Natural frequencies plots for three cases of empty pipeline, i.e. normal, corroded and leaky, using FE analysis

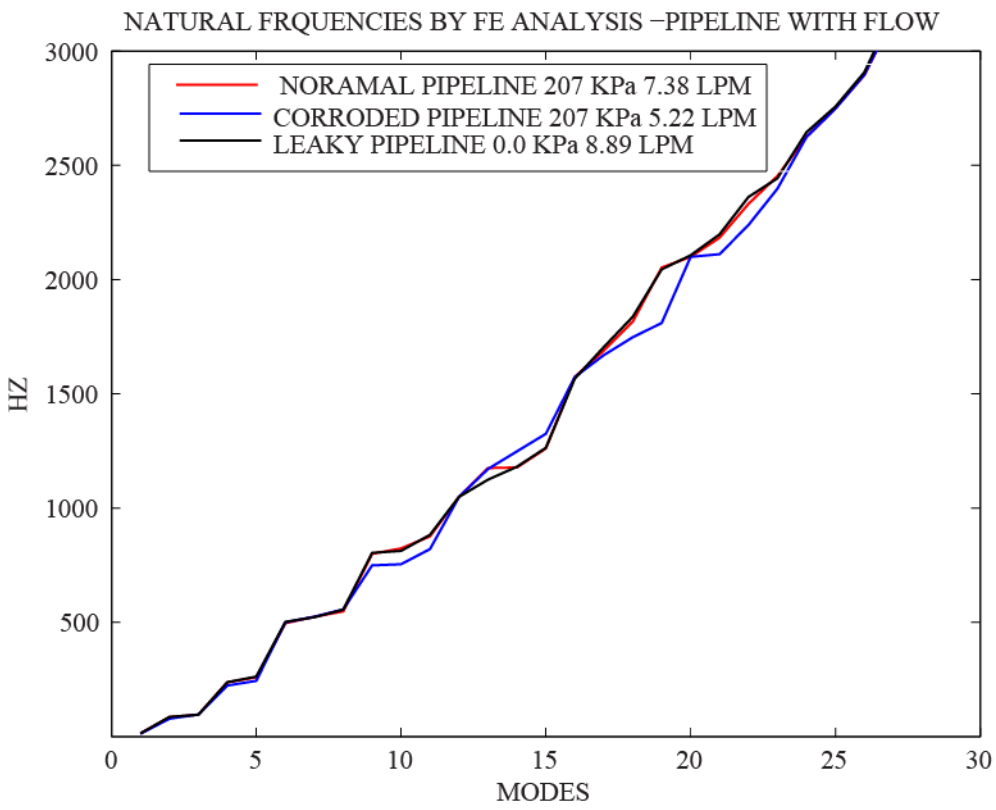

Figure 3.13: Natural frequencies plots for three cases of pipeline with flow, i.e. normal, corroded and leaky, using FE analysis

The combined plots for natural frequencies for the pipelines shown in Figures 3.12 and 3.13 indicate a very prominent variation of natural frequencies for the normal, corroded and leaky pipelines. The variation of natural frequencies was less between the normal and leaky pipelines, because not much material was removed from the normal pipeline to simulate the leakage, which done by drilling a 6.35 mm tapped hole.

The plot of natural frequencies for the three cases of pipeline with the water flow (Figure 3.13) showed that the natural frequencies changed with the presence of water flow compared to those of the empty pipeline condition. However, there was less variation in the natural frequencies for all modes between the normal, corroded and leaky pipelines with water flow.

3.4.5 Natural Frequency Plots from EMA

The following method was used to obtain the natural frequencies from the curves for FRFs from EMA of three cases of empty pipelines, i.e. normal, corroded and leaky. The fitting curve was plotted using MATLAB software for each condition of empty pipeline. The fitted curve was manually scanning, and two frequencies near the natural frequency for each resonance peak in the curve were selected using the frequency band method. The natural frequency was calculated from the selected two frequencies near the resonance peak using following formula:

$$\omega_n = \sqrt{(\omega_1^2 + \omega_2^2)/2}$$

The natural frequency curves shown in Figure 3.14 and Figure 3.15 for the empty pipeline conditions were very much comparable with the natural frequency curves from the FE analysis. The range of frequencies was also very similar to that of the natural frequencies from the FE analysis.

Similar to the results from the FE analysis, the natural frequencies plots from EMA for the pipeline with flow for all the three cases showed a variation in the natural frequencies due to the presence of flow of water in the pipeline, compared to those of the empty pipeline for all conditions. However, the variation was lower between the normal, corroded and leaky pipelines with water flow compared to that of the empty pipeline conditions.

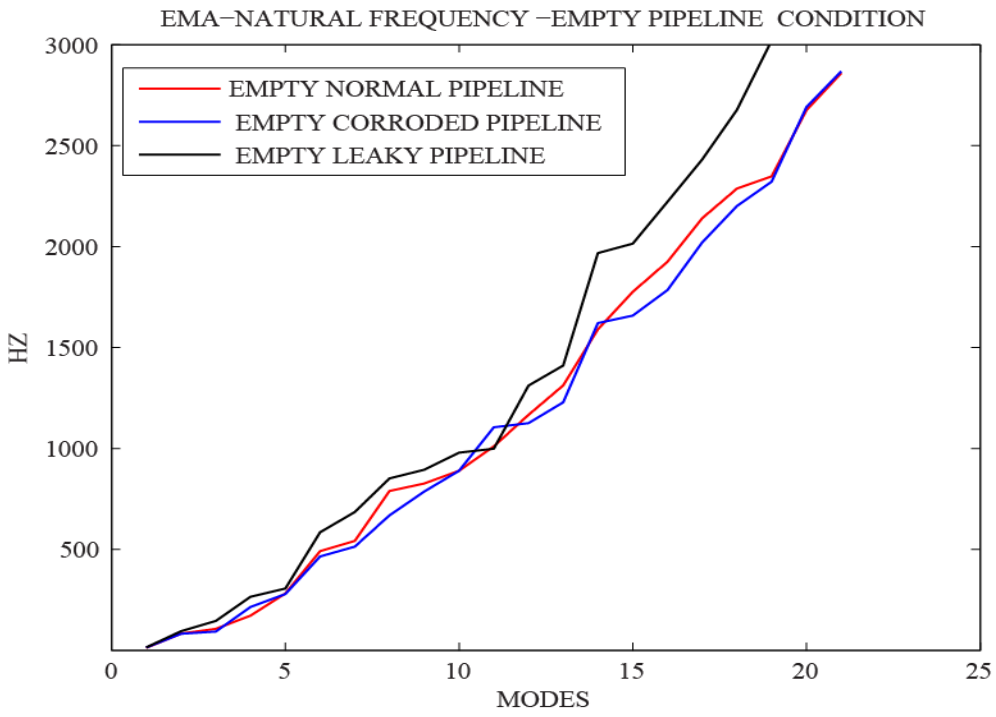

Figure 3.14: Natural frequency plot from EMA for empty pipeline conditions

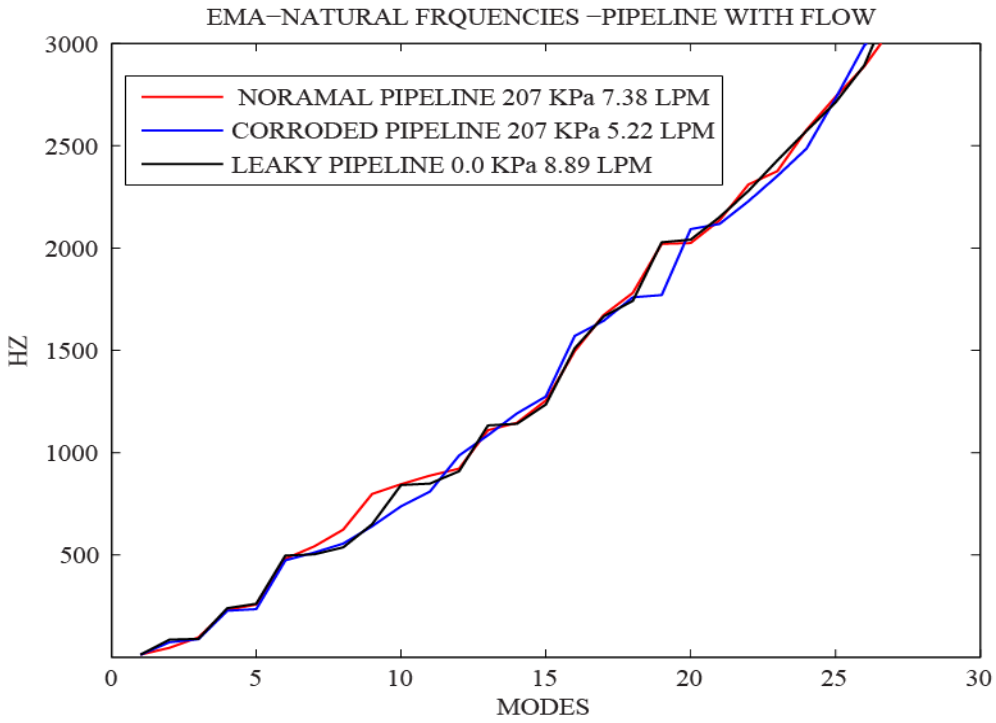

Figure 3.15: Natural frequency plots from EMA for flow pipeline conditions

3.4.6 Frequency Domain Plots (Transient Responses)

The time-domain signals were recorded at different conditions, as described in the experimental section. The time-domain signals were collected to detect change in the acoustic emission signals and correlate them to the leakage in the pipe. The locations of the AE (acoustic emission) sensors are as shown in Figure 3.1. All the time-domain plots had time along the x-axis and the transient signal response (volts) along the y-axis. The time-domain transient signal responses were converted to frequency-domain transient signal responses for all the recorded acoustic emissions signals for the various operating conditions of the pipeline.

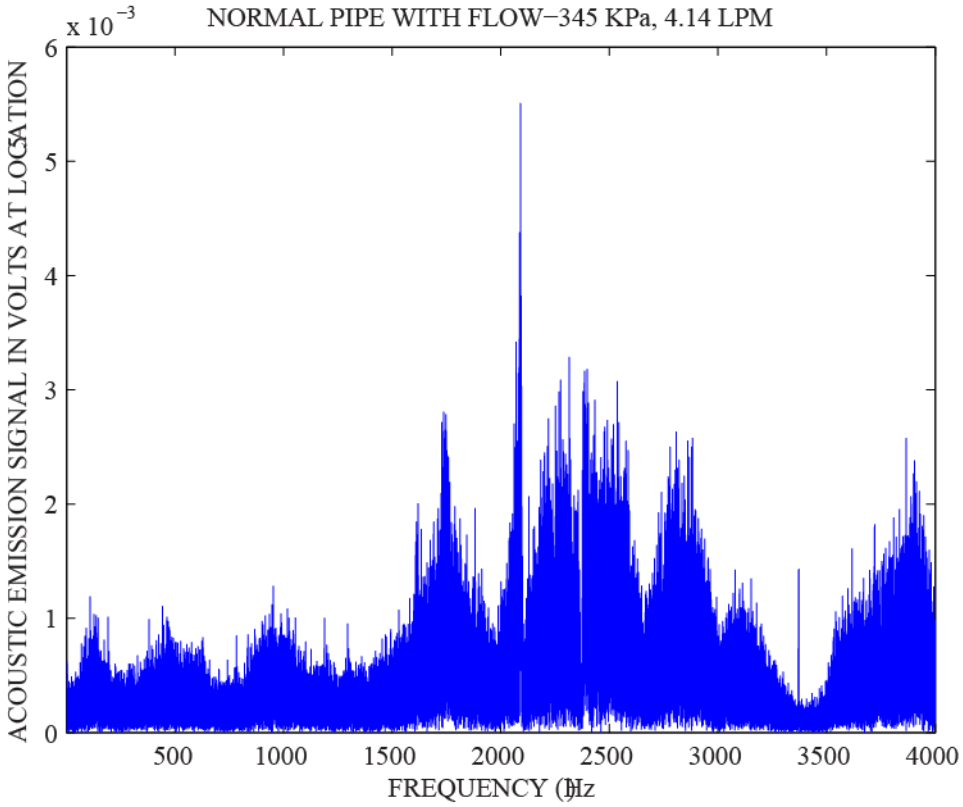

Figure 3.16: Transient response spectrum for normal pipeline with flow at location 5 (Pressure - 345 kPa, flow rate - 4.14 L/min)

Figure 3.16 shows the transient response spectrum recorded at location 5 using the AE sensor. The transient signal responses had significant values for AE signals in the frequency range of 1750 Hz to 3000 Hz. The maximum value of the calculated frequency-domain transient signal was approximately 5.5 millivolts.

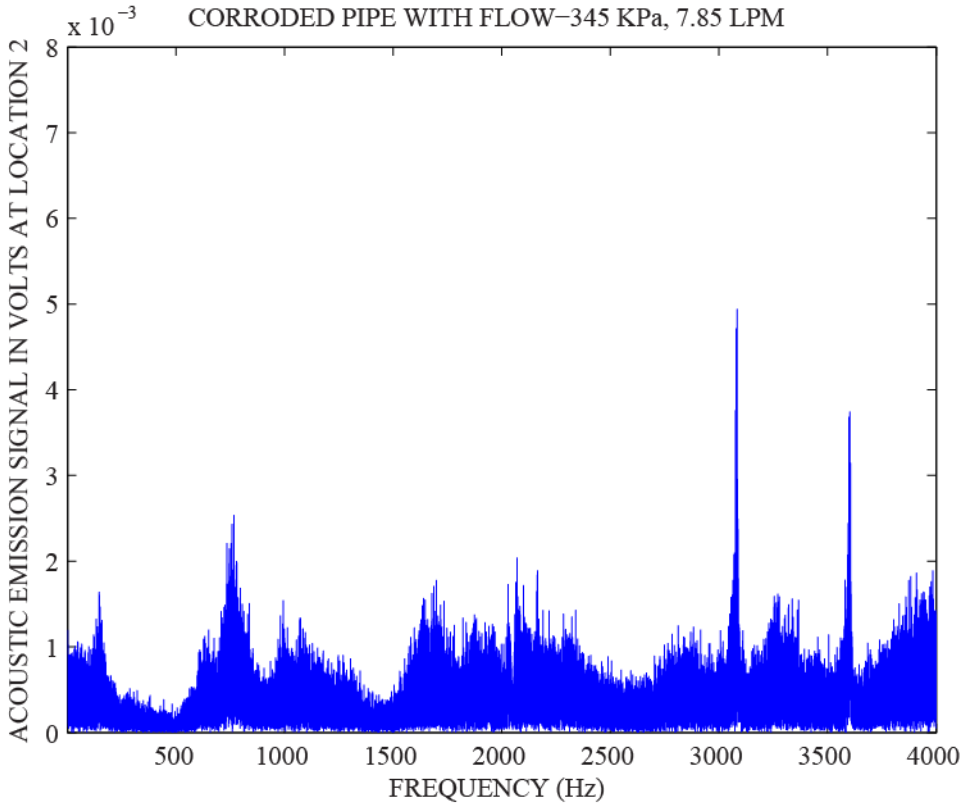

Figure 3.17: Transient response spectrum for corroded pipeline with flow at location 5 (Pressure - 345 kPa, flow rate - 7.85 L/min)

The middle spool of the pipeline assembly was thinned down from the outside to mimic the presence of corrosion in the pipeline. The depicted frequency-domain plot depicted in Figure 3.17 corresponds to the recorded time-domain transient signal at location 5 using an AE emission sensor. The maximum estimated value of acoustic emission signal was approximately 6.5

millivolts, which was about approximately 18% higher than that of the normal pipeline with water flow.

In general, the transient signals over the whole range of frequency were stronger with the corroded pipeline with flow compared to that of the normal pipeline with water flow. Therefore, it is clearly evident that corroded pipeline gives rise to a good variation of the transient signal responses, which can be considered a major factor for indicating the poor health or faulty condition of a pipeline.

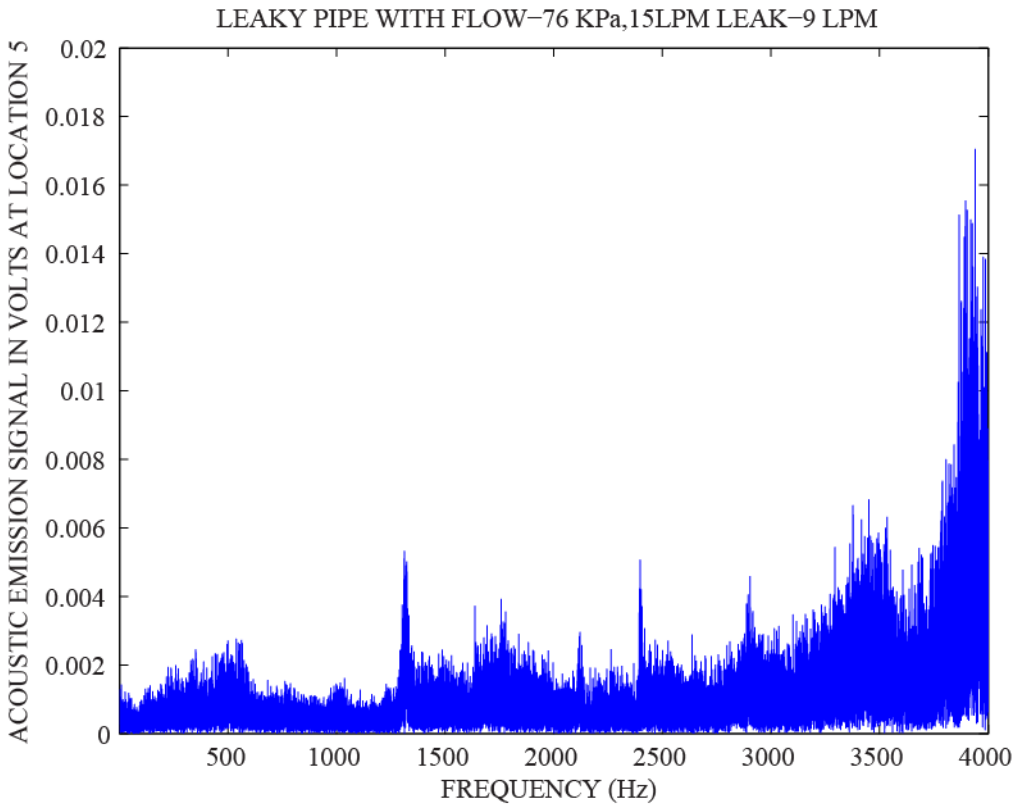

Figure 3.18: Acoustic emission signals for the leaky pipeline with flow at location 5 (Pressure - 76 kPa, flow rate - 15 L/min, leakage - 9 L/min)

A hole of the size 6.35 mm was drilled in the middle spool of the pipeline assembly to simulate leakage in the pipeline assembly. In this case of pipeline operation, the AEs were recorded at location 5 which are shown in Figure 3.18. The frequency-domain transient signal responses showed multiple jumps in the signal values compared to those of the normal and corroded pipelines. The maximum transient signal value was 17 millivolts, which was more than three times (a 200% increase) that of the normal pipeline signal response and a little less than three times that of the corroded pipeline. This variation in responses really proves the worthiness of consideration as a major factor to predict a faulty condition of the pipeline.

3.5 Comparison of EMA and FEA Results

The FRFs obtained from both the EMA and FE analysis showed the same trend for all pipeline operating conditions, i.e. normal pipeline with and without water flow, corroded pipeline with and without water flow, and leaky pipeline with and without water flow. There is a clear indication that the results obtained from the EMA and FE analysis are in agreement with each other; therefore, these results are reliable, and a novel pipeline health monitoring scheme using ANFIS architecture can be developed on the basis of the estimated variation of dynamic parameters, such as natural frequencies, FRFs and time-domain responses.

The results from the EMA and FE analysis showed that, when a pipeline system is put into operation, the dynamic behavior of the pipeline system changes from as-installed conditions. The dynamic parameters, such natural frequencies and time- and frequency-domain responses, change from as-installed condition to operating condition. In the case of a corroded condition, the FRFs had generally higher values for displacements for almost all natural frequencies. The change in FRF in the vicinity of the corroded portion was distinctly different from the other

locations. This difference can be very useful in distinguishing a corroded area from a non-corroded portion of the pipeline.

The transient response spectra for the normal, corroded and leaky pipelines showed variation in the voltage recorded using AE sensors. It was very clear from the frequency-domain transient signal response plots that the variation in the voltage increased for a corroded pipeline and increased further for a leaky pipeline.

3.6 Summary

The objective of performing the EMA and FE analysis for the pipeline assembly was the generation of datasets for the training and testing of the ANFIS-based pipeline monitoring scheme. It was also important that the generated datasets were reliable. To achieve this reliability, the FE analysis was performed by simulating the same physical and operating conditions of the pipeline. Accelerometer and AE sensors were installed on the critical locations to capture vibro-acoustic signals.

In view of the results from the EMA and FE analysis and their comparison, it can be concluded that the variation of dynamic parameters, such as natural frequencies and FRFs, are in agreement with each other and, therefore, form a reliable data source to develop the novel ANFIS-based monitoring scheme for the pipeline. The transient response spectra showed a logical trend in the variations of the AE signals in each of the pipeline conditions, also forming part of a reliable database for the development of the ANFIS-based pipeline monitoring scheme.

CHAPTER 4: TRAINING AND TESTING OF ANFIS-BASED PIPELINE MONITORING SCHEME

Reliability and serviceability are major challenges in the development of most advanced pipeline health monitoring systems. Successful monitoring of pipelines with the aid of an intelligent fault detection system can result in the identification of malfunctions and potential causes of failure in a timely fashion while the pipelines remain operational. This can prevent unnecessary and expensive breakdowns, minimize potentially fatal casualties, avoid environmental pollution and can, on the whole, increase the lifetime of an operating pipeline and prevent enormous economic losses.

Due to the advent of new technology in the field of vibration monitoring, it is possible to record vibrations in a broad range of frequencies using accelerometers and acoustic emission sensors and employing a data acquisition system. This pool of data can be further processed using CutPro-Modal^{TM} software to estimate dynamic properties, such as frequency response functions (FRFs) and natural frequencies. Time-domain signals are converted to frequency-domain signals for better interpretations of the transient responses of pipeline faults.

Dynamic parameter values have some amount of impreciseness, due to human error, the sensitivity of the equipment and the assumptions used while recording the data. Adaptive neuro fuzzy inference systems (ANFISs) are useful in processing recorded databases that are slightly imprecise and close to the real world, in terms of data collection and processing. An ANFIS employs fuzzy logic and a neural network to process the database and an optimization process to finalize the decision parameters in predicting the faults in the pipeline system. ANFIS architecture can have a feature that enables learning from the database for the known faults in the

pipeline, which is termed the training phase. When a trained ANFIS system is verified against the pool of data sets obtained for an unknown status of pipeline, it can then predict pipeline condition.

This novel pipeline monitoring scheme was developed in two steps, which are defined as the learning or training phase and the testing or verification phase. In the training phase, the database obtained from a finite element (FE) analysis was used; and, in the verification phase, the database obtained from actual recordings from an experimental modal analysis (EMA) was utilized. The operating conditions for the pipeline system were kept exactly the same in both analyses. The data from the recording of acoustic emission signals were utilized for the learning and testing phases of the ANFIS-based pipeline monitoring scheme.

4.1 Methodology

Artificial neural networks (ANNs) and fuzzy inference systems have been increasingly used in many engineering fields. Both of these computational techniques are branches of artificial intelligence and emulate humans in adaptation due to past experiences [Kuvulmaz et al., 2004]. An ANN is an information-processing paradigm that is inspired by the way biological nervous system, such as the brain, process information. Similar to a brain, an ANN consists of multiple layers of simple processing elements called as neurons. The neuron performs two functions, namely the collection of input and generation of output [Dongare et al., 2012].

In the present research, the collection of inputs refers to recordings of FRFs and frequency-domain signals (converted from recorded time-domain signals) using accelerometer and AE sensors; and, the output is achieved by using a fuzzy inference system technique to optimize the decision parameters to predict the health of the pipeline.

System modelling based on conventional mathematical tools (in this case, differential equations) is not well suited for ill-defined and uncertain systems [Jang et al., 1993]. By contrast, a fuzzy inference system employing fuzzy if-then rules can model the qualitative aspects of human knowledge and reasoning processes without employing precise quantitative analysis. Fuzzy inference systems are also known as fuzzy rule based systems, fuzzy models, fuzzy associative memories or fuzzy controllers when used as controller. A fuzzy inference system is shown in Figure 4.1 and is basically composed of five functional blocks [Jang et al., 1993]:

- A rule base containing a number of fuzzy if-then rules,
- A database that defines the membership functions of the fuzzy sets used in the fuzzy rules,
- A decision-making unit that performs the inference operations on the rules,
- A fuzzification interface that transforms the crisp inputs into linguistic values, and
- A defuzzification interface that transforms the fuzzy results of the inference into crisp output.

The aim of this research is the development of a reliable and accurate pipeline monitoring scheme that can be used during the operation of a pipeline network. Fusion of different sensor signals through an inference system is necessary in order to enhance the bandwidth of the sensors and achieve higher accuracy in predicting corrosion and leakage in a pipeline system.

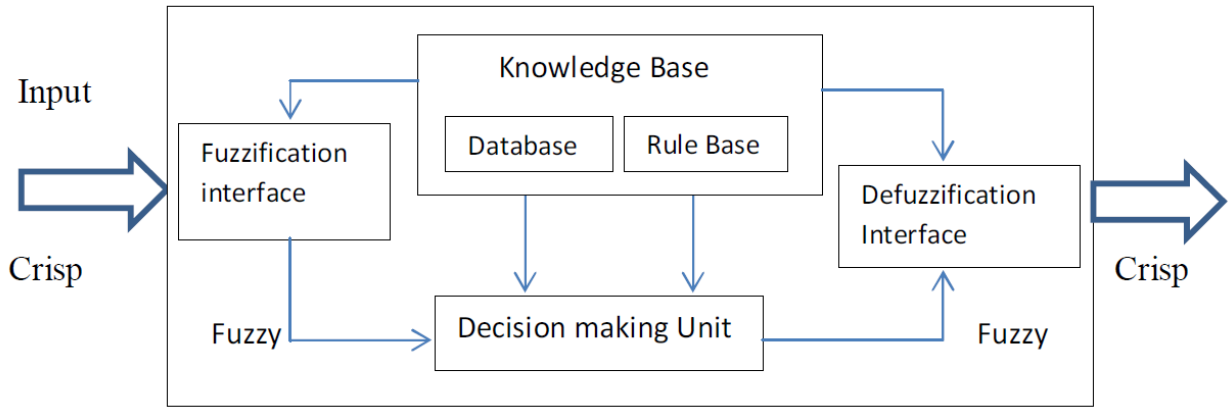

Figure 4.1: Fuzzy inference system [Jang et al., 1993]

An ANFIS model was chosen for fusing various sensor signals recorded using accelerometer and AE sensors, in order to predict the health of a pipeline for various operating conditions. The fusion of the signals was performed by a set of fuzzy rules that transformed the inputs, i.e. FRFs acquired using accelerometer sensors and transient signals obtained from AE sensors. The amalgamation of different signals compensates for the incomplete data of the sensors and increases the reliability of fault prediction, resulting in the increase of frequency bandwidth.

Figure 4.2 depicts the fuzzy analysis process where the quantitative outputs of different sensors and the estimated variations of the dynamic parameters are the inputs, generating a qualitative assessment of the pipeline conditions. The inference engine is located between the input and the output and consists of membership functions performing fuzzification, fuzzy rule-based aggregation and defuzzification (converting fuzzy values into crisp values) processes. In providing this qualitative assessment, the fuzzy logic model requires proper membership functions and weighting coefficients.

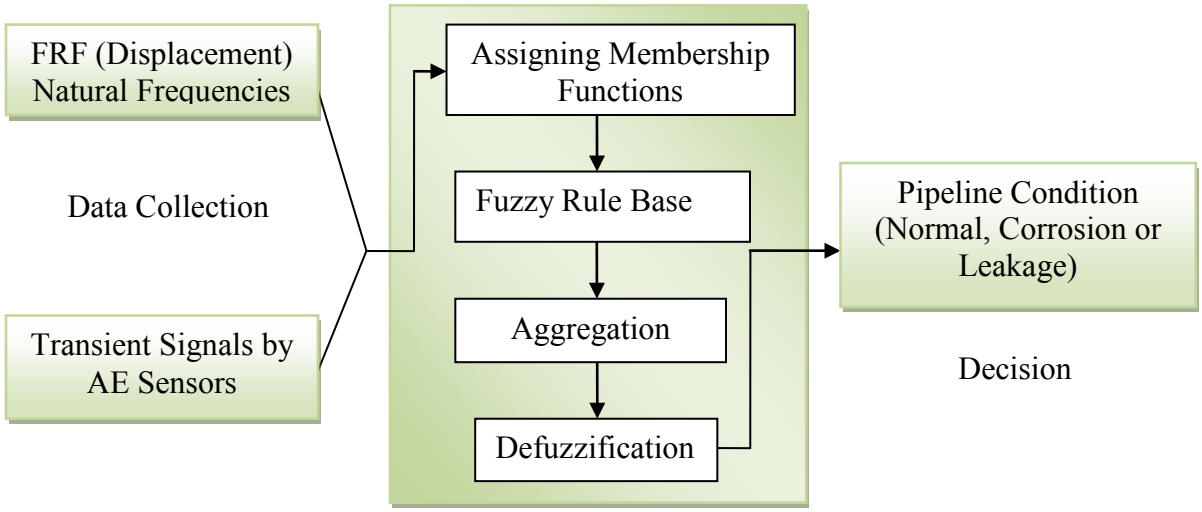

Figure 4.2: Fuzzy inference system structure

Finding the appropriate membership functions and required coefficients is, however, not easy. The ANFIS method employs a learning algorithm to determine the unknowns in the fuzzy inference engine [Jang et al., 1993]. Figure 4.3 illustrates a typical neuro fuzzy structure with *n* inputs, x_1 to x_n, and *m* membership functions in each fuzzy set. For a first-order Sugeno fuzzy model, a typical fuzzy rule can be written as:

$$\textbf{If } (x_1 \textbf{ is } A_{11}) \textbf{ and} \ldots (x_n \textbf{ is } A_{n1}) \textbf{ then } f_1 = p_{11}x_1 + \cdots + p_{1n}x_n + r_1 \qquad (4.1)$$

where *p* and *r* are coefficients of the linear relationship, and A is a nonlinear function that is found during the training process, which is also termed as a membership function.

The entire system architecture consists of five layers: a fuzzification layer, a product layer, a normalizing layer, a defuzzification layer and a total output layer, as depicted in Figure 4.3. The neuro fuzzy algorithm uses a supervised learning algorithm to determine a nonlinear model of input and output functions, namely the adaptive nodes. A hybrid method that uses the

gradient descent and least-squares methods is employed to identify the coefficients (p and r in Equation 4.1).

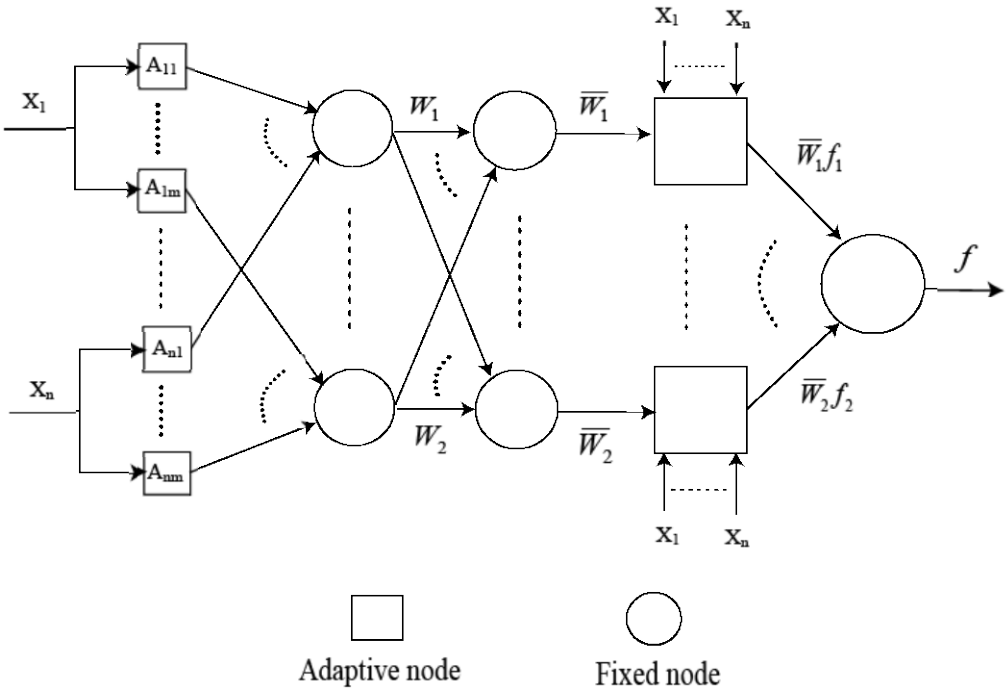

Figure 4.3: Adaptive neuro fuzzy inference system (ANFIS) structure [Jang et al., 1993]

4.1.1 Frequency Bandwidth of the Sensors

The fusion of different types of sensors provides a higher frequency bandwidth than with the use of only one type of sensor. This is particularly true for corroded and leaky pipeline conditions, where the signals are received in different ranges of frequency bands. For example, corroded pipes may give rise to signals that are in a different band of frequencies than transient signals.

In this research, accelerometer and AE sensors were used to cover a wide band of frequency range of signals emitting from a corroded or leaky pipeline. Figure 4.4 shows the

frequency bandwidths of the different sensors on a logarithmic scale. The features of the signals, such as the peak-to-peak and mean values and the root mean square (RMS), were extracted for use as inputs in the inference system.

It was found that the best feature of the signals in this study was the RMS, since it was a good representation of the energy of the signals and avoided unexpected signal jumps. The usage of the peak-to-peak value for the force signal did not significantly change the accuracy. Different combinations of sensor signals were fused with the ANFIS technique to determine the best combination for predicting pipeline conditions with accuracy.

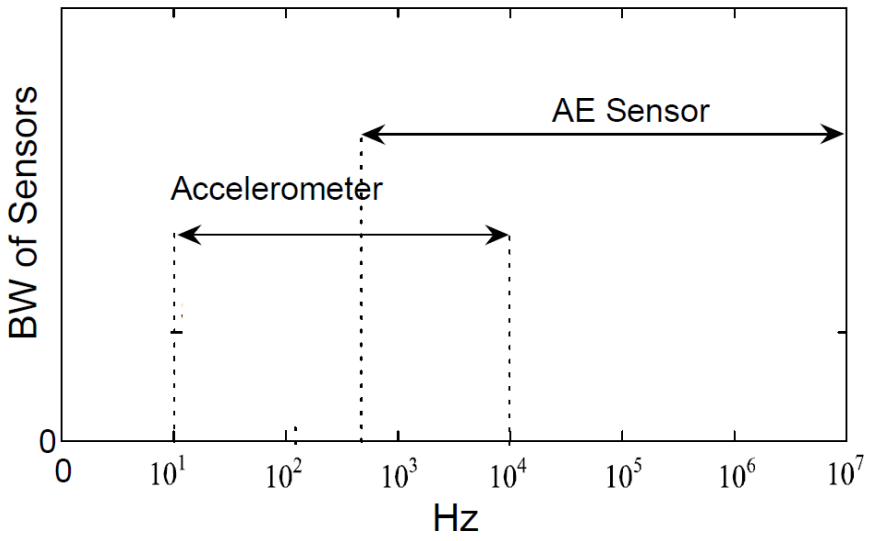

Figure 4.4: Frequency bandwidths of different sensors [Park et al., 2009]

4.2 Overall Strategy for the Development of the ANFIS-Based Pipeline Monitoring Scheme

The development of the ANFIS-based pipeline monitoring scheme was completed in two phases: training phase and verification phase. In the training phase, input variables, such as changes in natural frequency, vibro-acoustic signals and FRFs, were identified. Output variables predicted the pipeline condition. The datasets consisting of variations of the dynamic parameters for the corroded and leaky pipelines from the FE analysis were loaded to the ANFIS architecture as input variables. Considering the computational memory requirement, two independent pipeline monitoring schemes were planned: one for a corroded pipeline and one for a leaky pipeline.

The five input variables for the monitoring scheme of corroded pipelines were the changes of the natural frequencies in the empty corroded pipeline and the corroded pipeline with flow, ratios of FRFs for the empty corroded pipeline and corroded pipeline with flow, and changes in AE signals for the corroded pipeline with flow. Similarly, there were five input variables for the monitoring of leaky pipelines.

The training of the ANFIS-based scheme was an iterative process, which was performed using MATLAB^{TM} software. Once the training phase was completed, the verification of the trained ANFIS scheme was performed for multiple verification datasets of the input variables obtained from the EMA of the same pipeline in normal, corroded and leaky conditions at the same location on the pipeline.

4.2.1 Output Membership Functions

To predict the condition of the pipeline, the input datasets containing input variables and desirable output data was loaded to the ANFIS editor module of MATLAB^{TM}. A Sugeno type

fuzzy inference system was developed. The number of membership functions and types were defined for each of the input variables. If-then rules were generated by the ANFIS editor of MATLAB^{TM}, as were a set of the output membership.

All the output membership functions are defined as linear in a Sugeno type of ANFIS. The range of values for the output member ship functions were up to 0.3 for a normal pipeline, from 0.2 to 0.8 for mildly corroded or leaky pipeline, and more than 0.7 for corroded pipeline or leaky pipeline. In this way, the pipeline condition could be characterized with a certain percentage of two different conditions in the intersection region. This provided more robustness and suitability of the condition assignment of the pipeline system. The output membership functions for monitoring a corroded or leaky pipeline are shown in Figures 4.5(a) and 4.5(b), respectively

.

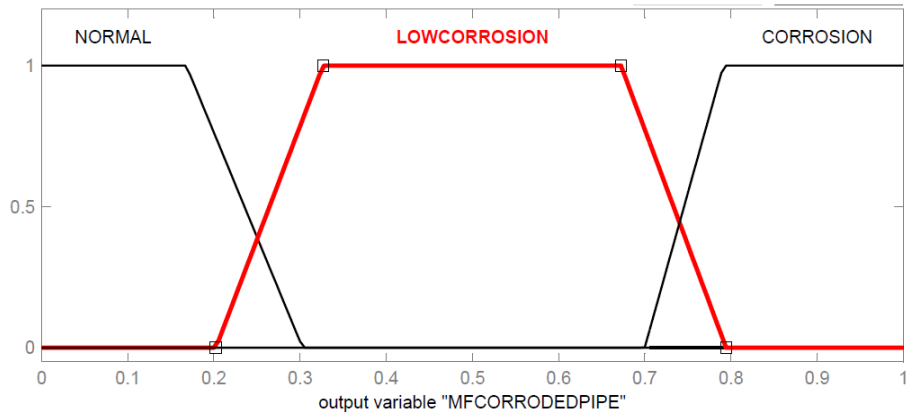

Figure 4.5(a): Output membership functions for a normal or corroded pipeline

In this study corroded condition is simulated by machining out 1.6 mm of pipe wall thickness in a single step from the outer surface of the middle spool of the pipeline setup for FE analysis and EMA. The output membership function with the value above 0.7 is used to train the

ANFIS for the corroded pipeline portion of the pipeline assembly. Physically there is no portion of pipeline which is simulated as low corroded, however one of the membership functions with the range of values from 0.2 to 0.8 is assigned to predict the pipeline condition as low corroded to account for variation in thickness of the pipeline assembly.

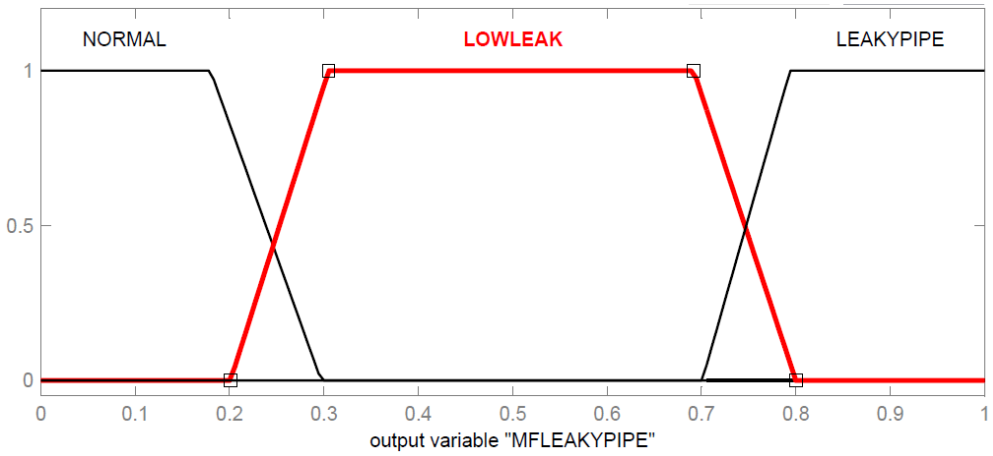

Figure 4.5(b): Output membership functions for a normal or leaky pipeline

Similarly, the leaky condition was simulated by making a hole of 6.35 mm in the middle pipe spool of the pipeline assembly. The output membership function with the value above 0.7 is used to train the ANFIS for the leaky pipeline portion of the pipeline assembly. Physically there is no portion of pipeline which is simulated as low leaky portion of the pipeline; however, one of the membership functions with the range of values from 0.2 to 0.8 is assigned to predict the pipeline condition as low leaky to account for variation in rate of leak from the pipeline assembly.

In all the output membership functions are designed to predict the normal, low leak, low corroded, leaky and corroded condition of the pipeline using ANFIS algorithm for the pipeline assembly in this study.

4.2.2 Training of the ANFIS-Based Pipeline Monitoring Scheme

In order to be able to verify the pipeline conditions from the input data obtained from the EMA, the ANFIS algorithm needed to be trained with an appropriate set of training data that was comprised of the variations in the dynamic parameters, such as FRFs estimated with the FE analysis and natural frequencies estimated from frequency-domain signals converted from the time-domain signals recorded using AE sensors.

The values of the output membership functions for predicting the pipeline condition are as shown in Figure 4.5(a) and Figure 4.5(b). FE analyses were performed for various physical conditions and operating conditions of the pipeline; and, the FRF values were estimated at five locations on the pipeline setup, as per the experimental setup for the EMA. Section 3.1.1 lists the physical and various operating conditions of the pipeline setup. AE signals captured with the AE sensors at the locations 2 and 5 on the pipeline were used for the training and verifying the ANFIS architecture

4.2.2.1 Input Variables for Corroded or Normal Pipelines

Five variables were selected for the monitoring scheme for corroded pipeline which are the changes of natural frequencies for an empty pipeline and a pipeline with flow in corroded condition from normal condition, ratios of FRFs of a corroded pipeline to FRFs of a normal pipeline in empty condition and with flow, and changes of AE signals. The AE signals were recorded in the time domain, which were represented as time versus AE signals in millivolts. To make the AE signals more meaningful for interpretation, the time-domain signals were converted to frequency-domain signals, which were represented as frequency versus AE signals in millivolts.

Each of the input variables was mapped by three membership functions. Bell type membership functions (MFs) were chosen to map the values for the input variables of the monitoring scheme for a normal or corroded pipeline. The range of values for the input variable is given in Table 4.1.

Table 4.1: Range of values for the MFs for the input variables for monitoring a normal or corroded pipeline

Input variables		Range of values	No. of MFs
Input1	Change of natural frequencies for corroded pipeline with flow	-250 Hz to 75 Hz	3 (Bell Type Curve)
Input 2	Ratio of FRFs for corroded pipeline with flow	0 to 50	3 (Bell Type Curve)
Input 3	Change of AE signals	0-6 mill-volts	3 (Bell Type Curve)
Input 4	Change of natural frequency for the corroded pipeline in empty condition	-175 Hz to 120	3 (Bell Type Curve)
Input 5	Ratio of FRFs for corroded pipeline in empty condition	0 to 20	3 (Bell Type Curve)

4.2.2.2 Input Variables for Normal or Leaky Pipelines

Similar to the monitoring scheme for corroded pipelines, five input variables for the monitoring scheme for leaky pipeline were selected. The AE signals were converted to frequency domain from the time domain signals, which were represented as time versus AE signals in millivolts. Each of the input variables was mapped by three membership functions. Bell type MFs were used to map the input variables. The ranges of values for the input variables are given in Table 4.2.

Table 4.2: Range of values for the MFs for monitoring a normal or leaky pipeline

Input variables		Range of values	No. of MFs
Input1	Change of natural frequencies for leaky pipeline with flow	-150 Hz to 50Hz	3 (Bell Type Curve)
Input 2	Ratio of FRFs for leaky pipeline with flow	0 to 50	3 (Bell Type Curve)
Input 3	Change of AE signals for leaky pipeline	0 to 18 mV	3 (Bell Type Curve)
Input 4	Change of natural frequency for the leaky pipeline in empty condition	-15 Hz to 1010 Hz	3 (Bell Type Curve)
Input 5	Ratio of FRFs for leaky pipeline in empty condition	0 to 50	3 (Bell Type Curve)

For the ANFIS training, the variations of natural frequencies were calculated for first 18 modes shapes for the corroded pipeline and leaky pipeline with and without water flow. The AE signals were converted from the time domain to frequency domain. Each of the data sets had values for five input variables. In total there are 18 datasets for ANFIS training and each dataset is independent of each other.

The next step was the development of a set of if-then rules to process the input variables. The ANFIS editor of MATLAB^{TM} generated if-then rules based on the number of input variables and the defined number of MFs for each input variable. The schematics for the completely developed plant dynamics from the ANFIS-based methodology are presented in Figure 4.6(a).

The schematics given in Figure 4.6(a) are applicable for monitoring corroded and leaky pipelines. In each case, there were five input variables, and each of the input variables were mapped by three MFs. Therefore, a total of 243 of if-then rules were developed. It is possible to

combine the ANFIS architecture for monitoring corroded and leaky pipelines; however, due to the limitation of memory requirement for the processing rule base of 243 x 243 (59,049), the schemes were designed separately.

Each of the ANFIS architectures for corroded or leaky pipeline to get trained from 90 values of five input variable calculated for 18 modes. However in the case of verification of ANFIS architecture, 21 modes were used while verifying ANFIS for corroded or leaky pipeline. Therefore there are 90 data points for ANFIS training and 105 data points for ANFIS verification.

Validity of ANFIS training algorithm

As described earlier 243 rules are automatically generated by ANFIS editor of MATLAB^{TM} based on the input and output membership functions to predict pipeline condition. When the datasets for 18 modes containing 90 values are loaded to ANFIS algorithm for training, each set of 5 values for input variables are checked against all the 243 rules and the aggregated output is computed as Equation 4.1. The objective of optimization process is to achieve aggregated output close to desired value for output membership function for pipeline condition during the training phase using hybrid learning mechanism. The hybrid learning mechanism optimises the parameter sets *p* and *r* as given in Equation 4.1 to arrive at aggregated value for the output membership function to predict pipeline condition.

The hybrid learning mechanism utilises the combination of least square estimates (LSE) and the gradient descend method. In a forward pass LSE is employed to update consequent parameters p and r and in a backward pass, the gradient descend method is used to update the

premise parameters and finally the aggregated output value is computed after selected numbers of epochs.

The errors are plotted for each epoch of optimisation process as shown in Figure 4.7 to Figure 4.10. The number of epoch are so selected that the error value stabilises for subsequent epochs. The amounts of error shown in Figures 4.7 to Figure 4.10 are very low which clearly proves the validity of using the rules to map the input variables for normal, corroded or leaky pipeline.

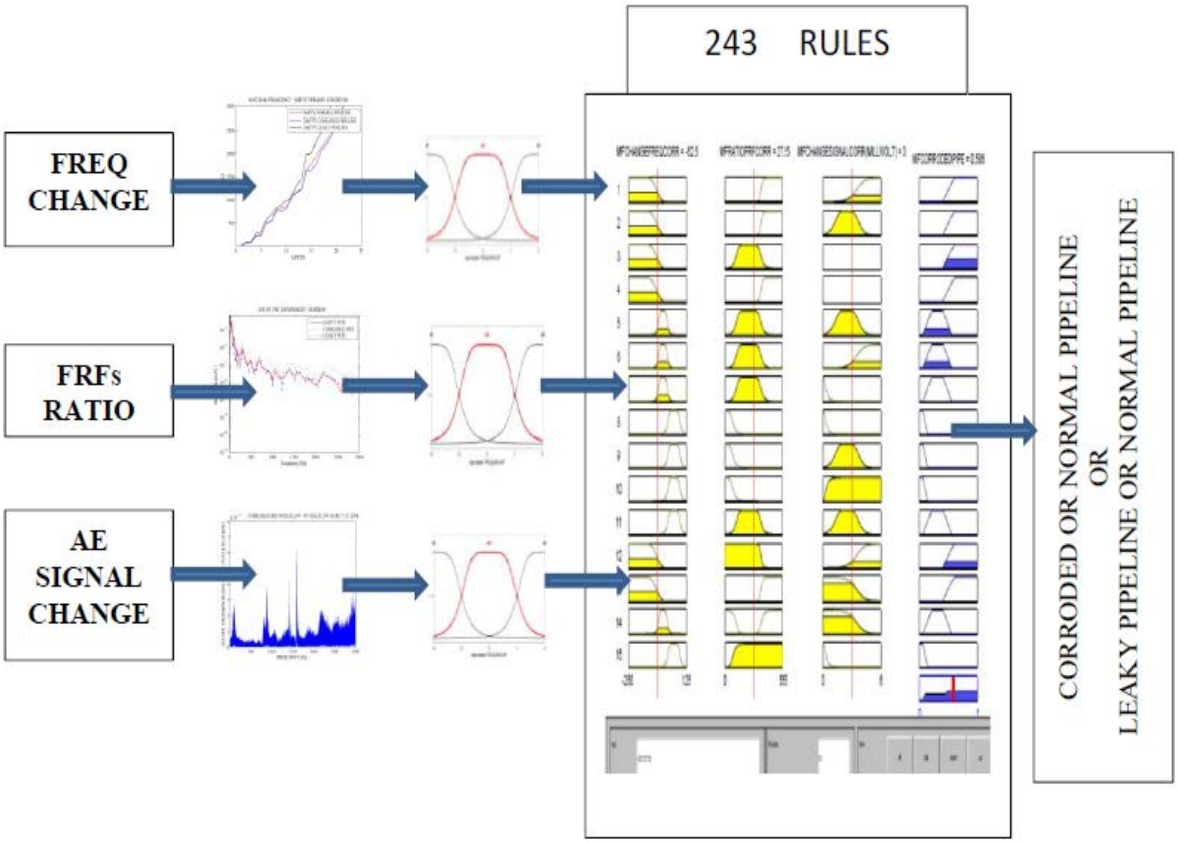

Figure 4.6(a): Schematics of fuzzy inference systems for corroded or leaky pipeline monitoring

The next step was the training of the ANFIS-based scheme. For the purpose of training, the database obtained from the FE analysis was used; and, AE signals recorded for a normal pipeline and a corroded or leaky pipeline were used. Locations 2 and 5 on the pipeline setup were chosen for the purpose of training.

ANFIS automatically generated if-then rules based MFs for the input variables. Based on the three MFs for each of the five variables, 243 if-then rules were generated. The typical ANFIS architecture for monitoring the corroded or leaky pipeline is shown in Figure 4.6(b).

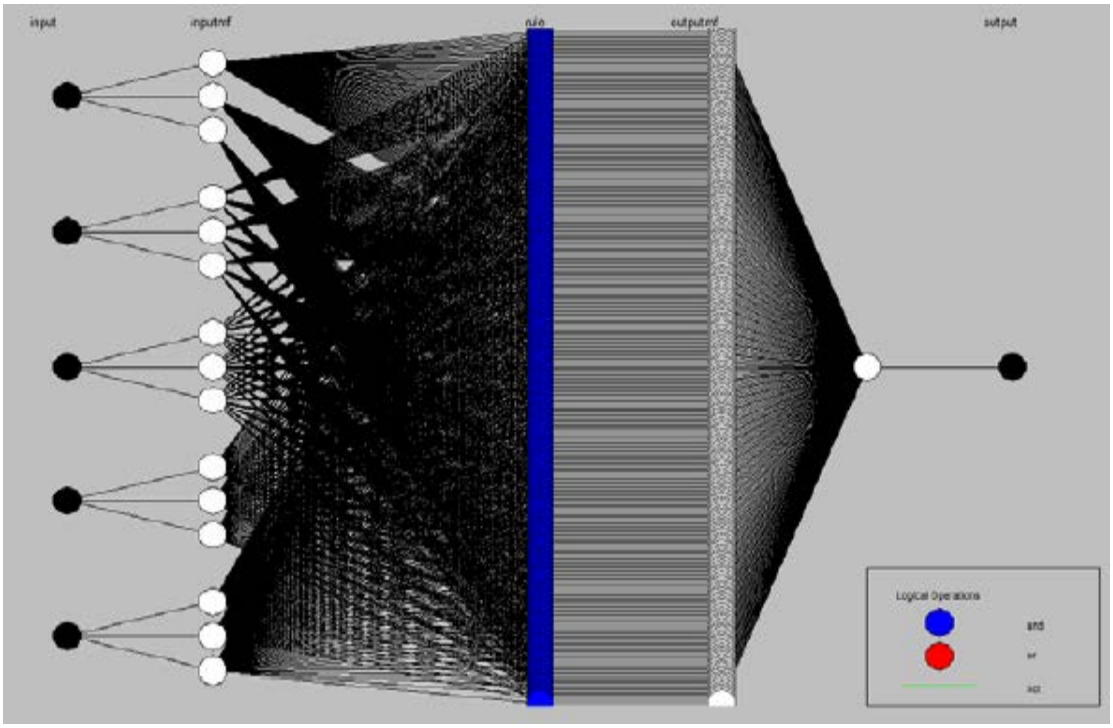

Figure 4.6(b): The typical ANFIS architecture for monitoring the corroded or leaky pipeline

4.2.3 Training the ANFIS Scheme for Normal or Corroded Pipelines

The middle of three pipe spools was thinned down to simulate corrosion during the EMA of the pipeline setup. Location 5 on the pipeline was to the right of the middle spool, which was

in fact in its normal condition. The training dataset obtained from the FE analysis at location 5 was used to train the ANFIS for the normal condition of the pipeline. The pressure in the pipeline was 207 kPa and the flow rate was 5.22 L/min. Table 4.3 contains the training dataset for the normal portion of the corroded pipeline. For the AE signals for the corroded pipeline the Pressure is 207 kPa and flow rate is 4.14 L/min

The values for the five input variables given in Table 4.3 were loaded to train the ANFIS architecture in MATLAB^{TM} toolbox for the normal portion of the corroded pipeline. The number of epochs was kept as twenty-five. The dataset for the training had five columns for five input variables, and the last column contained the index for the actual conditions of the pipeline. The index for the actual pipeline condition is given in the sixth column, which is based on the output membership function as per Figure 4.5 (a).

The training errors for 25 epochs for the training dataset for the normal portion of the corroded portion of the pipeline are shown in Figure 4.7. The training after 25 epochs is 4×10^{-7} which is almost negligible. Therefore the training phase has successfully mapped the training dataset using bell type of membership functions for the input variables.

Table 4.3: Values for the input variables for ANFIS training for the normal portion of the corroded pipeline at location 5

Data set index	Input 1 Change of natural frequency with flow (Hz)	Input 2 Ratio of FRFs with flow	Input 3 AE signal change (mV)	Input 4 Change of natural frequency in empty condition (Hz)	Input 5 Ratio of FRFs in empty condition	Output 1 Index for actual condition
1	-0.679	1	0.1	-1.024	1.2	0.2
2	-6.801	0.9	0.3	-6.622	1.2	0.2
3	1.17	0.8	0.3	1.479	1.3	0.2
4	-13.79	1.9	0	-13.39	1.4	0.2
5	-15.85	1.8	0	-15.32	1.3	0.2
6	3.77	0.8	0	5.3	1.2	0.2
7	0	0.7	0	10.45	1.9	0.2
8	8.81	0.6	0.1	-42.58	1.6	0.2
9	-50.67	0.5	0.1	-73.91	1.6	0.2
10	-69.38	6.2	0.2	-51.06	1.6	0.2
11	-54.92	2.7	0.2	111.7	1.9	0.2
12	0	2.1	0.1	-5.5	1.9	0.2
13	-3.6	1.2	0.5	-11.6	1.8	0.2
14	70.1	0.9	0	-33.9	1.7	0.2
15	65.1	0.5	0.4	-135.6	1.7	0.2
16	0	3.6	0.2	-174.6	1.8	0.2
17	-20	2.6	0.2	-67	2.5	0.2
18	-68.7	2.2	1.4	-88.8	3.4	0.2

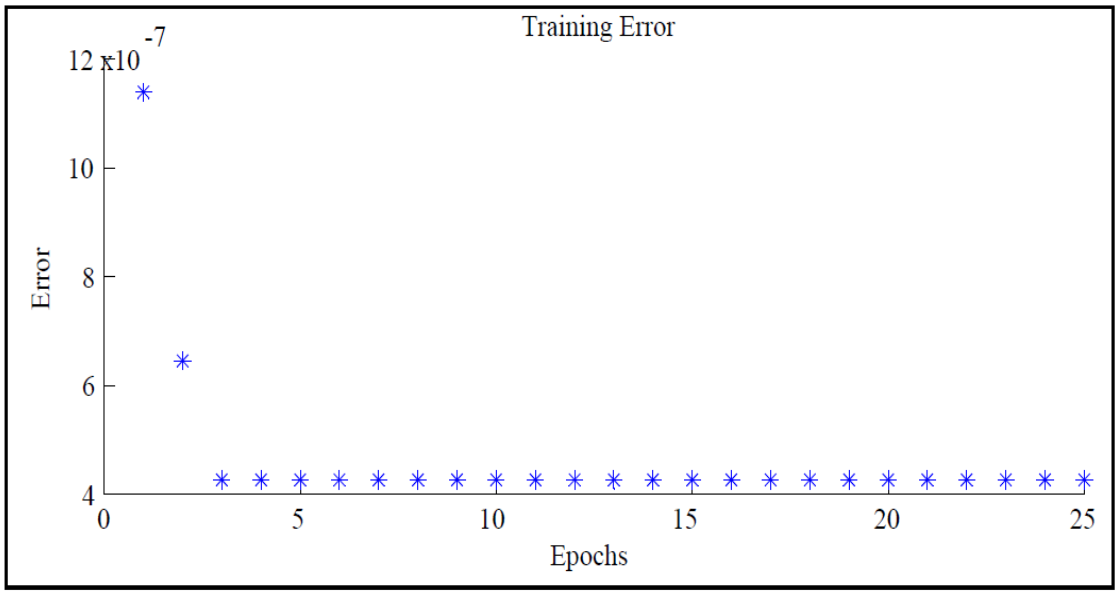

Figure 4.7: Training Error for the training data set for the normal portion of the corroded pipeline at location 5

To train the ANFIS algorithm for the corroded portion of the pipeline, location 2 on the pipeline was chosen, since the middle spool was used to simulate corrosion and leakage. The input variables were estimated for the first 18 mode shapes for the pipeline using FE analysis. The values for the input variables are listed in Table 4.4. The pressure and flow rate in the pipeline were 207 kPa and 5.22 L/min respectively.

The values for the five input variables given in Table 4.4 were loaded to train the ANFIS architecture for the corroded portion of the pipeline. The numbers of epochs were kept as twenty-five. The index for the actual pipeline condition is given in the sixth column, which is based on the output membership function as per Figure 4.5 (a).

Table 4.4: Values for the input variables for ANFIS training for the corroded portion of the pipeline at location 2

Data set index	Input 1	Input 2	Input 3	Input 4	Input 5	Output 1
	Change of natural frequency with flow(Hz)	Ratio of FRFs with flow	AE signal change (mV)	Change of natural frequency in empty condition(Hz)	Ratio of FRFs in empty condition	Index for actual condition
1	-0.679	0.9	0.8	-1.024	1.5	0.9
2	-6.801	0.8	0.1	-6.622	1.4	0.9
3	1.17	0.8	0.4	1.479	1.5	0.9
4	-13.79	1.7	0.1	-13.39	1.2	0.9
5	-15.85	1.5	0.4	-15.32	1.1	0.9
6	3.77	0.8	0.1	5.3	2	0.9
7	0	0.7	0.4	10.45	2.8	0.9
8	8.81	0.6	0.7	-42.58	1.5	0.9
9	-50.67	7.7	0.1	-73.91	1.5	0.9
10	-69.38	6.8	0.3	-51.06	1	0.9
11	-54.92	2.9	0.1	111.7	4.4	0.9
12	0	2.5	0.1	-5.5	4	0.9
13	-3.6	2	0.3	-11.6	3.4	0.9
14	70.1	1.4	0.1	-33.9	1.2	0.9
15	65.1	0.6	0.4	-135.6	1.1	0.9
16	0	5.8	0.2	-174.6	2.8	0.9
17	-20	4.3	0.4	-67	5.3	0.9
18	-68.7	3.8	1.3	-88.8	5.2	0.9

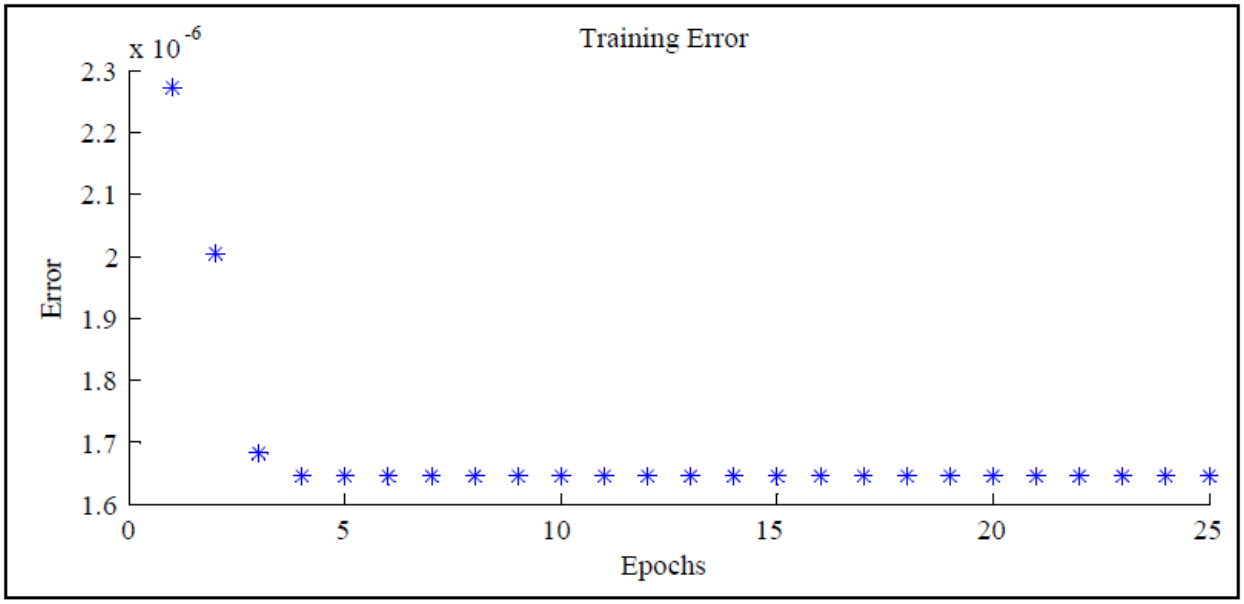

Figure 4.8: Training Error for the training data set for the corroded portion of the pipeline at location 2

The training error plot for the dataset for corroded portion of the pipeline at location 2 is as shown in Figure 4.8. The training error is 1.65 x 10^{-6}. The training error is small therefore the mapping of the training dataset for the corroded portion of the pipeline is quite good using bell type of membership functions for input variables.

4.2.4 Training the ANFIS Scheme for Normal or Leaky Pipelines

The training datasets obtained from the FE analysis at location 5 on the pipeline was used to train the ANFIS for the normal portion of the leaky pipeline. The pressure, flow rate and leakage rate in the pipeline were 0.0 kPa, 7.38 L/min and 8.89 L/min, respectively. Table 4.5 contains the training dataset for the normal portion of the leaky pipeline. For the AE signals for the leaky pipeline the pressure is 76 kPa and the flow rate is 15 L/min. The values for the five input variables given in Table 4.5 were loaded to train the ANFIS architecture for the normal portion of the leaky pipeline. The number of epochs was kept as twenty-five. The index for the

actual pipeline condition is given in the sixth column, which is based on the output membership function as per Figure 4.5 (b).

Table 4.5: Values for the input variables for ANFIS training for the normal portion of the leaky pipeline at location 5

Data set index	Input 1 Change of natural frequency with flow(Hz)	Input 2 Ratio of FRFs with flow	Input 3 AE signal change (mV)	Input 4 Change of natural frequency for empty condition(Hz)	Input 5 Ratio of FRFs in empty condition	Output 1 Index for actual condition
1	0.436	0.9	0.9	2.254	0.15	0.15
2	0.712	0.9	0.6	6.777	0.2	0.15
3	0.669	0.8	0.2	9.633	4	0.15
4	1.54	1.1	0	43.63	0.7	0.15
5	2.13	1.3	0.2	61.49	0.9	0.15
6	5.65	0.6	0.5	85.7	0.3	0.15
7	-1.58	0.6	0.1	139.76	8.9	0.15
8	7.86	0.5	0.2	33.53	1.3	0.15
9	3.63	2.2	0	69.31	0.9	0.15
10	-10.75	2.2	0.2	123.51	2	0.15
11	7.23	2.8	0	41	1.3	0.15
12	0.4	0.6	0	163.1	0.9	0.15
13	-50.5	0.5	0.1	194.3	7.5	0.15
14	2.1	0.5	0.4	321.4	0.6	0.15
15	3.5	0.4	0	225.4	0.5	0.15
16	-6.9	2.3	0.1	329.3	0.2	0.15
17	15.1	1.6	0.3	318.8	0.7	0.15
18	20.8	1.6	0.5	329.2	1.5	0.15

The plot for the training error for the training data set given in Table 4.5 is as shown in Figure 4.9. The training error after 25 epochs is 8.14×10^{-7}. It is obvious that the training error is

small and therefore the mapping of the training dataset is good using bell type membership functions.

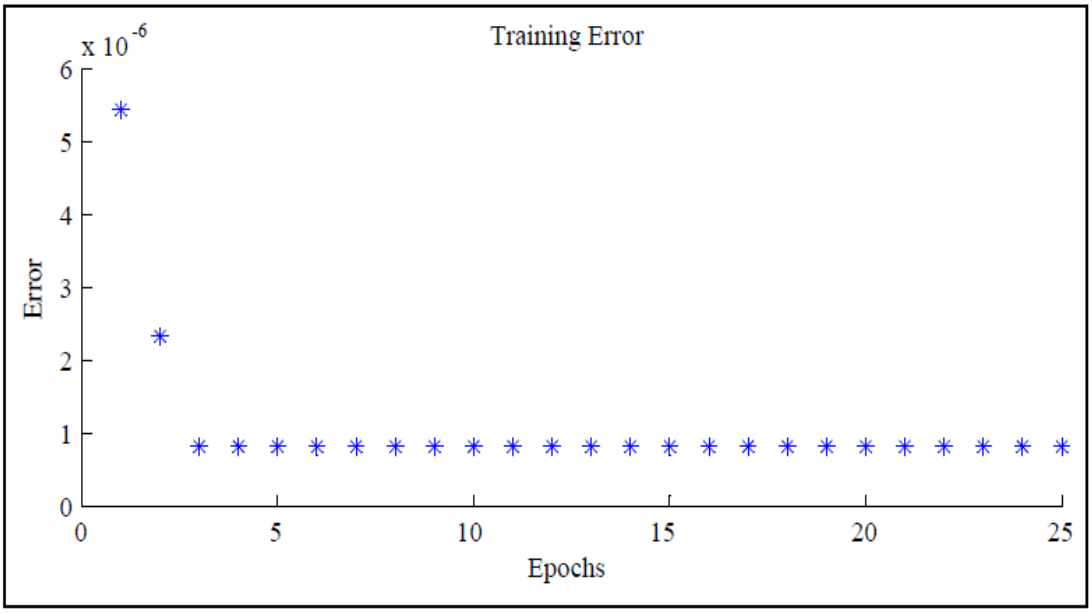

Figure 4.9: Training Error for the training data set for the normal portion of the leaky pipeline at location 5

As with the corroded pipeline, location 2 on the pipeline was chosen for the training dataset for the leaky portion of the pipeline, the middle spool was used to simulate leakage by drilling a hole in the middle. The input variables were estimated for first 18 mode shapes for the pipeline using FE analysis. The values for the input variables are listed in Table 4.6. The pressure, flow rate and the leakage rate in the pipeline were 0.0 kPa, 7.38 L/min and 8.89 L/min, respectively.

The values for the five input variables given in Table 4.6 were loaded to train the ANFIS architecture for the leaky portion of the pipeline. The numbers of epochs were kept as twenty-five.

The index for the actual pipeline condition is given in the sixth column, which is based on the output membership function as per Figure 4.5 (b).

Table 4.6: Values for the input variables for ANFIS training for leaky portion of the pipeline at location 2

Data set index	Input 1 Change of natural frequency with flow(Hz)	Input 2 Ratio of FRFs with flow	Input 3 AE signal change (mV)	Input 4 Change of natural frequency in empty condition(Hz)	Input 5 Ratio of FRFs in empty condition	Output 1 Index for actual condition
1	0.436	0.9	0.5	2.254	0.8	0.9
2	0.712	0.9	0.3	6.777	0.3	0.9
3	0.669	0.9	0.1	9.633	4.6	0.9
4	1.54	1.1	0.1	43.63	1.4	0.9
5	2.13	1.1	0.1	61.49	1.9	0.9
6	5.65	0.3	0.2	85.7	1.2	0.9
7	-1.58	0.3	0.0	139.76	8.6	0.9
8	7.86	0.3	0.2	33.53	2.2	0.9
9	3.63	1.6	0.1	69.31	2.4	0.9
10	-10.75	1.6	0.0	123.51	4.6	0.9
11	7.23	1.5	0.0	41	0.9	0.9
12	0.4	1.2	0.1	163.1	0.7	0.9
13	-50.5	1.4	0.0	194.3	8.1	0.9
14	2.1	0.2	0.2	321.4	1.5	0.9
15	3.5	0.3	0.1	225.4	1.3	0.9
16	-6.9	2	0.1	329.3	0.1	0.9
17	15.1	1.6	0.0	318.8	0.1	0.9
18	20.8	1.6	0.0	329.2	1.3	0.9

The training errors for the training dataset given in Table 4.6 is as shown in Figure 4.10. The training error is 3.9 x 10^{-6}. That means the training mapped accurately using bell type member ship functions.

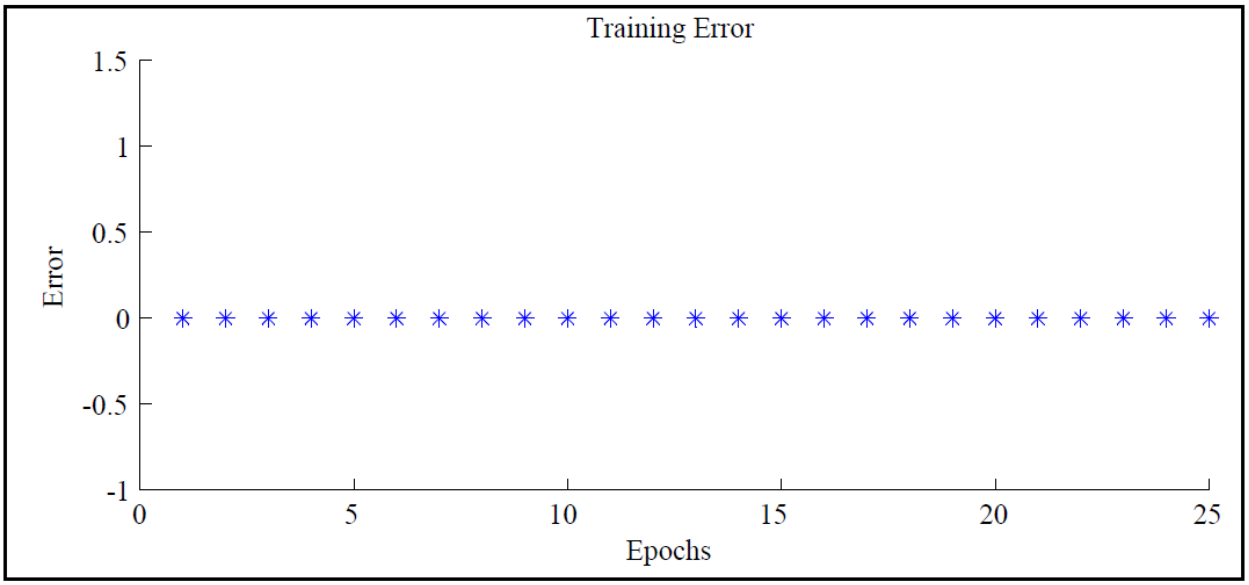

Figure 4.10: Training Error for the training data set for the leaky portion of the pipeline at location 2

4.2.5 Verification and Prediction Pipeline Conditions

In order to perform verification of the ANFIS algorithm, verification datasets from EMA were used; and, as in the training phase, locations 2 and 5 on the pipeline were used for the verification datasets of the leaky or corroded portions of the pipeline and the normal portions of the leaky or corroded pipeline. AE signals at locations 2 and 5 on the pipeline were used for verifying the ANFIS architecture for the pipeline health monitoring scheme. The format of the datasets for verifying the ANFIS architecture was kept the same as in the training phase.

4.2.5.1 Verifications of the ANFIS algorithm for Normal or Corroded Pipelines

Five input variables are estimated for each of the first 21 mode shapes for the pipeline using the EMA of the corroded pipeline. In total there are 105 data points for ANFIS verifications. The values for the input variables are listed in Table 4.7 for testing the ANFIS scheme at location 5 for the normal portion of the leaky pipeline. Table 4.8 contains the verification dataset for the corroded portion of the pipeline at location 2. The pressure in the pipeline was 207 kPa, and the flow rate was 5.22 L/min. For AE signals the pressure is 207 kPa and the flow rate is 4.47 L/min.

The verification dataset as per Table 4.7 was loaded to verify the ANFIS algorithm for the normal portion of the corroded pipeline. The verification data set as per Table 4.7 was loaded to verify the ANFIS algorithm for the normal portion of the corroded pipeline. The ANFIS editor of MATLAB^{TM} requires a desired reference output value to be loaded for comparison purpose and it is chosen from membership functions for normal condition of the pipeline for the comparison between ANFIS output and the desired output. Therefore, the value of 0.2 was chosen for the output membership function for the pipeline condition because the datasets under verification belongs to normal portion of the pipeline. The ANFIS results are plotted as shown in Figure 4.11.

Table 4.7: Values for the input variables for ANFIS verification for the normal portion of the corroded pipeline at location 5

Data set index	Input 1 Change of natural frequency with flow(Hz)	Input 2 Ratio of FRFs with flow	Input 3 AE signal change (mV)	Input 4 Change of natural frequency in empty condition(Hz)	Input 5 Ratio of FRFs in empty condition
1	-1	1	0.1	1	1.6
2	28	0.9	0	-1	1.1
3	-9	0.6	0	-14	0.9
4	-4	3.9	0.1	43	3.6
5	-23	2.6	0.1	-3	1.7
6	-8	1.2	0.1	-26	0.7
7	-30	1.4	0.1	-28	1
8	-68	1.6	0	-120	1.5
9	-158	0.7	0.1	-40	1.3
10	-108	1	0.1	0	0.4
11	-78	1.2	0.4	95	1.6
12	64	1.9	0.3	-41	1.8
13	-25	0.7	0.7	-84	0.5
14	45	21.5	0.2	31	2
15	19	2.8	0.8	-118	3
16	74	0.9	0.6	-141	3.2
17	-28	1.3	1.5	-120	1.9
18	-21	0.3	0.3	-87	2.2
19	-250	0.27	1.3	-26	1.8
20	68	1.6	0.9	16	0.9
21	-18	1.7	0.9	9	3.6

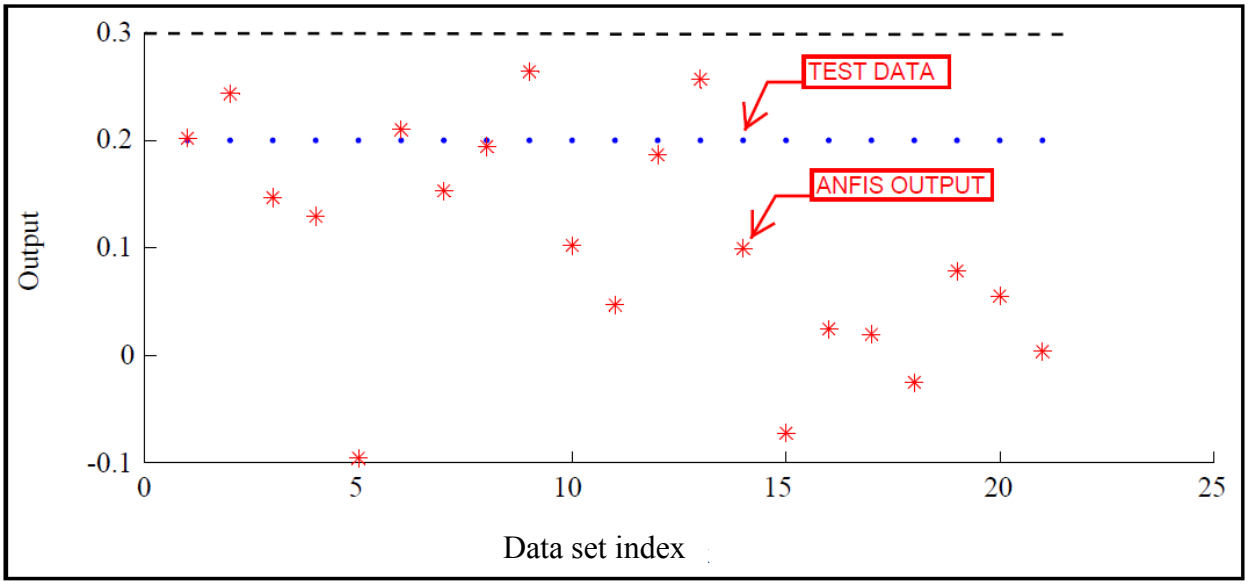

Figure 4.11: Testing the ANFIS scheme against the dataset for the normal portion of the corroded pipeline at location 5

As shown in Figure 4.5(a), the output membership functions for the normal conditions and low corroded condition have the range of reference values up to 0.3 and 0.2 to 0.8, respectively. The resultant values for 21 data sets from the ANFIS are below 0.3. The reference value for all the output values from ANFIS architecture was kept at 0.2 because the verification data sets are for location 5 on the pipeline which is in normal portion of the pipeline. As shown in the plot shown in Figure 4.11, four of the output values from ANFIS are between 0.2 to 0.3. The range of values 0.2 to 0.3 belongs to output membership functions for normal condition and low corroded condition and the membership grades are less than 1 in both the membership functions. That means these four output values predict pipeline condition as either normal condition or low corroded at location 5. Rest of the output values are below 0.2 or equal to 0.2, which clearly indicate that the pipeline condition is normal at location 5.

To verify the ANFIS algorithm for the corroded portion of the pipeline, the input variables were estimated at location 2 on the corroded portion of the pipeline and are given in Table 4.8. The range of values for the output MF for the corroded conditions of the pipeline is above 0.7 as shown in Figure 4.5(a). The values 0.2 to 0.8 are assigned to the output membership functions for low corrosion condition of the pipeline. The output membership for the low corrosion is defined to cover for the variation of the pipeline wall thickness due to allowable mill- tolerance on the wall thickness. The grid lines are shown in Figure 4.12 for the output values of 0.2 and 0.7. The desired reference output value is chosen from membership functions for corroded condition of the pipeline for the comparison between ANFIS output and the desired output. Therefore the value of 0.9 was chosen for the output membership function for the corroded pipeline condition because the datasets under verification belongs to corroded portion of the pipeline. Thirteen testing data values resulted in output values above 0.2, indicating the pipeline condition as either mildly or highly corroded.

The scatter of the testing output from the ANFIS predicted that there was a possibility for the pipeline to be highly corroded. Eight of the testing result values showed that the pipeline was normal at location 2 on the pipeline, which was an erroneous prediction. In general, the prediction from the ANFIS was that the pipeline had either low or high corrosion; however, there was an error of 39% in this prediction.

Table 4.8: Values for the input variables for ANFIS verification for the corroded portion of the pipeline at location 2

Data set index	Input 1 Change of natural frequency with flow(Hz)	Input 2 Ratio of FRFs with flow	Input 3 AE signal change (mV)	Input 4 Change of natural frequency in empty condition(Hz)	Input 5 Ratio of FRFs in empty condition
1	-1	1.8	0.3	1	5.9
2	28	2.8	0.2	-1	2.9
3	-9	2.7	0.2	-14	2.8
4	-4	1.2	0.3	43	3.6
5	-23	1.2	0.2	-3	3.7
6	-8	1.9	0.2	-26	0.7
7	-30	4.2	0.3	-28	2.3
8	-68	2.1	0.3	-120	2.7
9	-158	1.7	0.4	-40	26.6
10	-108	1.5	0.3	0	3.7
11	-78	2.8	0.3	95	6.3
12	64	1.8	0.1	-41	3.1
13	-25	1.7	0.4	-84	2.6
14	45	0.9	0.1	31	4.1
15	19	0.9	0.2	-118	11.8
16	74	2.1	0.5	-141	6.3
17	-28	2.6	0.7	-120	2.7
18	-21	0.5	0.2	-87	1.5
19	-250	0.5	0.8	-26	1.5
20	68	4.4	0.6	16	3.5
21	-18	3.8	1.1	9	16.5

The testing dataset was loaded to ANFIS editor and plotted against the ANFIS scheme output, as shown in Figure 4.12.

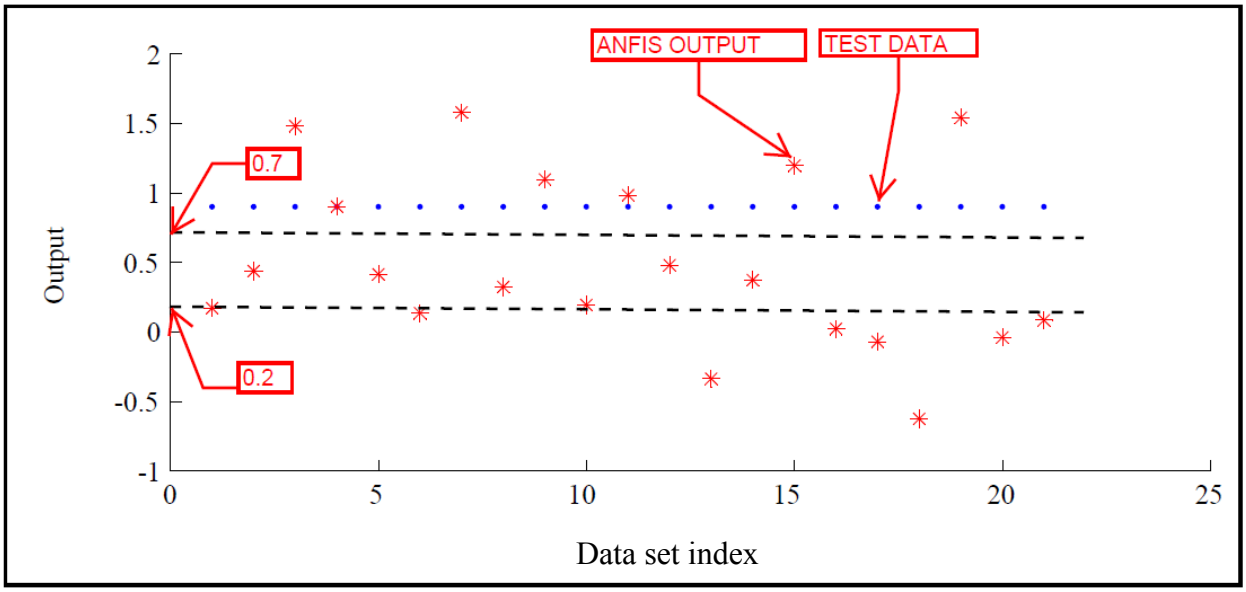

Figure 4.12: Testing results from ANFIS for the corroded portion of the pipeline at location 2

4.2.5.2 Verification of the ANFIS Algorithm for Normal or Leaky Pipelines

For the leaky pipeline, the input variables were estimated for first 21 mode shapes for the pipeline using EMA analysis. The values for the input variables are listed in Table 4.9 for the normal portion of the leaky pipeline at location 5, and Table 4.10 contains the verification dataset for the leaky portion of the pipeline at location 2. The pressure in the pipeline was 207 kPa, and the leakage rate was 8.89 L/min. For the AE signals the pressure is 34 kPa and the flow rate is 6.38 L/min with a leakage of 7.97 L/min

The verification dataset in Table 4.9 was loaded to the ANFIS algorithm for the normal portion of the leaky pipeline. The testing results from the ANFIS scheme were plotted against the testing data points and are shown in Figure 4.13.

Table 4.9: Values for the input variables for ANFIS verification for the normal portion of the leaky pipeline at location 5

Data set index	Input 1 Change of natural frequency with flow(Hz)	Input 2 Ratio of FRFs with flow	Input 3 AE signal change (mV)	Input 4 Change of natural frequency in empty condition(Hz)	Input 5 Ratio of FRFs in empty condition
1	0	1.7	0.1	2	0.8
2	40	0.9	0.1	12	1.1
3	-7	0.8	0.4	39	1.5
4	9	1.1	0.4	93	1.6
5	4	1.1	0.3	24	0.8
6	15	0.8	0.1	94	1.4
7	-39	0.9	0.4	143	1.5
8	-87	0.9	0	63	1.2
9	-148	1.6	0.1	68	0.7
10	-4	1.3	0.1	89	1.1
11	-39	1.2	0.5	-11	0.9
12	-13	1	0.2	145	0.8
13	23	0.1	0.2	98	0.7
14	-5	0.1	0.2	377	0.7
15	-20	1.9	0.3	238	2.2
16	14	0.8	0.5	297	2.7
17	-6	8.8	0.1	291	0.9
18	-38	1.1	0.2	389	0.5
19	8	0.5	0.7	674	1.6
20	16	0.6	1.1	469	3
21	15	0.9	0	862	0.7

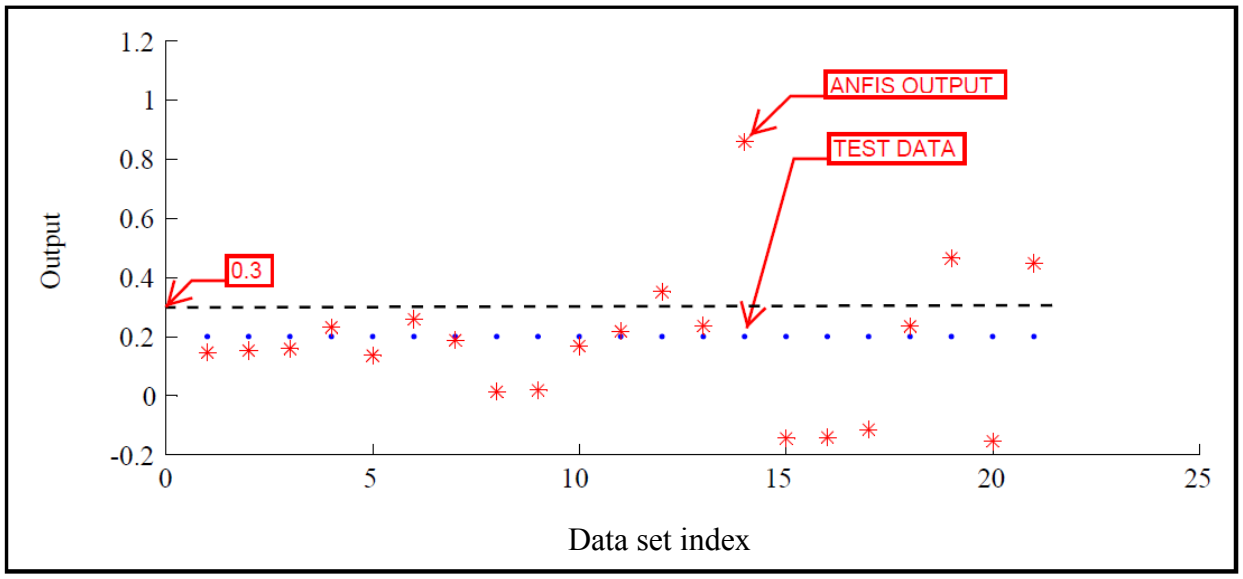

Figure 4.13: Testing result from the ANFIS scheme for the normal portion of the leaky pipeline at location 5

The value for the output MF for the normal pipeline condition was up to 0.3, as shown in Figure 4.5(b). The grid lines are shown in Figure 4.10 for the output value of 0.3. The reference value for the output MF for the normal portion of the pipeline was kept at 0.2, as per the testing dataset shown in Figure 4.13 Only three of output values for the testing data values were above 0.3, resulting in prediction error. The majority of the output values predicted that the pipeline was behaving normally at location 5. The prediction error was approximately 14%.

Table 4.10: Values for the input variables for ANFIS verification for the leaky portion of the pipeline at location 2

Mode Shapes	Input 1 Change of natural frequency with flow(Hz)	Input 2 Ratio of FRFs with flow	Input 3 AE signal change (mV)	Input 4 Change of natural frequency in empty condition(Hz)	Input 5 Ratio of FRFs in empty condition
1	0	1.4	0	2	2.5
2	40	1.6	0.4	12	1.9
3	-7	4.1	0.3	39	0.8
4	9	1.8	0.3	93	2.9
5	4	2.1	0.5	24	1.1
6	15	0.9	0.1	94	0.8
7	-39	1	0.4	143	2.1
8	-87	0.8	0.1	63	1.5
9	-148	0.9	0.3	68	0.9
10	-4	1.5	0.2	89	1.1
11	-39	1.6	0.6	-11	0.9
12	-13	0.8	0.1	145	0.6
13	23	1.5	0.1	98	1.1
14	-5	1.4	0.1	377	1.2
15	-20	1.2	0.7	238	1
16	14	2.1	0.4	297	1.3
17	-6	1.6	0	291	1.1
18	-38	2.3	0.6	389	1.9
19	8	0.8	0.5	674	2.2
20	16	0.8	0.6	469	2.8
21	15	0.2	0	862	2.7

Based on the testing dataset given in Table 4.10, the testing results from the ANFIS algorithm for the leaky pipeline are shown in Figure 4.14.

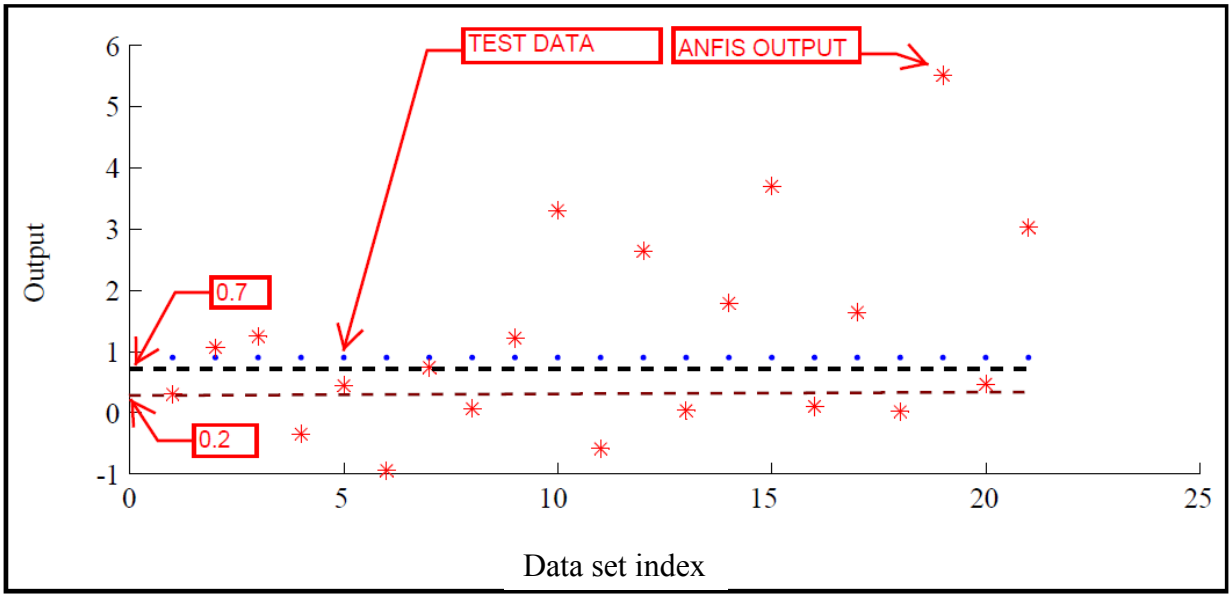

Figure 4.14: Verification of the ANFIS scheme for the leaky portion of the pipeline at location 2

The values for the output MF for mildly and severely leaky conditions of the pipeline were 0.2 to 0.7 and above 0.6, respectively, as shown in Figure 4.5(b). The grid lines are shown in Figure 4.14 for the values 0.2 and 0.7 for the output. The reference value for the output MF function for the corroded portion of the pipeline was kept at 0.9, as per the testing dataset shown in Figure 4.14

Fourteen test data values resulted in an output value above 0.2, indicating the pipeline condition were either mildly or severely leaky. The scatter of the test output from the ANFIS predicted that there was a more than 60% chance that the pipeline was severely leaky. Seven of the testing result values showed that the pipeline was normal at location 2 on the pipeline, which

were erroneous predictions. Therefore, the prediction from the ANFIS was that the pipeline was leaky. However, there was an error of 33% in this prediction.

4.3 Summary

The objectives of the training and testing of this novel ANFIS-based pipeline monitoring scheme were the provision of knowledge of the pipeline conditions and then the verification of the trained ANFI-based pipeline monitoring scheme, respectively. In total, four training datasets and four verification datasets were used. Two of the training and verification datasets were loaded to the ANFIS for the normal portions of the leaky and corroded pipelines. In both cases, the prediction from the ANFIS scheme strongly suggested that the pipeline condition was normal. The maximum prediction error was 14%, as shown in Figure 4.13.

The prediction for the corroded and leaky portions of the pipelines involved higher errors. In the case of the corroded portion of the pipeline, the prediction error was 39%, as shown in Figure 4.12. With the leaky portion of the pipeline, the prediction error was 33%, as shown in Figure 4.14.

The error in the predictions can be reduced by using larger training and verification datasets. Considering the ANFIS testing results for the normal, corroded and leaky pipelines, it can be inferred that the ANFIS-based architecture exhibits good potential for the prediction of pipeline conditions.

CHAPTER 5: SUMMARY

Pipeline inspection and monitoring are challenging tasks for owners and operators of pipeline networks. The pipeline industry is always looking for continuous improvements in pipeline integrity management. Safe and reliable operations of the pipeline network are of paramount importance for economic and environmental reasons.

5.1 Conclusions

The experimental modal analysis (EMA) of a small-scale pipeline analysis was performed to capture vibro-acoustic signals at five critical locations on a pipeline assembly setup. Separate setups of the pipeline were used to mimic the corroded and the leaky pipeline. The middle section of pipe spool was machined down to simulate corrosion (i.e. loss of materials); and, a hole was drilled at the centre of this middle pipe spool to allow leakage. Location 2 was located at the centre of the pipeline assembly and was a very important location for capturing the vibro-acoustic signal for the corroded or leaky portion of the pipeline. Locations 1 and 3 were characterised by the transition from the corroded/leaky portion of the pipe to normal pipeline portions on the both the sides; and, locations 4 and 5 are in the normal pipeline portions at the inlet and the outlet, respectively, for the flow of water in the pipeline assembly.

To investigate the variations of the dynamic parameters, algebraic differences were calculated for the natural frequencies and absolute difference were calculated for the AE signals between the corroded/leaky pipeline and normal operational pipeline. To obtain the changes infrequency response functions (FRFs), the ratios were calculated for the corroded/leaky portion

of the pipeline and the corresponding normal pipeline. The maximum variations of the dynamic parameters from the FE analysis and EMA are tabulated in Table 5.1.

The details of the variations of the dynamic parameters for the corroded/leaky pipeline with or without flow, as shown in Table 5.1, prove that the changes were appreciable. Therefore these variations of the variables, such as the natural frequencies, FRFs and AE signals, could be used to develop a novel scheme using the datasets of the variations of the dynamic parameters based on the ANFIS methodology.

As shown in Table 5.1, the ratios of the FRFs obtained from the EMA were relatively higher for the corroded/leaky pipeline with water flow than those of the empty corroded/leaky pipeline. However, the trend in the variations of the FRFs was not exactly the same in the case of the FE analysis for the maximum ratios of FRFs. The reason might be the assumption on the difference between the damping ratios for the EMA and FE. In the FE analysis, 2% damping was considered; which might have been quite different in the EMA, resulting in different trends for the maximum ratios of the FRFs. Another reason might be the assumption on the boundary conditions of the pipeline assembly.

The changes in the AE signals were higher for the leaky pipeline than those of the corroded pipeline, i.e. 5.36 millivolts for the corroded pipeline and 15.31 millivolts for leaky pipeline. This is self-evident, as the pipeline would experience higher disturbances in flow with leakage.

A novel contribution of this study is the fusion of sensor signals to broaden the frequency bandwidth while obtaining data for dynamic parameters for the pipeline using EMA in combination with ANFIS methodology to predict a pipeline's condition. This method does not disturb the operation of the pipeline, because the datasets are collected from the sensors. With

these datasets, computations using the ANFIS methodology can be performed to predict the condition of the pipeline; and, the operator can initiate action to prevent or minimise leakage.

Table 5.1: Maximum variation of dynamic parameters obtained from the FE analysis and EMA

Dynamic Parameters	EMA	FE Analysis
Maximum change of natural frequencies for empty corroded pipeline (Hz) for first 21 mode shapes	-141.0 (7.3%) for mode shape 16	-174.6 (9.9%) for mode shape 16
Maximum change of natural frequencies for empty leaky pipeline (Hz) for first 21 mode shapes	862.0 (30%) for mode shape 21	798.3 (29.2%) for mode shape 21
Maximum change of natural frequencies for the corroded pipeline with flow (Hz) for 21 mode shapes	-250.0 (12.3%) for mode shape 19	-242.4 (9.8%) for mode shape 19
Maximum change of natural frequencies for the leaky pipeline with flow (Hz) for first 21 mode shapes	-148.0 (18.5%) for mode shape 9	-50.5 (4.3%) for mode shape 13
Maximum ratio of FRFs for the empty corroded pipeline	32.27 @ location 2	14.48 @ location 2
Maximum ratio of FRFs for the empty leaky pipeline	12.79 @ location 2	47.59 @ location 1
Maximum ratio of FRFs for the corroded pipeline with flow	51.93 @ location 1	11.38 @ location 2
Maximum ratio of FRFs for the leaky pipeline with flow	43.95 @ location 5	17.31 @ location 4
Maximum change of AE signal for the corroded pipeline with flow (mV)	5.36 for Frequency 27411 Hz at location 5	
Maximum change of AE signal for the leaky pipeline with flow (mV)	15.31 for Frequency 51060 Hz at location 5	

In view of the analyses done on the variations of the dynamic parameters obtained from the EMA and FE analysis, it can be concluded that the changes in the natural frequencies were

appreciable and comparable, i.e. these variations in natural frequencies, FRFs and vibro-acoustic signals could be used to design and develop a monitoring scheme to predict pipeline health conditions.

Once the investigations of variations in the dynamic parameters of pipeline were completed, the main objective of this study was to develop an ANFIS-based pipeline monitoring scheme using these variations in the dynamic parameters. In the training and verification phases of the ANFIS scheme, the datasets from locations 2 and 5 on the pipeline were chosen. Location 2 was located on the corroded/leaky portion of the pipeline, and location 5 was on a normal portion of the corroded/leaky pipeline.

Four sets of data were used for the training and verification of the ANFIS-based pipeline monitoring scheme. Each of the training and verification datasets consisted of five input variables: changes in the natural frequencies for the corroded/leaky pipeline with or without water flow, the ratios of FRFs for the corroded/leaky pipeline with or without water flow, and changes in the AE signal for the corroded/leaky pipeline. Two of the four datasets were for the normal portion of the pipeline. The third and fourth training and verification datasets were for the corroded and leaky portions of the pipeline, respectively. The results of the training and testing are summarised as shown in Table 5.2.

As shown in Table 5.2, the ANFIS scheme predicted the normal portions of the corroded and leaky pipelines fairly accurately, with a maximum prediction error of 14%, as shown in Figure 4.13. For the third and fourth training and verification datasets, the prediction for the corroded or leaky portions of the pipeline involved higher errors. The prediction error was 39% for the corroded portion of the pipeline, as shown in Figure 4.12; and, the prediction error was 33% for the leaky portion of the pipeline, as shown in Figure 4.14. The higher prediction errors

could be reduced by using larger datasets and performing further investigations by reviewing the assumptions and accuracy of simulation of the pipeline conditions.

Table 5.2: Summary of the Predictions made by ANFIS based Pipeline monitoring scheme

Training and Verification Datasets	Training Error	Actual Pipeline Condition	Predicted Pipeline Condition	Verification or Prediction Error
First dataset at location 5 (normal portion in corroded pipeline)	4×10^{-7}	Normal	Normal	Very low
Second dataset at location 5 (normal portion in leaky pipeline)	8.14×10^{-7}	Normal	Normal	14%
Third dataset at location 2 (corroded portion of the pipeline)	1.65×10^{-6}	Corroded	Low corroded or Corroded	39%
Fourth dataset at location 2 (leaky portion of the pipeline)	3.9×10^{-6}	Leaky	Low leaky or Leaky	33%

This study was an effort to develop a novel approach to use ANFIS architecture to utilise the imprecise data of the variations of the dynamic parameters. Considering the ANFIS testing results for the normal, corroded and leaky pipelines, it can be inferred that ANFIS-based architecture for pipeline monitoring can be an excellent alternative to existing pipeline monitoring schemes for the safe operation of a pipeline network.

5.2 Assumption and Limitations

This research work used the combination of theoretical finite element analysis and experimental modal analysis (EMA) to gather data for variations of dynamic parameters. EMA was performed in the laboratory using 1 inch NPS carbon steel pipes joined by threaded couplings. The water flow from the existing domestic supply of water was used for the EMA. The simulation of the same physical and operating conditions was done while performing the FE analysis. The various assumptions and limitations of the FE analysis and EMA are described in the following subsection.

5.2.1 EMA and FE analysis

Water was used as the flowing medium in place of oil, due to its availability and the difficulty in making a laboratory pipeline setup using oil flow. Therefore, the study was limited to a single phase of a flowing medium in the pipeline, contrary to the presence of two phases in oil flow. The water flow in the pipeline was assumed to be isentropic and in-viscid (no viscous damping).

The pipeline size was 1 inch NPS for laboratory experiments, which is definitely not comparable to actual sizes of the pipeline in the field. Simulation was not possible using water to account for the noise generated by compressors in natural gas pipelines. In the field, most of the pipelines are buried, which largely affects the response of the pipeline. In the laboratory setup, the boundary conditions were kept very simple by clamping the pipeline on two ends. The overall length was kept as 1500 mm, due to the availability of space.

No specific simulation was made for the defects caused by stress corrosion cracking in the pipeline assembly setup. The corrosion in the pipeline was simulated by thinning the middle

portion of the pipeline; whereas corrosion in a pipeline is a very complicated phenomenon, and it is not possible to simulate corrosion just by thinning down the pipe in a pipeline assembly. Moreover, no consideration was given to sedimentation in the pipeline, which is very common in all pipelines in the field.

The acoustic pressure and displacement amplitudes were small relative to the fluid's ambient state in the experiments. To compute the response of the structure, it was assumed that the combination of forces was linear and applied simultaneously and that the resultant response of the pipeline was the sum of the individual responses to each of the forces acting alone.

Another basic assumption was that the structure was time invariant, i.e. the determined parameters were constants. In general, a system that is not time invariant will have components, such as mass, stiffness or damping, that depend on factors that are not measured or were not included in the model. For example, some components may be temperature dependent. In this case, the temperature of the component was viewed as a time-varying signal; hence, the component had time-varying characteristics. Therefore, the modal parameters that would be determined by any measurement and estimation process would depend on the time (by this temperature dependence) for any measurements made. If the structure that is being tested changes with time, the measurements made at the end and the beginning of the test period would determine a different set of modal parameters. Thus, the measurements made at the two different times will be inconsistent, violating the assumption of time invariance.

Another important assumption is that the structure obeys Maxwell's reciprocity (i.e. a force applied at degree of freedom (DOF) p causes a response at DOF q that is the same as the response at DOF p caused by the same force applied at DOF q). With respect to FRF measurements, the FRF between points p and q determined by excitation at p and response

measurement at q is the same FRF as found by excitation at q and response measurement at p ($H_{pq} = H_{qp}$).

A very basic assumption is that the structure is observable, i.e. the input-output measurements that are made contain enough information to generate an adequate behavioural model of the structure. Structures and machines that have loose components or, more generally, have DOFs of motion that are not measured are not completely observable.

The number and location of measurement sensors is another important issue that has not been addressed to any significant extent in the current literature. Many techniques that appear to work well in example cases actually perform poorly when subjected to the measurement constraints imposed by actual testing.

Computation difficulties due to software limitation also limit the extraction of the number of modes. This research was limited to the modes up to 3000 Hz; and, accordingly, the FRFs were estimated up to 3000 Hz. Even if the EMA response was available up to 8000 Hz and the AE signals were obtained for more than 65,000 Hz, the limitation of the response detection time for accelerometer and AE sensors would result in impreciseness of the collected data for the FRF and vibro-acoustic signals.

5.2.2 ANFIS

The consequent part of fuzzy rules should be a linear combination of the consequent parameters, and then only least square estimation (LSE) can be used to find the global optimal values for these parameters. The ANFIS architecture has been implemented with five inputs and a single output. This method is based on an assumption that the ANFIS model with the smallest

root mean squared error (RMSE) after one epoch of training has a greater potential to achieve a lower RMSE when given more epochs of training.

The training of a neural network may require a large number of iterative calculations. Furthermore, the network may not be able to adequately learn the desired function. In other words, transferring human knowledge into a fuzzy inference system and building a rule base is not always straightforward and simple. Therefore, a thorough understanding of plant dynamics is must.

Due to the limitations of the computational power of the computer used for developing the ANFIS-based pipeline monitoring scheme, two separate ANFIS schemes were proposed: one for corroded pipelines, and one for leaky pipelines. The combined ANFIS-based pipeline monitoring scheme for corroded and leaky pipelines can be developed using a computer with high computational power.

5.3 Recommendations for Future Work

The first and foremost task would be to overcome the limitations of the laboratory setup. A portion of operational pipelines in the field could be selected with oil or gas flow. The implementation of this novel approach for monitoring the pipeline health of an operational pipeline in the field is necessary to prove the usefulness of the scheme. It would also be useful for comparing the monitoring results of the ANFIS-based monitoring scheme for the pipeline, in order to prove the effectiveness of the ANFIS-based pipeline monitoring scheme. The selected pipeline should also have a buried section and properly defined boundary conditions. A large amount of the data would be generated from this setup for training and testing purposes.

Further study is required to see whether ANFIS plant dynamics can be used for the prediction of a water hammer or slug flow in a pipeline. Further research may also improve the ANFIS-based scheme ability to determine the thickness of the pipeline with an acceptable band of error. Future studies can also be initiated to predict a shock or explosion and its approximate location.

REFERENCES

Amirat, A., Benmoussat, A., Chaoui, K., 2009. "Reliability Assessment of Underground Pipelines under Active Corrosion Defects". International Journal of Pressure Vessels and Piping, vol.83, pp. 107–117.

Altintas, Y., 2006. "Manufacturing Automation Metal Cutting Mechanics, Machine Tool Vibrations and CNC Design". Cambridge University. Press pp. 79-97.

Andriashin, V.A., 2006. "Long-Term Inside Corrosion Attack of an Oil Operation". Published in Zashchita Metallov, Vol.42, and No.1 pp.52-56.

Barradas, I., Garza, L. E., 2009. "Leak Detection in a Pipeline Using Artificial Neural Networks". Progress in Pattern Recognition, Image Analysis, Computer Vision, and Applications Lecture Notes in Computer Science, Vol. 5856, pp. 637-644.

Bathe, K.J., 1997. "Displacement/Pressure Based Mixed Finite Element Formulations for Acoustic Fluid-Structure Interaction Problems". International Journal for Numerical Methods in Engineering, vol.40, pp. 2001-2017.

Battelle, J. Bruce Nestleroth., 2006. "Pipeline In-line Inspection – Challenges to NDT". ECNDT 2006 - Mo.2.5.1, pp.1-9.

Bill, Draft. 2001."Acoustic Wave Technology Sensors". IEEE Transactions on Microwave Theory and Techniques, VOL. 49, NO. 4, pp. 795-801.

Budenkov, B.A., 1999. "Use of Rayleigh Waves in Testing Stress-Corrosion Breaks in Pipelines by the Acoustic Emission Method". Izhevsk State Tech University Russia, pp.71-78.

Calcatelli, A., 2011. "Leak Detection: General Remarks and Examples". Integrity of Pipelines Transporting Hydrocarbons, NATO Science for Peace and Security Series C: Environmental Security, vol. 1, pp. 181-206.

Cist, David B., 2001." State of the Art for Pipe & Leak Detection". Geophysical Survey Systems Inc., DE-FC26-01NT41317, pp. 2-8.

De Jong, C. A. F. 1994. "Analysis of pulsation and vibrations in fluid-filled pipe system". Thesis-Eindhoven University of Technology, pp.1-13.

Diaz, A.A. 2001. "Mechanical Damage Characterization in Pipelines". Pacific Northwest National Laboratory, U.S. Department of Energy, National Energy Technology Laboratory, pp. 2-8.

DNV, 2006. "A Guidelines Famework for the Integrity Assessment of Offshore Pipelines". Det Norske Veritas, Technical Report NO. 44811520, Revision No. 2, pp.33-43.

Dongare, A.D., Kharde, R.R., 2012. "Introduction to Artificial Neural Network". International Journal of Engineering and Innovative Technology (IJEIT), Vol. 2, pp.189-194.

Feng, J., Zhang, H., 2006. "Algorithm of Pipeline Leak Detection Based on Discrete Incremental Clustering Method". Computational Intelligence: Lecture Notes in Computer Science. Vol. 4114, pp. 602-607.

George, R.G., 2008. "New methods of mathematical modeling of human behaviour in the manual tracking task". pp. 1-7.

Graf F.L., 1990. "Using ground-penetrating radar to pinpoint pipeline leaks". Materials Performance, Vol. 29, No. 4, pp.27-29.

Guo, Xin-lie., 2008. "Pure Frequency Domain Analysis for Detecting Pipeline Leakage". China Institute of Water Resources and Hydropower Research, pp.1713-1717.

Harrish, R. E., 1987. “On the generation of pipeline acoustic resonance”. Open Access Dissertations and Theses, pp.1-7.
Heidari, A.H., 2009. “Dynamic analysis and human analogous control of a pipe crawling robot”. Intelligent Robots and Systems, pp. 733 – 740.
Hennigar G. W., 1993. “Leak detection: new technology that works”, Gas Industries, Vol. 37, pp.16-18.
Hopkins, Phil., 2002. “The Structural Integrity of Oil And Gas Transmission Pipelines”. Elsevier Publishers: Comprehensive Structural Integrity, vol. 1, pp. 3-9.
Daniele, I. 2013.” Pipelines”. Verlag Berlin Heidelberg, Handbook of Technical Diagnostics, pp. 453-480.
Jang, R. J., 1993. “ANFIS Adaptive-Network-Based Fuzzy Inference System”. IEEE Transactions on the system, man and cybernetics, Vol. 43(3), pp.665-681.
Jang, R. J., 1991. “Fuzzy modeling using generalized neural networks and Kalman filter algorithm”. Proceedings of the ninth National conference on Artificial intelligence, Vol. 2, pp.762-767.
Jeffers, Kenneth E., 1999. “Electrochemical Impedance Spectroscopy for the Characterisation of Corrosion and Cathodic Protection of Burried Pipelines”. Thesis: University of Florida, pp.25-35.
Khalid, H.M., Rizvi, S.Z., 2010. “A PSO-Trained ANFIS for Fault Classification”. Fuzzy Computation and International Conference on Neural Computation, pp. 399 – 405.
Lobley, Graham R., 2009. “Pipeline Failure by Transit Fatigue”. A Case Study: J Failure Analysis and Prevention, vol. 9, pp. 35–38.
Murray, A., 2011. “Pipeline Regulations in Canada”. NATO Science for Peace and Security Series C, Environmental Security Vol. 1, pp. 3-8.
Malekian, M., Park, S.S., Jun, M.B., 2009. “Monitoring of Micro Milling Operations”. Journal of Materials Processing Technology, 209(10), pp. 4903-4914.
National Energy Board. 2009. “Focus on safety and Environment-A comparative analysis of performance 2000-2007”. National Energy Board (Canada), pp.2-5.
Odusina, E., 2008. “Software -based Pipeline leak Detection”. Advanced Chemical Engineering Design CHE 4273, Department of Chemical Engineering and Materials Science, University of Oklahoma, pp.1-11.
Ogwu, F.A., 2009. “Challenges of Oil and Gas Pipeline Network and the role of Physical Planners in Nigeria”. FORUM Ejournal, Vol. 10, pp. 41-51.
Peng, Z., Xie, X., Han, X., Fan, X., 2010. “Application Research of the Wavelet Analysis in Ship Pipeline Leakage Detecting”. Communications in Computer and Information Science Volume 97, pp. 47-55.
Pluvinage, G., Elwany., M.H., 2008 “Safety, Reliability and Risks Associated with Water, Oil and Gas Pipelines”. ENIM-UPV Metz (France), pp.1–22.
Polisetty, V.M.S., 2009. “ANFIS Generated dynamic path planning for mobile robots in a 3-D environment”. Electrical engineering, Northern Illinois University, pp. 2-15.
Porter, R.T., 1990. “Application of Inertial Systems for Precise Pipeline monitoring”. Thesis Surveying Engineering, University of Calgary, pp.1-10.
Ramsey. A., 1983. “Experimental Modal Analysis, structural modifications and FEM analysis on a desktop computer”. International Modal Analysis Conference sponsored by Union College, Orlando, FL, pp. 1-10.

Randall, J.A., 1998. “Vibrations: Analytical and Experimental Modal Analysis”. Structural Dynamics Research Laboratory, Department of Mechanical, Industrial and Nuclear Engineering, University of Cincinnati, UC-SDRL-CN-20-263-662, pp. 17-45

Ravanbod, H., 2005. “Application of neuro fuzzy techniques in oil pipeline ultrasonic non-destructive testing”. NDT&E International, Vol.38, pp. 643-653.

Roubidoux, John A., 2011. “Magnetic field and electric current effects on the corrosion and hydrogen absorption behavior of API line pipe steel grades”. Colorado School of Mines, pp 1-18.

Ryder, A.A., Rapson, S.C., 2008. “Pipeline Technology”. Springer Netherlands, pp. 229-230.

Saarenheimo, A., Haspaniemi, H., 2003. “Testing for modal analysis of a feed water pipeline”. Nuclear Engineering and Design, Vol. 235, pp. 1849–1865.

Schwarz, B. J., 1999. “Experimental Modal Analysis”. CSI Reliability Week, Orlando, pp.1-12.

Shawki, S., 2002. “Internal Corrosion of Petroleum Pipelines”. Journal of Engineering and Technology, pp. 112-117.

Shcherbinin, V.E., 2011.” On the Measures that are Necessary for Providing the Safe Operation of Pipeline Transport with Nondestructive Testing Facilities”. Russian Journal of Nondestructive Testing, vol. 47, No. 12, pp. 842–851.

Sivathanu, Y., 2001. “Natural Gas Leak Detection in Pipelines”. Technology Status Report: U.S. Department of Energy, National Energy Technology Laboratory, pp. 1-10.

Sinha, D.N., 2005. “Acoustic Sensor for Pipeline Monitoring: Technology Report”. Gas Technology Management Division Strategic Center for Natural Gas and Oil National Energy Technology Laboratory, LA-UR-05-6025, pp.1-23.

Stevenson, J.D., 1980. “Structural Damping values as a function of Dynamic Response Stress and deformation levels”. Nuclear Engineering and Design, vol. 60, pp. 211-237.

Tung, W.L., Quek, C., 2002. “DIC: A Novel Discrete Incremental Clustering Technique for the Derivation of Fuzzy Member ship Function”. PRICAI 2002: Trends in Artificial Intelligence Lecture Notes in Computer Science, Vol. 2417, pp. 178-187.

Taieb, E., 2008 “Leakage Detection By Using Impedance Method”. NATO Science for Peace and Security Series 2008, pp.79-97.

Wang, X., Bathe, K. J., 1997. “Displacement/pressure based mixed finite element formulations for acoustic fluid-structure interaction problem”. International journal for numerical methods in engineering, Vol.40, pp. 2001-2017.

Weil G.J., “Non-contact, remote sensing of buried water pipeline leaks using infrared thermography”, Water Resources Planning and Management and Urban Water Resources, pp. 404-407.

Yang, J., 2008. “Acoustic Emission Source Identification Technique for Buried Gas Pipeline Leak”. Key Laboratory of Electromagnetic Field and Electrical Apparatus Reliability of Hebei Province, Hebei University of Technology, pp. 1-5.